FINITE DIFFERENCE SOLUTIONS OF THE VON MISES EQUATION

John Y. Thomson

A Thesis Submitted for the Degree of PhD
at the
University of St Andrews

1958

# <u>FINITE DIFFERENCE SOLUTIONS</u>

# <u>OF THE</u>

# <u>VON MISES EQUATION</u>

being a thesis presented by

John Y. Thomson, B.Sc.

to the University of St.Andrews

in application for

the degree of

Doctor of Philosophy.

2040

# CERTIFICATE.

We certify that John Y. Thomson, B.Sc., has spent eleven ~~twelve~~ terms in research work under our direction, and so is qualified to submit the accompanying thesis in application for the degree of Doctor of Philosophy.

DIRECTORS OF RESEARCH.

## DECLARATION.

I declare that the following thesis is based on research work carried out by me, that the thesis is my own composition, and that it has not previously been presented for a higher degree.

The research has been carried out in the Mathematics Department of St.Salvator's College, University of St.Andrews, under the supervision of Drs. D.E. Rutherford and A.R. Mitchell.

## PERSONAL PREFACE.

In October, 1950 I matriculated at St. Andrews University and read for a degree in Mathematics in St. Salvator's College. In June, 1954 I graduated with first class honours in Mathematics.

In October, 1954 I commenced upon a three year course of research study in the Mathematics Department of St. Salvator's College. This course ended in September, 1957.


## ACKNOWLEDGEMENT.

The Author is indebted to the Carnegie Trust for a Research Scholarship held during the period of research.

# INDEX.

## PREFACE.

Prandtl in 1904, discovered that the flow of a fluid over a thin obstacle can be adequately represented by an approximate set of equations, much simpler than the complex Navier-Stokes equations which govern the motion of the fluid.

A particularly simple form of these equations, for the two-dimensional steady flow of a fluid past a flat plate, are the Von Mises Boundary layer equations. Unfortunately the Von Mises transformation introduces a singularity at the plate and this discouraged the use of the equations as a means for obtaining numerical solutions of boundary layer problems in incompressible and compressible flow.

In this thesis, we show that this difficulty can be overcome and the Von Mises equations are used as a basis for a finite difference evaluation of the velocity and temperature in the boundary layer adjacent to a flat plate, particular attention being given to conditions near the plate and more especially to the separation point.

In the section on compressible flow, the calculations also yield a check on certain common simplifying assumptions.

## LIST OF SYMBOLS.

| | |
|---|---|
| $x, y, z$ | Cartesian co-ordinates. |
| $C_p$ | Specific heat at constant pressure. |
| $C_v$ | Specific heat at constant volume. |
| $i$ | Enthalpy. |
| $M$ | Mach number. |
| $p$ | Pressure. |
| $R$ | Reynold's Number. |
| $\mathcal{R}$ | Gas constant. |
| $t$ | Time. |
| $T$ | Absolute temperature. |
| $u, v, w$ | Velocity components in the x, y and z directions respectively. |
| $\Delta x$ | Mesh length in the x-direction. |
| $\Delta \psi$ | Mesh length in the $\psi$-direction. |
| $\delta$ | Mesh Ratio. |
| $\rho$ | Density. |
| $\gamma$ | Ratio of specific heats. |
| $\sigma$ | Prandtl number. |
| $\mu$ | Coefficient of viscosity. |
| $\nu$ | Coefficient of kinematic viscosity. |
| $\tau$ | Shearing stress. |
| $\psi$ | Stream function. |

| | |
|---|---|
| Subscript $o$ | Conditions on the plate. |
| Subscript $1$ | Conditions in the free stream. |
| Subscript $M$ | Conditions in the main stream. |
| Subscript $s$ | Conditions at separation. |

# SECTION I.

## INTRODUCTION.

SURVEY OF HISTORY AND DEVELOPMENT OF TWO DIMENSIONAL BOUNDARY LAYER THEORY.

In this section it is hoped to show how we arrive at the concept of a boundary layer, with reference to the general field of fluid dynamics. The subject matter of fluid dynamics has increased so rapidly in the past fifty or sixty years, that it is now necessary to specialise to a considerable extent. Because of this it is advisable to show where the particular problem investigated fits into the general theory.

The theory of fluid dynamics has as its basis a set of standard equations, including the equation of conservation of mass and the equation of conservation of momentum. Unfortunately the set of equations is so complex that certain approximations and restrictions must be made in order to attempt a solution, different approximations being appropriate for different types of flow.

In this section also, we shall show how the fundamental boundary layer equations are derived and we shall sketch briefly some of the work carried out in attempting to solve these equations.

In the thesis, and more particularly in the introduction, an acknowledgement must be made to the following three text books,

"Modern Developments in Fluid Dynamics", [1]

"Modern Developments in Fluid Dynamics, High Speed Flow", [2]

"Boundary layer Theory" by L. Schlichting. [3]

Real and ideal fluids.

Fluid dynamics can be divided into two major sections, the study of real fluids and the study of ideal fluids. The fact that a fluid, such as air, offers in the main little internal resistance to any change of shape has led to the concept of a perfect or ideal fluid, such a fluid offering no internal resistance to a change of shape. This property is best demonstrated by considering two layers of an ideal fluid moving parallel and adjacent to one another with different velocities. In such a case, the forces between the layers are all acting normal to the interface. No tangential stresses are allowed in ideal fluid theory. Another important example of this is when an ideal fluid flows past a fixed boundary, in which case, the fluid in contact with the boundary maintains the velocity of the main stream. This is the condition of slip on a wall.

The science of ideal flow theory has been expanded considerably and has produced some elegant results - the equations of motion being considerably simpler than those for a real fluid.

It has been shown experimentally that if we consider a real fluid flowing past a fixed boundary the fluid in contact with the wall is at rest. This phenomenon of "no slip at a wall" is more readily seen if the fluid is "thick" (e.g. glycerine) than if the fluid is "thin" (e.g. air). The condition of no slip at a wall produces the main difference between results arising from the two theories.

If we now consider two adjacent layers of a real fluid moving parallel to each other along the x-axis, one with a greater velocity than the other, then there are tangential stresses acting along the interface which tend to speed up the slow layer and retard the fast layer. In this simple example the tangential stress at any point is found to be proportional to the velocity difference normal to the direction of flow. This can be expressed for a continuous flow as,

$$\tau \propto \frac{\partial u}{\partial y}, \quad \text{or } \tau = \mu \frac{\partial u}{\partial y},$$

where $\tau$ is the tangential stress and $u$ is the velocity in the x-direction. The above relation, known as Newton's law of friction can be used to define the coefficient of viscosity $\mu$. The ratio of the viscosity $\mu$ to the density $\rho$ is called the coefficient of kinematic viscosity $\nu$. This coefficient is of prime importance in problems where viscous and inertia forces act together. The coefficient of viscosity is nearly independent of pressure but varies considerably with temperature.

Viscous flow equations.

If we are to specify the motion of a real fluid, with respect to three mutually perpendicular axes and time, we must, at any point in the fluid, at any time, be able to give expressions for the following set of variables; the three components of velocity, $u$, $v$, $w$, parallel to the three axes, the density $\rho$, the pressure $p$, the absolute temperature $T$, and the coefficient of viscosity $\mu$. There are thus seven dependent variables to be expressed in terms of the four independent variables $x$, $y$, $z$ and $t$, in customary notation. We shall now proceed to sketch the derivation of the set of equations which are to be solved for the above dependent variables.

Equation of conservation of mass.

The equation of conservation of mass, or the continuity equation, expresses the fact that in a fluid motion the mass of fluid entering a volume in unit time is equal to the mass leaving the same volume in unit time.

The equation which is easily derived is,

$$\frac{\partial \rho}{\partial t} + \underline{\nabla} \cdot (\rho \underline{u}) = 0, \tag{1,1}$$

in vector form, where $\underline{u}$ is the velocity vector and

$$\underline{\nabla} \equiv \left( \frac{\partial}{\partial x}, \frac{\partial}{\partial y}, \frac{\partial}{\partial z} \right).$$

In Cartesian form, (1,1) becomes

$$\frac{\partial \rho}{\partial t} + u \frac{\partial \rho}{\partial x} + v \frac{\partial \rho}{\partial y} + \frac{\partial \rho}{\partial z} + \rho \left( \frac{\partial u}{\partial x} + \frac{\partial v}{\partial y} + \frac{\partial}{\partial z} \right) = 0. \tag{1,2}$$

Equations of conservation of momentum.

The equation of conservation of momentum follows from Newton's second law of motion. Considering now a small volume of the fluid the law can be expressed as

$$\rho \frac{D\underline{u}}{Dt} = \underline{F} + \underline{P}, \qquad (1,3)$$

where $\frac{D\underline{u}}{Dt}$ is the acceleration of any particle of fluid following the motion of the particle and can be written in the usual form

$$\frac{D\underline{u}}{Dt} = \frac{\partial \underline{u}}{\partial t} + u \frac{\partial \underline{u}}{\partial x} + v \frac{\partial \underline{u}}{\partial y} + w \frac{\partial \underline{u}}{\partial z} .$$

$\underline{F} \equiv F_x \underline{i} + F_y \underline{j} + F_z \underline{k}$ , is the external force per unit volume acting on a volume of fluid.

$\underline{P} \equiv P_x \underline{i} + P_y \underline{j} + P_z \underline{k}$ , is the total force on the boundary of the unit volume, this force being the resultant of normal pressures and tangential frictional forces.

Stoke's law of friction for fluids, a particular case of which is Newton's law, states that the forces which oppose the deformation of a volume of fluid are proportional to the rate of strain. We use this empirical law to establish a relation between the stresses and strains on a unit volume. In other words we establish a relation connecting $\underline{P}$ with the derivatives of $\underline{u}$.

If we substitute such an expression for $\underline{P}$ in (1,3) and split up the resulting equation into its three components we arrive at the equations of conservation of momentum in the three cartesian directions as follows;

$$\frac{\partial u}{\partial t} + u\,\frac{\partial u}{\partial x} + v\,\frac{\partial u}{\partial y} + w\,\frac{\partial u}{\partial z} = \frac{F_x}{\rho} - \frac{1}{\rho}\,\frac{\partial p}{\partial x} + \frac{1}{\rho}\,\frac{\partial}{\partial x}\Big[\mu\Big(2\,\frac{\partial u}{\partial x} - \frac{2}{3}\underline{\nabla}\cdot\underline{u}\Big)\Big]$$
$$+ \frac{1}{\rho}\,\frac{\partial}{\partial y}\Big[\mu\Big(\frac{\partial u}{\partial y} + \frac{\partial v}{\partial x}\Big)\Big] + \frac{1}{\rho}\,\frac{\partial}{\partial z}\Big[\mu\Big(\frac{\partial w}{\partial x} + \frac{\partial u}{\partial z}\Big)\Big],$$

$$\frac{\partial v}{\partial t} + u\,\frac{\partial v}{\partial x} + v\,\frac{\partial v}{\partial y} + w\,\frac{\partial v}{\partial z} = \frac{F_y}{\rho} - \frac{1}{\rho}\,\frac{\partial p}{\partial y} + \frac{1}{\rho}\,\frac{\partial}{\partial y}\Big[\mu\Big(2\,\frac{\partial v}{\partial y} - \frac{2}{3}\underline{\nabla}\cdot\underline{u}\Big)\Big] \qquad (1.4)$$
$$+ \frac{1}{\rho}\,\frac{\partial}{\partial z}\Big[\mu\Big(\frac{\partial v}{\partial z} + \frac{\partial w}{\partial y}\Big)\Big] + \frac{1}{\rho}\,\frac{\partial}{\partial x}\Big[\mu\Big(\frac{\partial u}{\partial y} + \frac{\partial v}{\partial x}\Big)\Big],$$

$$\frac{\partial w}{\partial t} + u\,\frac{\partial w}{\partial x} + v\,\frac{\partial w}{\partial y} + w\,\frac{\partial w}{\partial z} = \frac{F_z}{\rho} - \frac{1}{\rho}\,\frac{\partial p}{\partial y} + \frac{1}{\rho}\,\frac{\partial}{\partial z}\Big[\mu\Big(2\,\frac{\partial w}{\partial z} - \frac{2}{3}\underline{\nabla}\cdot\underline{u}\Big)\Big]$$
$$+ \frac{1}{\rho}\,\frac{\partial}{\partial x}\Big[\mu\Big(\frac{\partial w}{\partial x} + \frac{\partial u}{\partial z}\Big)\Big] + \frac{1}{\rho}\,\frac{\partial}{\partial y}\Big[\mu\Big(\frac{\partial v}{\partial z} + \frac{\partial w}{\partial y}\Big)\Big].$$

The equations (1,2) and (1,4) were first derived by Navier [4] in 1827 and later by Poisson [5] in 1831, in both cases it was assumed that the density was constant.

The Navier-Stokes equations (1,4), derived from Stokes' empirical law, depend on the accuracy of this law. Their validity has been demonstrated by experimental results.

<u>Equation of conservation of energy.</u>

We must now consider some of the principles of thermodynamics in order to derive the energy equation.

The equation of conservation of energy expresses the fact that the heat added per unit volume to a volume of fluid in unit time, both from external sources and from frictional heating, is equivalent to the increase in internal energy of the fluid and the work done in expansion. This may be written in the form

$$dQ = \Delta V\,.\,d\,(C_v T) + p\,.\,d\,(\Delta V), \qquad (1,5)$$

where $\Delta V$ is an infinitesimal volume and $C_v$ is the specific heat at constant volume. The quantity of heat added, viz. $dQ$ can be divided into two parts and written as

$$dQ = dQ_c + dQ_f \,,$$

where $dQ_c$ is the amount of heat added due to conduction and $dQ_f$ is the amount of heat added due to frictional effects. The former quantity can be expressed in terms of temperature gradients using Fourier's equation of heat flux. The latter quantity can be evaluated in terms of the velocity gradients by relating the total work done by the frictional forces and the total increase in mechanical energy, the heat evolved being the difference between the two.

Substituting for the heat added in (1,5) we eventually arrive at the energy equation in the form,

$$\rho \frac{D}{Dt}\left(C_v T + \frac{p}{\rho}\right) = \frac{Dp}{Dt} + \frac{\partial}{\partial x}\left(k\,\frac{\partial T}{\partial x}\right) + \frac{\partial}{\partial y}\left(k\,\frac{\partial T}{\partial y}\right) + \frac{\partial}{\partial z}\left(k\,\frac{\partial T}{\partial z}\right) + \mu\Phi, \qquad (1,6)$$

where $k$ is the conductivity and $\Phi$, the dissipation function, can be expressed as

$$\Phi = 2\left[\left(\frac{\partial u}{\partial x}\right)^2 + \left(\frac{\partial v}{\partial y}\right)^2 + \left(\frac{\partial w}{\partial z}\right)^2\right] + \left(\frac{\partial v}{\partial x} + \frac{\partial u}{\partial y}\right)^2 + \left(\frac{\partial w}{\partial y} + \frac{\partial v}{\partial z}\right)^2 + $$
$$+ \left(\frac{\partial u}{\partial z} + \frac{\partial w}{\partial x}\right)^2 - \frac{2}{3}\left(\frac{\partial u}{\partial x} + \frac{\partial v}{\partial y} + \frac{\partial w}{\partial z}\right)^2 . \qquad (1,7)$$

In actual practice it is generally assumed that for air the conductivity $k$ is a constant, resulting in a simplification of the energy equation.

Equation of state.

Another equation required in the specification of viscous fluid flow is the equation of state, which connects the pressure, density and temperature. In the absence of a general equation of state we shall list the equation of state for a perfect gas, viz.,

$$\frac{p}{\rho} = RT, \tag{1,8}$$

where $R$ is the gas constant.

Equation connecting viscosity and temperature.

As was stated earlier the coefficient of viscosity varies appreciably with the temperature. For air, the fluid we shall be concerned with, the generally accepted law is Sutherland's law,

$$\mu = \frac{AT^{1.5}}{T + 114^{\circ}\ K}, \tag{1,9}$$

where $A$ is a constant and the temperature is measured in absolute units.

As will be discussed later various approximations to this law have been offered, notably that due to Hartree, which asserts that over a large range of temperature,

$$\mu = aT^{0.89}.$$

A linear relation of the form $\mu = bT$, produces worthwhile simplifications when it is used in the equations of motion.

Totality of equations.

We have now given seven equations for the seven dependent variables. Together with the appropriate boundary conditions these equations require solution in any flow problem.

The equations are listed below.

The complexity of the general equations and the need for approximations is evident from the list below.

Equations of motion of a viscous fluid.

$$\frac{\partial \rho}{\partial t} + u\frac{\partial \rho}{\partial x} + v\frac{\partial \rho}{\partial y} + w\frac{\partial \rho}{\partial z} + \rho\left(\frac{\partial u}{\partial x} + \frac{\partial v}{\partial y} + \frac{\partial w}{\partial z}\right) = 0.$$

$$\frac{\partial u}{\partial t} + u\frac{\partial u}{\partial x} + v\frac{\partial u}{\partial y} + w\frac{\partial u}{\partial z} = F_x - \frac{1}{\rho}\frac{\partial p}{\partial x} + \frac{1}{\rho}\frac{\partial}{\partial x}\left[\mu\left(2\frac{\partial u}{\partial x} - \frac{2}{3}\underline{\nabla}\cdot\underline{u}\right)\right]$$
$$+ \frac{1}{\rho}\frac{\partial}{\partial y}\left[\mu\left(\frac{\partial u}{\partial y} + \frac{\partial v}{\partial x}\right)\right] + \frac{1}{\rho}\frac{\partial}{\partial z}\left[\mu\left(\frac{\partial w}{\partial x} + \frac{\partial u}{\partial z}\right)\right].$$

$$\frac{\partial v}{\partial t} + u\frac{\partial v}{\partial x} + v\frac{\partial v}{\partial y} + w\frac{\partial v}{\partial z} = F_y - \frac{1}{\rho}\frac{\partial p}{\partial y} + \frac{1}{\rho}\frac{\partial}{\partial y}\left[\mu\left(2\frac{\partial v}{\partial y} - \frac{2}{3}\underline{\nabla}\cdot\underline{u}\right)\right]$$
$$+ \frac{1}{\rho}\frac{\partial}{\partial z}\left[\mu\left(\frac{\partial v}{\partial z} + \frac{\partial w}{\partial y}\right)\right] + \frac{1}{\rho}\frac{\partial}{\partial x}\left[\mu\left(\frac{\partial u}{\partial y} + \frac{\partial v}{\partial x}\right)\right].$$

$$\frac{\partial w}{\partial t} + u\frac{\partial w}{\partial x} + v\frac{\partial w}{\partial y} + w\frac{\partial w}{\partial z} = F_z - \frac{1}{\rho}\frac{\partial p}{\partial z} + \frac{1}{\rho}\frac{\partial}{\partial z}\left[\mu\left(2\frac{\partial w}{\partial z} - \frac{2}{3}\underline{\nabla}\cdot\underline{u}\right)\right]$$
$$+ \frac{1}{\rho}\frac{\partial}{\partial x}\left[\mu\left(\frac{\partial w}{\partial x} + \frac{\partial u}{\partial z}\right)\right] + \frac{1}{\rho}\frac{\partial}{\partial y}\left[\mu\left(\frac{\partial v}{\partial z} + \frac{\partial w}{\partial y}\right)\right].$$

$$\rho\frac{D}{Dt}\left(c_vT + \frac{p}{\rho}\right) = \frac{Dp}{Dt} + \frac{\partial}{\partial x}\left(k\frac{\partial T}{\partial x}\right) + \frac{\partial}{\partial y}\left(k\frac{\partial T}{\partial y}\right) + \frac{\partial}{\partial z}\left(k\frac{\partial T}{\partial z}\right) + \mu\Phi.$$

$$\underline{\Phi} = 2\left[\left(\frac{\partial u}{\partial x}\right)^2 + \left(\frac{\partial v}{\partial y}\right)^2 + \left(\frac{\partial w}{\partial z}\right)^2\right] + \left(\frac{\partial v}{\partial x} + \frac{\partial u}{\partial y}\right)^2 + \left(\frac{\partial w}{\partial y} + \frac{\partial v}{\partial z}\right)^2 + \left(\frac{\partial u}{\partial z} + \frac{\partial w}{\partial x}\right)^2$$
$$- \frac{2}{3}\left(\frac{\partial u}{\partial x} + \frac{\partial v}{\partial y} + \frac{\partial w}{\partial z}\right)^2.$$

$$\frac{p}{\rho T} = R.$$

$$\mu = \frac{AT^{1.5}}{T + 114^{\circ}K}.$$

Approximate equations of flow.

As we have shown in the previous section the motion of a real fluid is governed by a set of differential equations, the complexity of which forbids the possibility of a general solution. In order to make any progress we must restrict ourselves to certain special cases of flow, each producing different simplifications in the general system of equations. Below are listed some of the simplifications which can be made.

(a) Steady flow.

As an example we consider the flow of air in a wind tunnel. It is found that some time after the flow has been started, and with the right conditions, a state is reached when the motion is such that, if a photograph is taken at one time and at a later time, the photographs of the motion will be the same. Such a state is called a steady state and obviously if we are concerned with steady flow the time variable can be eliminated from the equations. The assumption of steady flow can not be applied to turbulent motion in which changes with time are important.

(b) Two-dimensional flow.

To demonstrate "two-dimensional" flow we consider the flow of a fluid past an obstacle which is of infinite length in the z-direction, the flow approaching the obstacle in say, the direction of x. It is obvious that if we take any plane section perpendicular to the z-direction, a picture of the flow will be the same no matter the section. In other words, the flow equations become independent of the variable z and we can represent the flow by a two dimensional picture.

Two dimensional flow can also be assumed in the case of parallel flow past an obstacle of finite length, such as an aeroplane wing of rectangular plan form, provided we are interested in the flow inboard of the tips. It is, however, the reduction in the number of equations and variables rather than any practical considerations which justify the assumption of two dimensional flow.

(c) Non Viscous flow.

The assumption of a non viscous irrotational fluid produces what is called the potential or ideal flow theory, which has been subject to exhaustive mathematical treatment and which has produced many valuable results. If we are considering the flow of air past an obstacle it is noted that since the viscous forces are of the order of the coefficient of viscosity times a velocity gradient, and the coefficient of viscosity is very small, the viscous stresses can be neglected if the velocity gradients are not large. In such a flow it is found that the velocity gradients are only large in a very narrow region bordering the obstacle, and so in the major part of the flow field we can neglect the viscous forces. In fact when the inertia forces far outweigh the viscous forces we can choose $\mu = o$ in the equations of motion and so produce a much simpler set of equations.

In ideal flow theory however we assume that $\mu = o$ throughout the flow field, even on the obstacle; this of course yields full slip over the obstacle, a contradiction of experimental evidence.

(d) Very Viscous flow.

An exactly opposite assumption to (c) is the assumption which is valid in the case of the slow flow of a very viscous fluid such as tar. In the equations of motion of this flow we can assume that the viscous terms far outweigh the inertia terms and the latter may be neglected, again simplifying the equations.

(e) Incompressible flow.

We define the Mach number M at a point in a fluid as the ratio of the local velocity to the local speed of sound in the fluid, that is, $M = \frac{u}{c}$. It can be shown that density changes in a fluid are negligible provided the Mach number of the flow is much less than unity at all points in the field. If there are regions in the fluid where the Mach number is of the order of unity we can not assume that the density there is constant. For incompressible fluid flow the equations of momentum and continuity are much simplified since $\rho =$ const. The equations of energy and state do not apply to the calculation of the flow field and the viscosity can be assumed constant.

(f) Perfect gas flow.

We can make the assumption that the fluid is a perfect gas, a valid approximation if the fluid is air, and this is accompanied by a simple equation of state, namely,

$$\frac{p}{\rho T} = R.$$

The above equation of state can also be used to simplify the energy equation.

(g) Adiabatic gas flow.

Since air has a low value of conductivity we can assume that any heat processes are adiabatic, this assumption producing the simplifying relation

$$\frac{p}{\rho^{\gamma}} = \text{const.}$$

The adiabatic approximation can be applied in regions of approximately non-viscous flow but is not valid in regions of high stress such as a boundary layer or shock wave.

(h) Elimination of external forces.

If, in the case of two dimensional flow, we choose our plane section to be horizontal, the effects of gravity can be ignored and we simplify the equations of motion by the elimination of external force components.

There are other approximations and restrictions which can be made on fluid flow and these may be combined, each set of approximations being valid in certain regions of a flow field under a given set of conditions.

The concept of boundary layer flow is perhaps the most important example of this idea of specialised flow. In such a flow we divide the field into two regions; one region, the free stream, in which the inertia terms in the equations are much larger than the viscous terms, and a second region, the boundary layer, in which the inertia and viscous terms are of the same order of magnitude.

Qualitative concept of a boundary layer.

For the sake of simplicity, we shall assume the fluid to be steady, two dimensional and incompressible.

In the problem of flow over a semi-infinite plate we consider the plate stretching along the positive part of the x-axis and the fluid approaching the plate with a constant velocity $U$ in the positive x direction. We examine the fluid in layers parallel to the x-axis.

The layer of fluid immediately in contact with the plate, by the condition of no slip, is at rest. A particle of fluid approaching the plate in the next adjacent layer moves along with a constant velocity $U$ until it reaches a position near the nose of the plate at which there is a velocity gradient in the y-direction which produces a shearing force retarding the particle, the retardation being proportional to the velocity gradient, and so the velocity decreases as we move downstream along this layer.

As we proceed along the next adjacent layer it too is retarded but to a lesser extent, since the velocity gradient is less than that encountered by the first layer. If we now examine the velocity of the fluid at points along a normal to the plate it is seen that the retardation decreases as we move out from the plate until the free stream velocity is approximately reached by the fluid in a very short distance.

We have thus demonstrated how the effects of viscosity are confined to a very thin layer next to the plate. The thickness of the layer increases as we move downstream. The definition of the outer edge of the boundary layer is to some extent arbitrary. It can be defined as the locus of points at which the velocity of the fluid first differs from the free stream velocity by a given small percentage. A better definition is the locus of points along which the shearing stress first becomes negligible as we move out from the plate, in other words, the locus of points at which $\frac{\partial u}{\partial y} \doteq 0$ to the required degree of accuracy. It can be proved that the thickness of the boundary layer $\delta = O(\nu^{\frac{1}{2}})$.

Figure (1,1) is an exaggerated diagram of a boundary layer with velocity profiles drawn at various stations of x. We shall now proceed to establish the boundary layer equations.

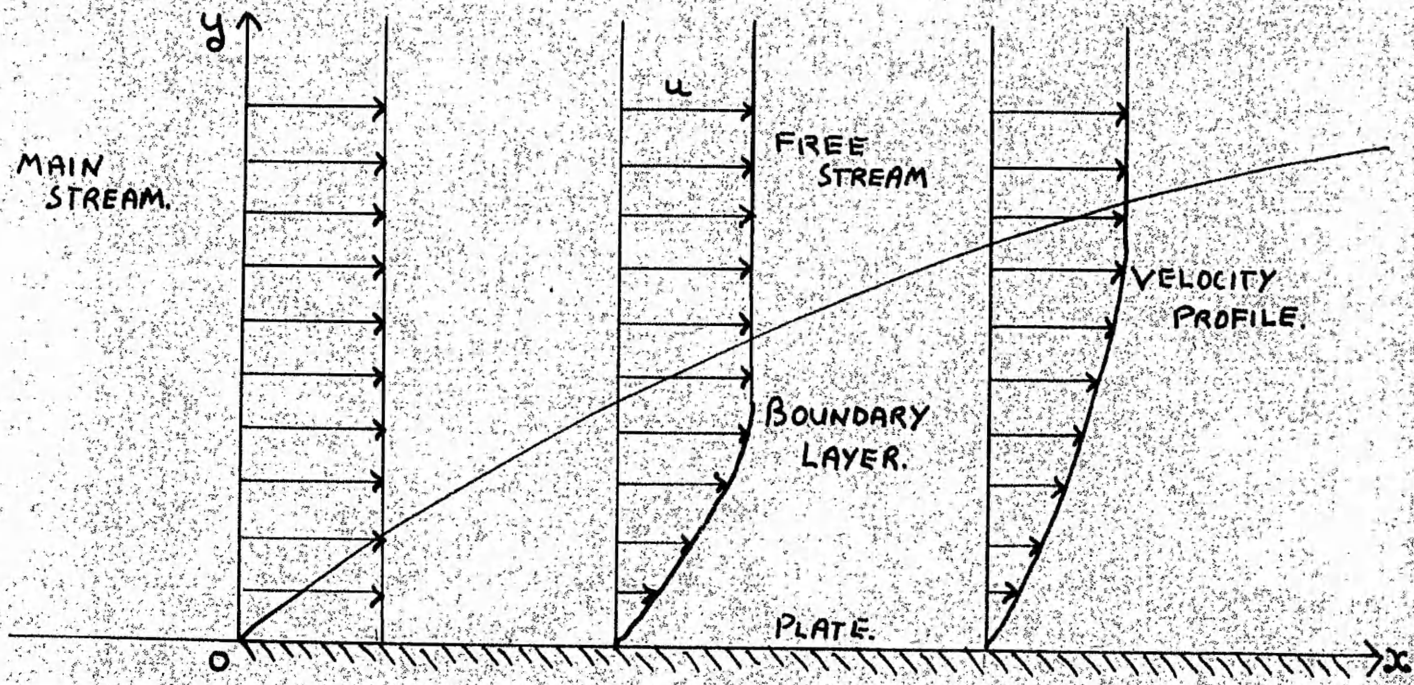


FIGURE (1,1)

Establishing the incompressible boundary layer equations.

As in the previous section, we shall consider the two dimensional, steady, laminar flow of an incompressible fluid past the semi-infinite flat plate shown in figure (1,1).

The equations of conservation of momentum and mass, the only relevant equations for incompressible flow, are first simplified to the extent that the flow is steady and two dimensional and that the fluid is incompressible. The resulting equations are,

$$u\frac{\partial u}{\partial x} + v\frac{\partial u}{\partial y} = -\frac{1}{\rho}\frac{\partial p}{\partial x} + \nu\left(\frac{\partial^2 u}{\partial x^2} + \frac{\partial^2 u}{\partial y^2}\right), \tag{1,10}$$

$$u\frac{\partial v}{\partial x} + v\frac{\partial v}{\partial y} = -\frac{1}{\rho}\frac{\partial p}{\partial y} + \nu\left(\frac{\partial^2 v}{\partial x^2} + \frac{\partial^2 v}{\partial y^2}\right), \tag{1,11}$$

$$\frac{\partial u}{\partial x} + \frac{\partial v}{\partial y} = 0, \tag{1,12}$$

the symbols representing the same variables as before.

We may assume now that $x$ and $u$ are of a finite size, that is, $x \equiv O(1)$, $u \equiv O(1)$ and since we are interested in the flow in a very thin layer of thickness $\delta$, $y \equiv O(\delta)$ where $\delta$ is the first order of small quantities. In (1,12) we have $\frac{\partial u}{\partial x} \equiv O(1)$ and so $\frac{\partial v}{\partial y} \equiv O(1)$ and so $v = O(\delta)$.

This means that the velocity in the y direction is very small, in fact, in actual calculations, it is neglected and only the component of velocity in the x-direction is considered.

We now examine the order of the terms in equation (1,10). $\frac{\partial^2 u}{\partial x^2} = O(1)$ whereas $\frac{\partial^2 u}{\partial y^2} = O(\delta^{-2})$ and so we can neglect $\frac{\partial^2 u}{\partial x^2}$ in comparison with $\frac{\partial^2 u}{\partial y^2}$. The inertia terms in (1,10) are of order unity and so, on the assumption that the viscous term is of comparable order, we require that $\nu = O(\delta^2)$ or $\delta = O(\nu^{\frac{1}{2}})$. This again demonstrates the small thickness of the boundary layer.

Equation (1,11) subjected to a similar scrutiny reduces to

$$-\frac{1}{\rho}\frac{\partial p}{\partial y} = 0,$$

signifying that the pressure is a constant through the boundary layer, along any normal to the plate.

We now establish the equation governing the motion of the fluid in the free stream. We assume that the velocity $v$ is negligible and the resulting equation is the equation of motion of a one dimensional steady non viscous flow, namely,

$$u_1 \frac{du_1}{dx} = -\frac{1}{\rho} \frac{\partial p_1}{\partial x} = -\frac{1}{\rho} \frac{\partial p}{\partial x}, \qquad (1,13)$$

where the subscript 1 denotes conditions in the free stream.

Combining (1,13) with the reduced form of (1,10) we arrive at the following set of governing equations,

$$\begin{aligned} u \frac{\partial u}{\partial x} + v \frac{\partial u}{\partial y} &= u_1 \frac{du_1}{dx} + \nu \frac{\partial^2 u}{\partial y^2}, \\ \frac{\partial p}{\partial y} &= 0, \\ \frac{\partial u}{\partial x} + \frac{\partial v}{\partial y} &= 0. \end{aligned} \qquad (1,14)$$

The above set of equations was first suggested by Prandtl [6], in 1904. The Prandtl boundary layer equations are obviously more readily solved than the Navier-Stokes equations.

For the case of flow past a flat plate we now specify the boundary conditions under which a solution can be obtained. Since the equations are of the second order in y we require two boundary conditions in the y-direction, namely

$$\begin{aligned} u = v = 0 \quad &\text{when} \quad y = 0, \\ u = u_1(x), \ v = 0 \quad &\text{when} \ \frac{\partial u}{\partial y} \doteq 0. \end{aligned} \qquad (1,15)$$

We must now specify one boundary condition in the x direction. This can be done by assuming a known velocity profile $u = u\ (x_o, y)$ at some initial station $x = x_o$.

As is seen from the boundary conditions, in order to solve (1,14) we must specify the free stream velocity as an external boundary condition. Since it must be compatible with the actual conditions in the non-viscous free stream it is generally taken to be the value of velocity derived from the potential flow solution of the same problem. In the case of flow past a flat plate at zero incidence the free stream velocity is simply $u_1 = U$, a constant.

It has been found advantageous however, to investigate the somewhat artificial problem of flow past a flat plate against adverse pressure gradients. Thus, instead of the pressure being a constant (as in (1,13) with $u_1 = U$), we require that the pressure increases as x increases. This technique is used to give a mathematical model of a section of the flow over an aerofoil as demonstrated below in figure (1,2).

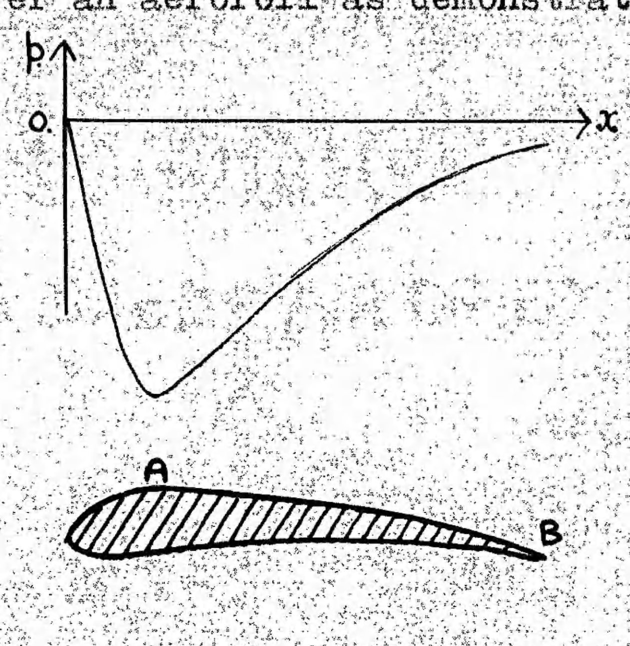


FIGURE (1,2)

Figure (1,2) shows a graph of the pressure over the top surface of an aerofoil, plotted against position on the aerofoil. It is seen that there is a section AB of the surface over which the pressure increases as we move downstream. It is found that if the pressure gradient $\frac{\partial p}{\partial x}$ is sufficiently large, the laminar flow can not continue and at some point it breaks away from the surface, causing the aerofoil to stall. We can mathematically represent such a flow by adding an adverse pressure gradient to the flow over a flat plate, in the hope that we can create the conditions of stall and examine the mechanics of flow separation.

From equation (1,13) we see that instead of specifying the pressure gradient we could equally specify the corresponding free stream velocity, this is in fact the specification used in the calculations to follow.

We now examine qualitatively the theory of boundary layer separation.

Separation point in a boundary layer.

Consider the flow of air along a flat plate against an adverse pressure gradient. From the second of equations (1,14) it is seen that the pressure is transmitted normally through the boundary layer to the fluid adjacent to the plate. The layer of fluid on the plate is at rest and the next layer has a very small forward velocity and so may not have sufficient momentum to overcome the pressure gradient.

At some point along the plate it may be brought to rest and downstream of this point the flow will be reversed. This position of breakaway is called the separation point and is defined to be the station x at which $\left(\frac{\partial u}{\partial y}\right)_o = 0$, the subscript o denoting conditions on the plate. A diagrammatic representation of such a flow is given in figure (1,3).

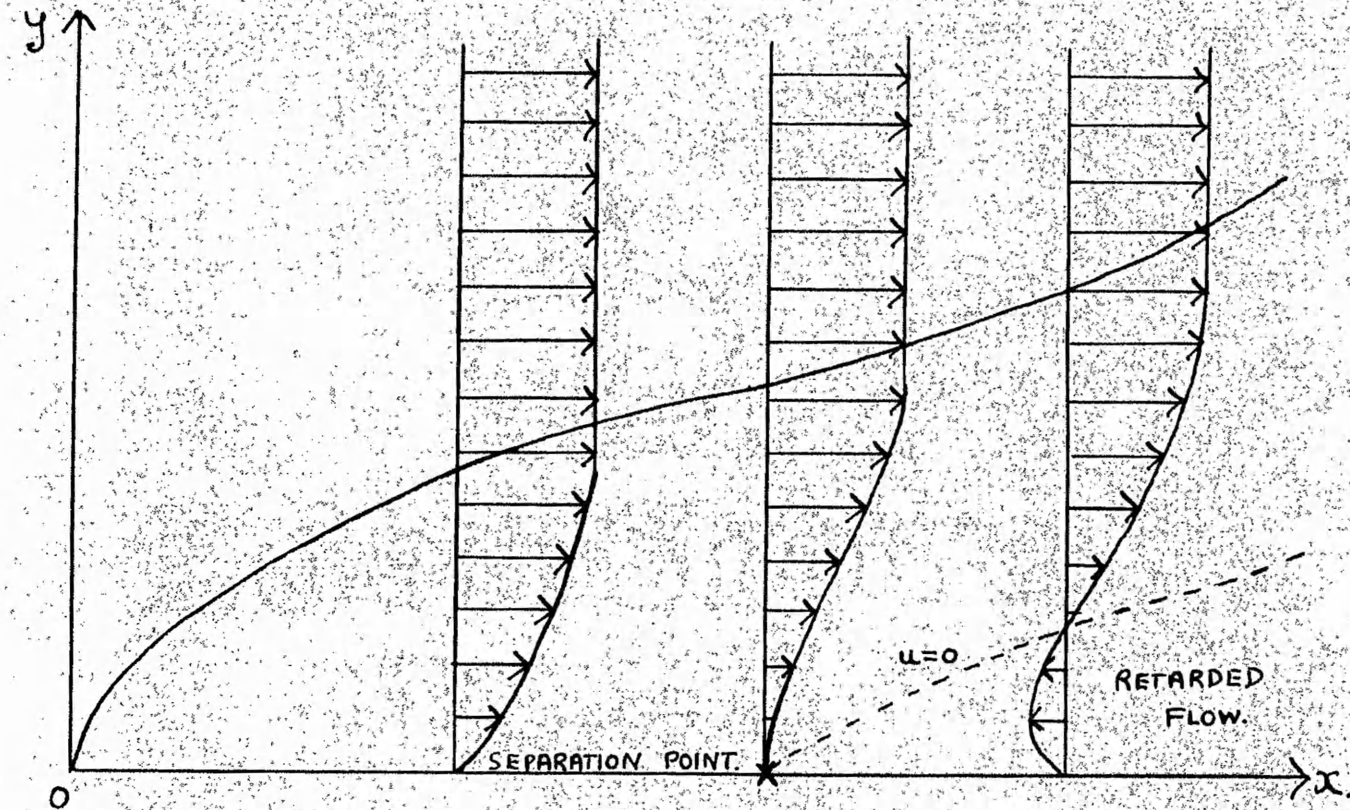


FIGURE (1,3)

Aircraft design has demanded a great deal of effort, both theoretical and experimental, concerning calculations of the separation point and the mechanics of separation with a view to the design of an optimum aerofoil shape over which the major part of the flow would be laminar.

The compressible boundary layer equations.

The considerations which have been employed in establishing the boundary layer concept in incompressible flow can be readily carried over to compressible flow. We now have not only a velocity boundary layer, in which are concentrated all the viscous stresses, but also a thermal boundary layer in which are confined all viscous heating effects. The problem is much more complex because of the interdependence of the two layers and the temperature variations of the density and viscosity. It is found that the two layers are comparable in thickness if the Prandtl number of the fluid is of the order of unity, the Prandtl number being $\sigma = \frac{\mu c_p}{k}$, where $c_p$ is the specific heat at constant pressure. For air, the fluid we are considering, the Prandtl number is taken to be $\sigma = 0.72$.

Applying the same techniques as are used in incompressible flow we can establish the simplified form of the equations of motion for a steady, two dimensional, compressible boundary layer. These equations, in which it is more convenient to use the enthalpy $i$ ($= C_p T$) than the temperature, are given below,

$$\rho u \frac{\partial u}{\partial x} + \rho v \frac{\partial u}{\partial y} = \rho_1 u_1 \frac{du_1}{dx} + \frac{\partial}{\partial y}\left(\mu \frac{\partial u}{\partial y}\right),$$

$$\rho u \frac{\partial i}{\partial x} + \rho v \frac{\partial i}{\partial y} = -\rho_1 u_1 \frac{du_1}{dx} u + \frac{\partial}{\partial y}\left(\frac{\mu}{\sigma} \frac{\partial i}{\partial y}\right) + \mu\left(\frac{\partial u}{\partial y}\right)^2, \qquad (1,16)$$

$$\frac{\partial \rho u}{\partial x} + \frac{\partial \rho v}{\partial y} = 0,$$

together with the equation of state for a perfect gas and the equation connecting viscosity and temperature.

As in incompressible flow we require the appropriate number of boundary conditions. With regard to boundary conditions it should be noted that there are two main types of problem which can be considered, the thermometer problem in which we specify the temperature on the plate, and the problem of no heat transfer across the plate where the boundary condition there is $\left(\frac{\partial T}{\partial y}\right)_0 = 0$.

It should be mentioned that we shall ignore the possible existence of shock waves.

<u>Variation of viscosity with temperature.</u>

The generally accepted law of variation of viscosity with temperature is Sutherland's law,

$$\mu = \frac{\text{const.}\ T^{1.5}}{T + C} \tag{1,9}$$

where $C = 114^\circ K$ for air.

However it is found to be more convenient to frame a law in the form

$$\mu = \text{const.}\ T^{\omega}.$$

Such a representation, suggested by Cope and Hartree [7] with $\omega = 8/9$ is applicable over the range $90^\circ K \leq T \leq 300^\circ K$, with a percentage error of less than five per cent. The special case $\omega = 1$ is often considered for convenience.

The assumptions $\omega = 1$ and $\sigma = 1$ produce startling simplifications in the compressible boundary layer equations and a section of the work on compressible flow in this thesis is devoted to assessing the validity of these assumptions.

We shall now sketch a brief history of the development of boundary layer theory.

History of the development of boundary layer theory.

In this thesis we are considering a particular aspect of boundary layer theory, namely the two dimensional steady boundary layer flow along a semi-infinite flat plate. We have made no mention of three dimensional boundary layers, or boundary layers on circular cylinders and we have restricted ourselves to laminar flow, neglecting the effects of turbulence. In the compressible flow section we do not consider the interaction of shock wave and boundary layer. With all the above restrictions it is still not possible to discuss all the work which has been carried out in this field. It would be undesirable, however, to proceed to our specific calculation without a brief mention of some of the work already published on the subject.

The concept of a boundary layer was first given in the famous paper delivered by Prandtl [6] to the Mathematical Congress at Heidelberg in 1904. In this paper Prandtl showed how the motion of a slightly viscous fluid past a body could be divided into two regions, pointing to the simplifications this would produce in the Navier-Stokes equations.

The first solution of the boundary layer equations for flow past a flat plate at zero incidence was given by Blasius [8] in a Doctor's thesis at Göttingen. The essential feature of this solution is an expansion of velocity as an infinite series, the first few terms of which are evaluated. Similar types of solution were developed by Töpfer [9], Bairstow [10] and S. Goldstein [11].

Howarth [12], solved the equations for boundary layer flow past a flat plate against a linear adverse pressure gradient, and found the position of the separation point. Hartree [13] solved the same problem and his results agree favourably with those of Howarth.

In the approximate methods of Von Karman [14] and Polhausen [15] the momentum integral form of the equation of motion was used. In this technique the boundary layer equations were satisfied in average over the boundary layer thickness.

Another class of solutions consists of the step-by-step solutions, here again motivated by Prandtl [16] and expanded by Görtler [17]. Here the velocity profile at a station $(x + \delta x)$ is obtained in terms of the velocity profile at the station x. Görtler [18] improved upon his method later, whilst Schroeder [19] produced a finite difference solution of the Prandtl boundary layer equations, his method being improved by Witting [20] in 1953. One of the most recent papers on this type of solution is that of Leigh [21] who, from the results of Hartree at a small distance upstream of the separation point, proceeds to calculate to a high accuracy using step-by-step methods the actual position of the separation point.

In the theory of compressible boundary layers the large number of different boundary conditions which can be applied and the various approximations which can be made concerning the viscosity and the Prandtl number make it difficult to present the work done in the field in an orderly manner.

Howarth [22] calculates the flow fields of compressible boundary layers on a flat plate with and without adverse pressure gradients. He makes the assumption that $\sigma = \omega = 1$. In Howarth's paper he transforms the compressible equations into incompressible equations for which the solution is known. A general conclusion reached by Howarth is that as the initial Mach number increases, the boundary layer thickens, and separation can be expected to occur nearer the nose of the plate. Stewartson [23] used a similar technique to that used by Howarth.

Crocco [24], using u and x as independent variables, solves the problem of flow past a flat plate using different values for $\mu$ and $\sigma$, one interesting result being that as the Mach number increases, corresponding velocity profiles become more linear. Busemann [25], assuming $\sigma = 1$ solves a corresponding problem by expressing the shearing stress $\tau$ as a quadratic in $u$.

Hantsche and Wendt [26], assuming $\omega = 1$, and using a similar method to that of Crocco, tackled the same problem with various wall conditions. They found that as the Mach number increased the discrepancy between results calculated with $\sigma = 1$ and $\sigma = 0.70$ increased.

In a recent paper Illingworth [27] found a solution for flow past a flat plate against a linear adverse pressure under differing conditions of temperature and Mach number by fitting various functions of $y/\delta$ as solutions for $u$.

Brainerd and Emmons [28] and Cope and Hartree [7] numerically solved the problems with the aid of computing machinery, in each case the changes being rung on the values of $\omega$ and $\sigma$. Another numerical approach to the same problem is that of Gadd [29] using a step-by-step method. Flugge Lotz [30] put forward the first finite difference approach to the problem, and more recently a further finite difference solution was given by Siekmann [31] in a doctoral thesis.

The above is a brief sketch of some of the work carried out in this field, sufficient to show the great concentration of effort devoted to the subject. No mention has yet been made of the Von Mises transformation which, since it forms the basis of the work done in this thesis, is considered in more detail in the next part of the introduction.

# THE VON MISES TRANSFORMATION.

The differential equations governing boundary layer flow can be given in several different forms, depending on the variables used, each form of the equations having its own advantages and disadvantages. For several reasons we have chosen to use the form of equations first discovered by Von Mises [32] in 1927.

The Prandtl boundary layer equations for two dimensional, steady, incompressible flow were shown in (1 A) to be

$$u \frac{\partial u}{\partial x} + v \frac{\partial u}{\partial y} = u_1 \frac{du_1}{dx} + \nu \frac{\partial^2 u}{\partial y^2} , \qquad (1,17)$$

$$\frac{\partial p}{\partial y} = 0, \qquad (1,18)$$

$$\frac{\partial u}{\partial x} + \frac{\partial v}{\partial y} = 0. \qquad (1,19)$$

Equation (1,19) tells us of the existence of a stream function $\psi$ such that

$$u = \frac{\partial \psi}{\partial y} , \quad v = - \frac{\partial \psi}{\partial x} . \qquad (1,20)$$

After the method of Von Mises we change the independent variables from $x$ and $y$ to $x$ and $\psi$, such a change being governed by the following transformation formulae.

$$\left(\frac{\partial u}{\partial x}\right)_y = \left(\frac{\partial u}{\partial x}\right)_\psi + \left(\frac{\partial u}{\partial \psi}\right)_x \left(\frac{\partial \psi}{\partial x}\right)_y = \left(\frac{\partial u}{\partial x}\right)_\psi - v \left(\frac{\partial u}{\partial \psi}\right)_x ,$$

$$\left(\frac{\partial u}{\partial y}\right)_x = \left(\frac{\partial u}{\partial \psi}\right)_x \left(\frac{\partial \psi}{\partial y}\right)_x = u \left(\frac{\partial u}{\partial \psi}\right)_x ,$$

$$\left(\frac{\partial^2 u}{\partial y^2}\right)_x = \left(u \frac{\partial}{\partial \psi} \left[u \frac{\partial u}{\partial \psi}\right]\right)_x ,$$

where $\left(\frac{\partial u}{\partial x}\right)_y$ represents the partial derivative of u with respect to x; y being kept constant.

Using the above formulae equation (1,17) becomes

$$u \frac{\partial u}{\partial x} = u_1 \frac{du_1}{dx} + \nu u \frac{\partial}{\partial \psi}\left(u \frac{\partial u}{\partial \psi}\right),$$

or, since $u_1$ is a function of $x$ only

$$\frac{\partial}{\partial x}(u_1^2 - u^2) = \nu u \frac{\partial^2}{\partial \psi^2}(u_1^2 - u^2).$$

Writing $z = u_1^2 - u^2$ we arrive at the Von Mises equation for incompressible flow,

$$\frac{\partial z}{\partial x} = \nu\sqrt{u_1^2 - z}\;\frac{\partial^2 z}{\partial \psi^2} . \qquad (1,21)$$

Equation (1,19) moreover is identically satisfied so that the flow in an incompressible boundary layer is completely specified by (1,21). This equation is much more adaptable to a finite difference method of solution than (1,17) and (1,19). In the subsequent numerical work we shall use the Von Mises boundary layer equation.

Turning our attention now to the case of steady, two dimensional, compressible boundary layer flow, we have shown in (1 A) that the equations of momentum, energy and continuity (1,16) are

$$\rho u \frac{\partial u}{\partial x} + \rho v \frac{\partial u}{\partial y} = \rho_1 u_1 \frac{du_1}{dx} + \frac{\partial}{\partial y}\left(\mu \frac{\partial u}{\partial y}\right), \tag{1,22}$$

$$\frac{\partial p}{\partial y} = 0, \tag{1,23}$$

$$\rho u \frac{\partial i}{\partial x} + \rho v \frac{\partial i}{\partial y} = -\rho_1 u_1 \frac{du_1}{dx} u + \frac{\partial}{\partial y}\left(\frac{\mu}{\sigma}\frac{\partial i}{\partial y}\right) + \mu\left(\frac{\partial u}{\partial y}\right)^2, \tag{1,24}$$

$$\frac{\partial \rho u}{\partial x} + \frac{\partial \rho v}{\partial y} = 0. \tag{1,25}$$

Equation (1,25) yields a stream function $\psi$ such that

$$\rho u = \frac{\partial \psi}{\partial y} \;;\; \rho v = -\frac{\partial \psi}{\partial x}.$$

As before we change the independent variables from $x$ and $y$ to $x$ and $\psi$, in terms of which (1,22) and (1,24) become,

$$\rho u \frac{\partial u}{\partial x} = \rho_1 u_1 \frac{du_1}{dx} + \rho u \frac{\partial}{\partial \psi}\left(\rho \mu u \frac{\partial u}{\partial \psi}\right), \tag{1,26}$$

$$\rho u \frac{\partial i}{\partial x} = -\rho_1 u_1 \frac{du_1}{dx} u + \rho u \frac{\partial}{\partial \psi}\left(\frac{\mu}{\sigma}\rho u \frac{\partial i}{\partial \psi}\right) + \mu \rho^2 u^2 \left(\frac{\partial u}{\partial \psi}\right)^2. \tag{1,27}$$

If however, as was explained in (1 A), we assume that our fluid is a perfect gas we have,

$$\frac{p}{\rho T} = R = c_p - c_v,$$

$$\text{thus} \quad \frac{p}{\rho} = c_p T\left(1 - \frac{cv}{cp}\right) = i\left(1 - \frac{1}{\gamma}\right),$$

$$\text{and so} \quad \rho = \frac{\gamma}{\gamma - 1}\frac{p}{i}, \quad \rho_1 = \frac{\gamma}{\gamma - 1}\frac{p}{i_1}$$

and since from equation (1,23) $p$ is a function of $x$ alone we can substitute for $\rho$ in (1,26) and (1,27) and obtain

$$\frac{\partial q}{\partial x} = \left[\frac{1}{i_1}\frac{dq_1}{dx}\right] i + \left[\frac{\gamma p}{\gamma - 1}\right] q^{\frac{1}{2}} \frac{\partial}{\partial \psi}\left(\frac{\mu}{i}\frac{\partial q}{\partial \psi}\right), \tag{1,28}$$

$$\frac{\partial i}{\partial x} = -\left[\frac{1}{2i_1}\frac{dq_1}{dx}\right] i + \left[\frac{\gamma p}{\sigma(\gamma-1)}\right]\frac{\partial}{\partial\psi}\left(\frac{\mu q^{\frac{1}{2}}}{i}\frac{\partial i}{\partial\psi}\right) + \left[\frac{\gamma p}{4(\gamma-1)}\right]\frac{\mu}{i q^{\frac{1}{2}}}\left(\frac{\partial q}{\partial\psi}\right)^2 \quad (1,29)$$

where $q = u^2$ and the quantities in square brackets are functions of $x$ alone.

Equations (1,28) and (1,29) will be the governing equations in all subsequent calculations on compressible boundary layers.

We shall now give a summary of the history of the Von Mises equations. In 1939 Prandtl [16] suggested that the Von Mises equation might be used as the basis of a step-by-step finite difference technique to solve the problem of incompressible flow past a semi-infinite flat plate with a linear adverse pressure gradient. Görtler [17] pointed out that since the velocity is zero on the plate it follows from (1,21) that $\left(\frac{\partial^2 z}{\partial\psi^2}\right)_0$ must be infinite and for this reason he abandoned the method as a possible means of solving the problem. This singularity has discouraged most authors from considering the Von Mises equation as a means of solving either incompressible, or compressible boundary layer equations.

Luckert [33] however, was able to use the Von Mises equation for incompressible flow to evaluate the velocity in the wake of a finite flat plate placed parallel to the stream, since in this case the velocity is nowhere zero and consequently $\frac{\partial^2 z}{\partial\psi^2}$ remains finite in the field.

Von Karman and C.B. Millikan [34] used the Von Mises equation in their method of inner and outer solutions of the incompressible flow past a flat plate with a linear adverse pressure gradient. They found the separation point at $x_{\rho} = .102$ which we may compare with the presently accepted result of $x_{\rho} = .1198$ calculated by Leigh [21] in 1955.

The first application of the Von Mises equations for solving compressible flow problems was an iterative method of solution of the flow past a flat plate with no pressure gradient and with the assumptions $\sigma = 1$ and $\mu = aT^{0.76}$. This piece of work was carried out by Von Karman and Tsien [35] in 1938 and was extended later to flow past various cylindrical profiles by Illingworth [36] in 1949.

In this thesis we hope to show that both in compressible and incompressible flow, the Von Mises form of the equations provides an excellent basis for an easy and relatively speedy numerical solution of problems in boundary layer flow, the chief difficulty being a relatively large amount of simple numerical computation. It should be pointed out that the method which we shall describe, is primarily intended for compressible flow calculations. From our solutions, it is hoped to check the accuracy of simplifying assumptions which have been made by other authors in previous calculations.

Since the method is much less elaborate when applied to incompressible flow problems it has been so employed in the first place in order to examine inherent difficulties of the transformation as well as a means of solution in itself.

FINITE DIFFERENCE SOLUTION OF PARABOLIC DIFFERENTIAL EQUATIONS.

As seen in the previous section, the boundary layer equations in which we are interested are non linear parabolic differential equations, the highest derivative in the x-direction being of the first order and in the $\psi$ direction of the second order. The method of solution used in this thesis is the method of finite differences and before attempting any specific solution it seems advisable to sketch the technique as applied to the simplest of parabolic differential equations, viz. the equation of heat conduction,

$$\frac{\partial z}{\partial x} = \frac{\partial^2 z}{\partial y^2} . \qquad (1,30)$$

The equation is to be solved inside a "horseshoe" boundary on which the values of $z$ are known, the field of computation is shown in figure (1,4).

The area inside the "horseshoe" is covered by a rectangular mesh with the nodal points labelled (j,k), the mesh length in the x direction being $\Delta x$ and in the y-direction $\Delta y$. If the starting position in the x-direction is $x = x_o$ and in the y-direction $y = y_o$ then the point labelled (j,k) corresponds to the point with co-ordinates $x = x_o + j\Delta x, \quad y = y_o + k\Delta y$.

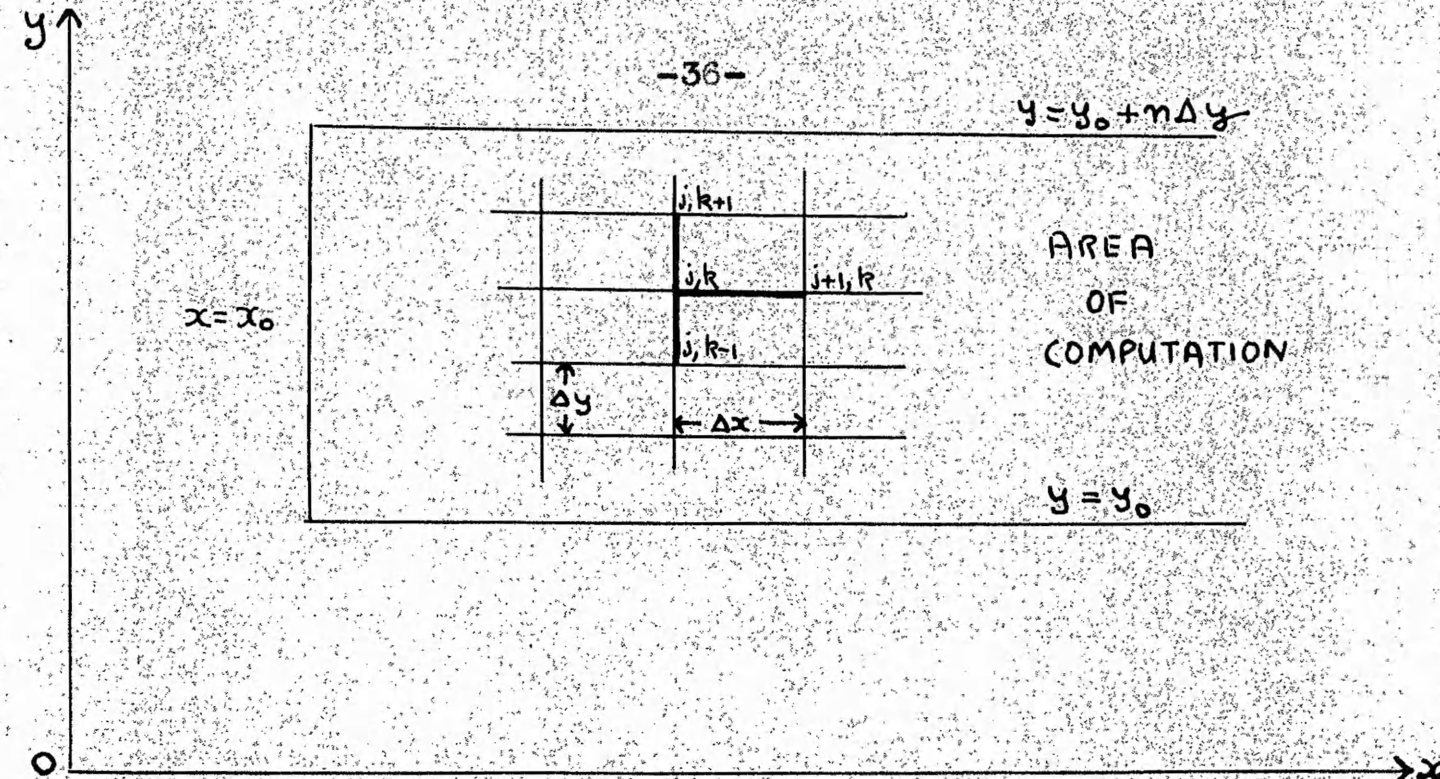


FIGURE (1,4)

We express the function $z(x + \Delta x, y)$ in terms of $z(x,y)$ and the partial derivatives of $z(x,y)$ with respect to x, using Taylor's series in the form

$$z(x + \Delta x, y) = z(x,y) + \Delta x \frac{\partial}{\partial x} z(x,y) + \frac{(\Delta x)^2}{2!} \frac{\partial^2}{\partial x^2} z(x,y) + \cdots\cdots$$

If we neglect terms of greater order than the first in $\Delta x$ we can represent $\frac{\partial z}{\partial x}$ approximately by,

$$\frac{\partial z}{\partial x} \doteq \frac{z(x + \Delta x, y) - z(x,y)}{\Delta x},$$

In a similar fashion we approximate $\frac{\partial^2 z}{\partial y^2}$ by

$$\frac{\partial^2 z}{\partial y^2} \doteq \frac{z(x, y + \Delta y) - 2 z(x,y) + z(x, y - \Delta y)}{(\Delta y)^2},$$

this formula being accurate to $(\Delta y)^3$.

If now the point $(x,y)$ corresponds to the node $(j,k)$ and we represent $z(x,y)$ by $z_{j,k}$ the above replacements can be written as

$$\left(\frac{\partial z}{\partial x}\right)_{j,k} \doteq \frac{z_{j+1,k} - z_{j,k}}{\Delta x} ; \left(\frac{\partial^2 z}{\partial y^2}\right)_{j,k} \doteq \frac{z_{j,k+1} - 2z_{j,k} + z_{j,k-1}}{(\Delta y)^2} . \tag{1,31}$$

Substituting these approximations in (1,30) we obtain,

$$z_{j+1,k} = z_{j,k} + \delta \left(z_{j,k+1} - 2z_{j,k} + z_{j,k-1}\right) , \tag{1,32}$$

where $\delta = \Delta x/(\Delta y)^2$ is the mesh ratio.

Equation (1,32) is the four point forward finite difference replacement of (1,30). There are other replacements which can be used but the one above is the simplest minimum order replacement.

We now suppose that we have reached a stage in the calculation where values of $z$ are known at all the nodes on the $j$-line and we wish to calculate the values of $z$ on the $(j+1)$ line, using the equation (1,32).

The value of $z$ at $(j+1,0)$ is known from the boundary conditions, the value at $(j+1,1)$ is obtained using (1,32) and the values at $(j,0)$, $(j,1)$ and $(j,2)$. Continuing in this way we evaluate $z$ at all points on the $(j+1)$ line, the final value at $(j+1,n)$ being given by the boundary conditions. The next step is to evaluate $z$ on the $(j+2)$ line and so on. Eventually we cover the area of computation in a step-by-step fashion.

We must now try to estimate how near the solution we have obtained is to the proper solution of (1,30). At any node (j,k) there are three associated values, $Z_{j,k}$ the correct solution of the differential equation (1,30), $z_{j,k}$ the correct solution of the difference equation (1,32) and $\eta_{j,k}$ the numerical solution we have obtained, $\eta_{j,k}$ being a number rounded off after a prescribed number of decimal places.

In any calculation there are two different types of error involved, the difference between $z_{j,k}$ and $Z_{j,k}$ and the difference between $\eta_{j,k}$ and $z_{j,k}$. The vanishing or otherwise of the former error as the mesh size is reduced is the problem of convergence. This error will not be considered in the thesis. It will be assumed that this error is small for the mesh lengths used and it is also known that this error is of comparable magnitude over the entire field of calculation.

Considerations of the error in $\eta_{j,k}$ (as compared with $z_{j,k}$) is the problem of stability. This problem is much more important in a step-by-step calculation as is demonstrated below.

Rounding off errors occur at every stage and it may happen that when these errors are transmitted to the next stage by (1,32), they increase. In this case the procedure is said to be unstable, whilst if the errors do not grow the procedure is said to be stable. Errors in any unstable difference solution can become so large that the calculated values obtained bear no resemblance to the true solution.

In the manner of O'Brien, Hyman and Kaplan [37] we discuss the stability of (1,32). Suppose that for all $j$ and $k$ $\eta_{j,k}$ can be expressed as $\eta_{j,k} = z_{j,k} + \epsilon_{j,k}$, where $\epsilon_{j,k}$ is small. From (1,32) we obtain

$$\eta_{j+1,k} = \eta_{j,k} + \delta\,(\eta_{j,k+1} - 2\eta_{j,k} + \eta_{j,k-1}),$$

and if we assume that $\eta_{j+1,k} = z_{j+1,k} + \epsilon_{j+1,k}$ we obtain

$$z_{j+1,k} + \epsilon_{j+1,k} = z_{j,k} + \epsilon_{j,k} + \delta(z_{j,k+1} - 2z_{j,k} + z_{j,k-1})$$
$$+ \delta(\epsilon_{j,k+1} - 2\,\epsilon_{j,k} + \epsilon_{j,k-1}). \qquad (1,33)$$

Since $z_{j,k}$ is the true solution of (1,32) we can simplify (1,33) and obtain the error equation,

$$\epsilon_{j+1,k} = \epsilon_{j,k} + \delta\,(\epsilon_{j,k+1} - 2\epsilon_{j,k} + \epsilon_{j,k-1}). \qquad (1,34)$$

It is now assumed that $\epsilon_{j,k}$ can be expressed as a series of the form

$$\epsilon_{j,k} = \sum_m A_m\, e^{\alpha_m j\Delta x}\, e^{i\beta_m k\Delta y},$$

where $\alpha_m = a_m + ib_m$, $\beta_m$ is real and $i^2 = -1$.

The above form for $\epsilon_{j,k}$ is chosen because as $j$ increases, that is as the calculation proceeds, the modulus of the error can increase or decrease. The condition for stability is that the modulus does not increase.

Since the error equation (1,34) is linear we need only consider one term in the expansion and in fact we may choose $\epsilon_{j,k} = Ae^{\alpha j\Delta x}\, e^{i\beta k\Delta y}$ where $\alpha = a + ib$, $\beta$ is real.

The modulus of this number is $|A|(e^{a\Delta x})^j$ . As $j$ increases we require this modulus not to increase and so our condition for stability is

$$\left| e^{a\Delta x} \right| \leq 1. \tag{1,35}$$

Substituting $A e^{aj\Delta x} \; e^{i\beta k\Delta y}$ for $\epsilon_{j,k}$ in (1,34) and simplifying we arrive at the result

$$e^{a\Delta x} = 1 + \delta \, (e^{i\beta\Delta y} - 2 + e^{-i\beta\Delta y}),$$

$$= 1 - 4\, \delta \sin^2 \frac{\beta\Delta y}{2} .$$

Taking the modulus of both sides we obtain

$$\left| e^{aj\Delta x} \right| = \pm \left(1 - 4\delta \sin^2 \frac{\beta\Delta y}{2}\right),$$

and so our stability condition becomes

$$-1 \leq 1 - 4\,\delta \sin^2 \frac{\beta\Delta y}{2} \leq 1. \tag{1,36}$$

The upper condition is satisfied automatically since $\delta \geq 0$ and the lower condition becomes,

$$\delta \sin^2 \frac{\beta\Delta y}{2} \leq \tfrac{1}{2} .$$

For stability this must be satisfied for all $\beta$ in the range $0 \leq \beta \leq 2\pi$. Thus the condition for stability is

$$\delta \leq \tfrac{1}{2} \tag{1,37}$$

We have thus demonstrated that if (1,37) is satisfied our difference equation is stable and the results obtained in the calculation will be an accurate representation of the solution of (1,30).

The technique described above will be used in our solution of boundary layer problems.

SUMMARY.

Before going on to describe the actual calculations carried out in this thesis, it is adviseable to assess the situation by giving some of the motives which prompted the research carried out in this thesis.

(a) The method developed can be applied equally to incompressible and compressible flow problems, and so direct comparison can be made between the calculated flow fields.

(b) The Von Mises form is by far the simplest of the forms of the boundary layer equations. This can be more readily appreciated in the incompressible case where the flow is governed by a single equation of a relatively simple form. Because of the simplicity of the governing equations they are more readily adapted to numerical methods of solution.

(c) As in most numerical techniques the limitation on accuracy is governed by the minimum mesh size possible, which in turn is governed by the time available. Modern high speed computing machines eliminate this difficulty to a large extent and it is hoped, at a later date, to make use of such machines to exploit the method more fully.

(d) In the light of numerical methods the problem is interesting in that we are confronted with an equation which has an inherent instability over a section of the field. A method of overcoming this difficulty will be demonstrated in the section on incompressible flow.

(e) Since the technique is numerical it can be used when the boundary conditions are derived from experimental data.

(f) Perhaps the most significant discovery in this thesis concerns the use of the Von Mises transformation. Although the Von Mises equations have a simple form, Prandtl [16] pointed out that they could not be used in numerical techniques because of the singularity of the equations at the plate as mentioned in (I B). In this thesis it is hoped to show that the difficulty of this singularity can be overcome in a numerical calculation, and so the major objection to the use of the Von Mises equations is eliminated.

# SECTION II.

## INCOMPRESSIBLE BOUNDARY LAYER.

## 2 A

## GOVERNING DIFFERENTIAL EQUATIONS AND BOUNDARY CONDITIONS.

The problem which we are attempting is the evaluation of the velocity at all points in the two-dimensional, steady, incompressible boundary layer on a semi-infinite flat plate placed parallel to the stream. Two types of flow will be considered, the first, in section (2 B), in which no extraneous pressure gradient is present and the second, in section (2 C), in which the fluid is subjected to a linear adverse pressure gradient.

In terms of the variables $x$ and $\psi$, we consider the plate to be lying along the x-axis $x \geq 0$, and the fluid to be approaching the plate with a constant velocity $U$, in the positive x-direction. This is illustrated in figure (2,1).

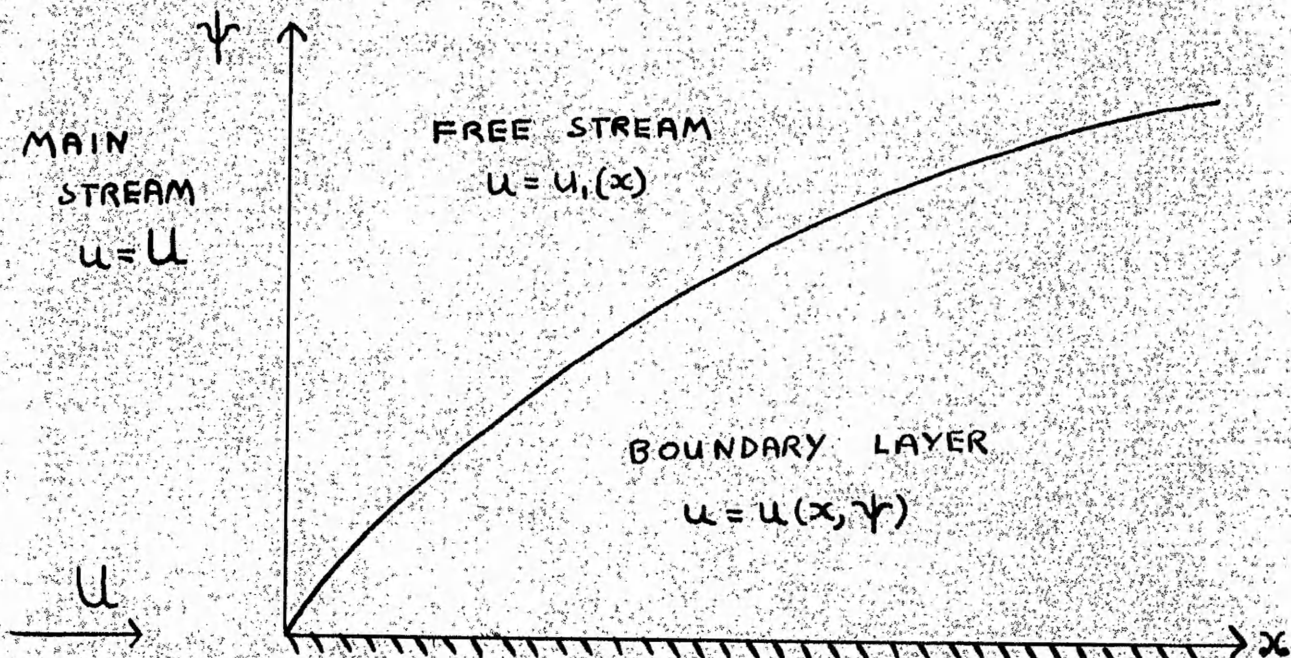


FIGURE (2,1)

As was shown in (1 A) the outer edge of the boundary layer is defined to be the locus of points at which, to the degree of accuracy required, $\frac{\partial u}{\partial y} \doteq 0$. In the $(x, \psi)$ plane this curve which divides the boundary layer from the free stream is given as the locus of points at which $\frac{\partial u}{\partial \psi} \doteq 0$ or $\frac{\partial z}{\partial \psi} \doteq 0$, to the required degree of accuracy.

The line of separation of the boundary layer from the free stream is not known until the calculation has been completed but for demonstration purposes it is drawn in Figure (2,1).

In (1,B) we have shown that for incompressible boundary layer flow the governing equation, in terms of $x$ and $\psi$, is

$$\frac{\partial z}{\partial x} = \nu\sqrt{u_1^2 - z} \quad \frac{\partial^2 z}{\partial \psi^2}, \tag{2,1}$$

where $z = (u_1^2 - u^2)$ and $u_1 = u_1(x)$ is the free stream velocity.

Equation (2,1) is a non linear parabolic differential equation and as such, for a unique solution we must specify one boundary condition in the x-direction and two boundary conditions in the $\psi$ direction.

On the plate, that is on the line $\psi = 0$, $x \geq 0$, the velocity $u$ vanishes, by the property of a viscous fluid of no slip on a wall. In the free stream, that is when $\frac{\partial z}{\partial \psi} \doteq 0$ we have $u = u_1(x)$. If we now suppose that $z$ is specified as a function of $\psi$ at some station $x = x_0$

we have the following set of boundary conditions.

$$\begin{aligned} &\text{(i)} \quad z = u_1^2 \quad \text{when} \quad \psi = 0, \\ &\text{(ii)} \quad z = 0 \quad \text{when} \quad \frac{\partial z}{\partial \psi} \doteq 0, \\ &\text{(iii)} \quad z = z\,(x_0, \psi) \text{ when } x = x_0. \end{aligned} \tag{2,2}$$

Knowing the values of $z$ on this "horseshoe" boundary our problem is to evaluate $z$ in its interior.

The first problem to be tackled is that in which the pressure is a constant in the free stream, and as seen from (1,13) the free stream velocity is also a constant $u_1(x) = U$.

In this case the equation (2,1) can be expressed more simply in the form

$$\frac{\partial u}{\partial x} = \frac{1}{2} \nu \frac{\partial^2 u^2}{\partial \psi^2}, \tag{2,3}$$

subject to the following set of boundary conditions,

$$\begin{aligned} &\text{(i)} \; u = 0 \text{ when } \psi = 0, \\ &\text{(ii)} \; u = U \text{ when } \frac{\partial u}{\partial \psi} \doteq 0, \\ &\text{(iii)} \; u = u\,(x_0, \psi) \text{ when } x = x_0. \end{aligned} \tag{2,4}$$

Section (2 B) is concerned with a numerical solution of (2,3) subject to (2,4).

FLOW ALONG A FLAT PLATE WITH CONSTANT PRESSURE.

This, the first problem, is intended as a prototype calculation in which the method is tested as a means of solution and a plan of computation is laid down.

Governing equations in non dimensional form.

In this problem in which the free stream velocity is of constant magnitude and the plate is infinite in extent there is no characteristic length. However, in order to conform with subsequent work we shall denote the characteristic length by L (although no characteristic length apart from $U/\nu$ exists in the problem) and non dimensionalise the equations in terms of a general Reynolds number R. We choose as the characteristic velocity U, the main or initial stream velocity.

Consider the non-dimensional variables

$$x' = x/L, \quad u' = u/U, \quad \psi' = \psi/\Psi ,$$

where $\Psi$, the characteristic stream function, has to be determined. Substituting for x,u and $\psi$ in (2,3) we obtain,

$$\frac{\partial u'}{\partial x'} = \tfrac{1}{2} \frac{\partial^2 u'^2}{\partial \psi'^2} \quad \frac{U L \nu}{\Psi^2} ,$$

for convenience we choose

$$\Psi = \frac{UL}{\sqrt{R}} ,$$

and with the above choice of $\Psi$ the resulting equation is

$$\frac{\partial u'}{\partial x'} = \tfrac{1}{2} \; \frac{\partial^2 u'^2}{\partial \psi'^2} \; .$$

The boundary condition $u = U$ becomes $u' = 1$, whilst the other two boundary conditions remain the same in terms of the dashed variables.

We shall now drop the dashes for convenience to produce the differential equation in its final form

$$\frac{\partial u}{\partial x} = \tfrac{1}{2} \; \frac{\partial^2 u^2}{\partial \psi^2} \; , \qquad (2,5)$$

subject to the boundary conditions,

$$\begin{aligned} &(i)\ u = 0 \quad \text{when} \quad \psi = 0, \\ &(ii)\ u = 1 \quad \text{when} \quad \frac{\partial u}{\partial \psi} = 0, \qquad\qquad (2,6) \\ &(iii)\ u = u(x_o, \psi) \quad \text{when}\ x = x_o. \end{aligned}$$

All the variables in (2,5) and (2,6) are non dimensional. We now form a finite difference replacement of (2,5) in the manner of (1 C).

Finite difference replacement of (2,5).

As discussed in (1 C) the $(x, \psi)$ field is divided by a square net with nodal points labelled $(j,k)$, the value of velocity at such a node being denoted by $u_{j,k}$. The mesh length in the x-direction is $\Delta x$ and in the $\psi$-direction is $\Delta \psi$, and so if the calculation is started at $x = x_o$ the node $(j,k)$ corresponds to the point $(x_o + j\Delta x,\ k\Delta\psi)$ and $u_{j,k} \equiv u\ (x_o + j\Delta x,\ k\Delta\psi)$.

As in (1 0) we make the following approximations,

$$\frac{\partial u}{\partial x} \doteq \frac{u_{j+1,k} - u_{j,k}}{\Delta x}, \quad \frac{\partial^2 u^2}{\partial \psi^2} \doteq \frac{u^2_{j,k+1} - 2u^2_{j,k} + u^2_{j,k-1}}{(\Delta\psi)^2},$$

by means of which (2,5) can be replaced by the difference equation

$$u_{j+1,k} = u_{j,k} + {}^{\delta}/_{2} \ (u^2_{j,k+1} - 2u^2_{j,k} + u^2_{j,k-1}), \quad (2,7)$$

where $\delta = \Delta x/(\Delta\psi)^2$ is the mesh ratio.

The boundary conditions are now given as

(i) $u_{j,o} = 0$ for all j,

(ii) $u_{j,k} = 1$ when $u_{j,k+1} \doteq u_{j,k}$ for all j and k,

(iii) $u_{o,k}$ known for all k.

Equation (2,7) is the four point forward difference replacement of (2,5) so called because it makes use of the four points, (j,k+1), (j,k-1), (j,k) and (j+1,k) as demonstrated below.

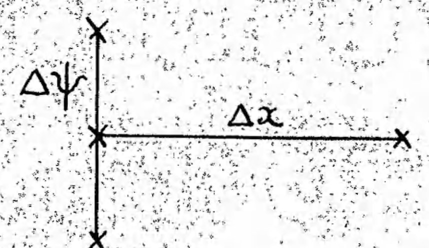


From equation (2,7) it is readily seen that if the velocity is known at all nodes on the line j then the velocity at each of the nodes (j+1,k) can be calculated in turn. Using (2,7) and the boundary conditions, we can thus cover the boundary layer in a step-by-step manner.

Before proceeding to describe the actual computation we must first discuss the stability of the difference equation.

Stability of the finite difference equation (2,7).

We shall now examine the stability of (2,7) using the method outlined in (1 C). Associated with the difference equation,

$$u_{j+1,k} = u_{j,k} + \delta/2\,[u^2_{j,k+1} + u^2_{j,k-1} - 2u^2_{j,k}], \quad (2,7)$$

is the equation

$$u_{j+1,k} + \varepsilon_{j,k} = u_{j,k} + \delta/2\,[(u_{j,k+1} + \varepsilon_{j,k+1})^2$$

$$- 2(u_{j,k} + \varepsilon_{j,k})^2 + (u_{j,k-1} + \varepsilon_{j,k-1})^2\,],$$

where at any node $(j,k)$, $\varepsilon_{j,k}$ represents the small error in the calculated value of $u_{j,k}$, this error arising from rounding off after so many decimal places.

Rewriting the above equation and neglecting powers of $\varepsilon_{j,k}$ higher than the first we arrive at the following linear error equation,

$$\varepsilon_{j+1,k} = \varepsilon_{j,k} + \delta(u_{j,k+1}\varepsilon_{j,k+1} - 2u_{j,k}\varepsilon_{j,k} + u_{j,k-1}\varepsilon_{j,k-1}). \quad (2,8)$$

As described in (1 C) we assume that we can express $\varepsilon_{j,k}$ in the form $\varepsilon_{j,k} = Ae^{\alpha j\Delta x}e^{\beta k\Delta\psi}$ where $\alpha = a + ib$ and $\beta$ is real. Substituting this value of $\varepsilon_{j,k}$ in (2,8) we obtain

$$Ae^{\alpha(j+1)\Delta x}e^{i\beta k\Delta\psi} = Ae^{\alpha j\Delta x}e^{i\beta k\Delta\psi} + \delta[u_{j,k+1}Ae^{\alpha j\Delta x}e^{i\beta(k+1)\Delta\psi}$$

$$- 2u_{j,k}\,Ae^{\alpha j\Delta x}e^{i\beta k\Delta\psi} + u_{j,k-1}\,Ae^{\alpha j\Delta x}\,e^{i\beta(k-1)\Delta\psi},$$

which simplifies to

$$e^{\alpha\Delta x} = 1 + \delta\,(u_{j,k+1}\, e^{i\beta\Delta\psi} - 2u_{j,k} + u_{j,k-1}\, e^{-i\beta\Delta\psi}). \quad (2,9)$$

According to (1 C) the condition that the difference equation is stable, that is, that any errors introduced do not grow as the caluulation proceeds, is that

$$|e^{\alpha\Delta x}| \leq 1 \quad .$$

From (2,9), writing $h = \Delta\psi$

$$|e^{\alpha\Delta x}|^2 = [1 + \delta\,(u_{j,k+1}\cos\beta h - 2u_{j,k} + u_{j,k-1}\cos\beta h)]^2 + \delta^2\,(u_{j,k+1} - u_{j,k-1})^2 \sin^2\beta h,$$

and so the condition for stability is obtained, viz.

$$0 \leq \delta \leq 2\,[-(u_{j,k+1} - 2u_{j,k} + u_{j,k-1}) + 2\sin^2\frac{\beta h}{2}(u_{j,k+1} + u_{j,k-1})] \left\{[(u_{j,k+1} - 2u_{j,k} + u_{j,k-1}) - 2\sin^2\frac{\beta h}{2}(u_{j,k+1} + u_{j,k-1})]^2 + 4\sin^2\frac{\beta h}{2}(1 - \sin^2\frac{\beta h}{2})(u_{j,k+1} - u_{j,k-1})^2\right\}^{-1}. \quad (2,10)$$

If we now write

$$w = \sin^2\frac{\beta h}{2}\,, \quad 0 \leq \omega \leq 1\,,$$

$$B = u_{j,k+1} - 2u_{j,k} + u_{j,k-1}\,,$$

$$C = u_{j,k+1} + u_{j,k-1}\,,$$

$$D = u_{j,k+1} - u_{j,k-1}\,,$$

the condition (2,10) is simplified to,

$$0 < \delta \leq \frac{2(-B + 2\omega C)}{(B - 2\omega C)^2 + 4\omega(1-\omega)D^2} = F \quad (2,11).$$

A necessary condition arising from (2,11) is that $F \geq 0$, in other words

$$B < 2\omega C,$$

or

$$u_{j,k+1} - 2u_{j,k} + u_{j,k-1} < \sin^2 \frac{\beta h}{2} (u_{j,k+1} + u_{j,k-1}).$$

The above condition must be satisfied for all values of $\beta$ in the range $0 \leq \beta < 2\pi$ and in particular for the worst value of $\beta$, in this case $\beta = 0$, which provides us with,

$$u_{j,k+1} - 2u_{j,k} + u_{j,k-1} < 0. \quad (2,12)$$

If (2,12) is satisfied then the previous condition is certainly satisfied for all values of $\beta$.

Returning now to the condition $\delta \leq F$. For stability this must be satisfied at all nodes in the field and for all values of $\beta$. To attempt such an examination of stability would be extremely laborious and in order to overcome this we establish a lower bound for $F$.

To find a lower bound for $F = \dfrac{2}{-B + 2\omega C + \dfrac{4\omega(1-\omega)D^2}{-B + 2C\omega}}$,

we need only find an upper bound for the denominator

$$-B + 2\omega C + \frac{4\omega(1-\omega)D^2}{-B + 2\omega C} \leq -B + 2\omega C + 2(1-\omega)\frac{D^2}{C},$$

$$= -B + 2C\omega + \frac{2}{C}(1-\omega)(C^2 - 4u_{j,k+1} \cdot u_{j,k-1}),$$

$$= -B + 2C\omega + 2C(1-\omega),$$

$$= - B + 2C,$$

$$= u_{j,k+1} + 2u_{j,k} + u_{j,k-1},$$

$$\leq 4,$$

Thus a lower bound for $F$ is $\frac{1}{4}$ and if we choose

$$\delta \leq \tfrac{1}{2}, \tag{2,13}$$

and

$$u_{j,k+1} - 2u_{j,k} + u_{j,k-1} < 0, \tag{2,12}$$

the stability condition (2,10) is satisfied at all points in the field for all values of $\beta$.

The condition (2,12) is inherent in the differential equation as will now be demonstrated. Suppose that by suitably adjusting the boundary condition at $x = x_0$ we find a solution of (2,6) in the form $u + \varepsilon$ where $u$ is the solution compatible with the original boundary condition. We thus have

$$\frac{\partial}{\partial x}(u + \varepsilon) = \frac{1}{2}\,\frac{\partial^2}{\partial\psi^2}(u + \varepsilon)^2 ,$$

and if we choose $\varepsilon$ to be sufficiently small this will reduce to

$$\frac{\partial\varepsilon}{\partial x} = u\,\frac{\partial^2\varepsilon}{\partial\psi^2} + 2\,\frac{\partial u}{\partial\psi}\,\frac{\partial\varepsilon}{\partial\psi} + \varepsilon\,\frac{\partial^2 u}{\partial\psi^2} .$$

We now assume that $\varepsilon = Ae^{\alpha x}\, e^{i\beta\psi}$, a form corresponding to that of the function in the difference equation.

Substituting for $s$ we arrive at the result

$$\alpha = -u\beta^2 + 2i\beta + \frac{\partial^2 u}{\partial\psi^2},$$

and so $a = Rl\alpha = -u\beta^2 + \dfrac{\partial^2 u}{\partial\psi^2}$ .

The condition that $s$ does not increase as $x$ increases leads to the result

$$|e^{\alpha}| \leq 1 \text{ or } e^{a} \leq 1 \text{ or } a \leq 0.$$

Using the calculated value of $a$ this condition can be written as,

$$-u\beta^2 + \frac{\partial^2 u}{\partial\psi^2} \leq 0.$$

This condition is true for all values of $\beta$ if

$$\frac{\partial^2 u}{\partial\psi^2} \leq 0. \qquad (2,14)$$

It is readily seen that (2,12) is the finite difference replacement of (2,14).

Although the analysis used to derive (2,14) is not strictly accurate it does show that the condition (2,12) is inherent in the differential equation and so in any difference replacement of the same order as the differential equation.

It should also be pointed out at this stage that although the condition (2,13) can always be satisfied by a suitable choice of mesh ratio the condition (2,12) is entirely out of our control. At any node (j,k) the condition (2,12) is either satisfied or not satisfied and we can do nothing to alter this fact.

To sum up we may say that in order that our solution of the difference equation (2,7) will adequately represent the required solution we must ensure that the following two conditions are satisfied.

$$\text{(i)} \quad u_{j,k+1} - 2u_{j,k} + u_{j,k-1} \leqq 0,$$

$$\text{(ii)} \qquad \delta \leq \tfrac{1}{2}\,.$$

Bearing the above restrictions in mind we shall now proceed to the first numerical calculation.

Numerical calculation of the velocity in the boundary layer.

We have shown that the numerical calculation will be a simple step-by-step technique in which the values of $u$ at nodes on the line $x = x_o + (j+1)\Delta x$ can be found from the values of $u$ at nodes on the line $x = x_o + j\Delta x$. In order to start the calculation we must therefore specify the velocity at some station $x = x_o$.

In 1934 Howarth found expressions for the velocity in the problem we are at present considering, the results can be found in [1] page 107. In his solution he expands the velocity $u$ and stream function $\psi$ in terms of the variable $\eta = \dfrac{y}{\sqrt{x}}$. From the results of Howarth we tabulate $u$ and $\psi$ in terms of $\eta$ at the station $x_o = .0025$, and from this tabulation we extract the values of $u$ at $\psi$ nodes on this line.

In the present calculation we choose $x = .001$, $\psi = .05$ and thus $\delta = .4$, ensuring that the stability condition (2,13) is satisfied. The specific equation to be used in this calculation is (2,7) with $\delta = .4$, namely

$$u_{j+1,k} = u_{j,k} + .2\,(u^2_{j,k+1} - 2u^2_{j,k} + u^2_{j,k-1}). \qquad (2,15)$$

As in later examples the actual numerical computation was carried out as efficiently as possible on a desk calculating machine, the routine of operations is given in Programme (1).

| OPERATION $u_{j+1,k} = u_{j,k} + .2\,(u^2_{j,k+1} - 2u^2_{j,k} + u^2_{j,k-1})$ | | | |
|---|---|---|---|
| $(1)_k$ | $u_{j,k}$ | $(4)_k$ | $.2\times(3)_k$ |
| $(2)_k$ | $(1)^2_k$ | $(5)_k$ | $(1)_k+(4)_k = u_{j+1,k}$ |
| $(3)_k$ | $(2)_{k+1} - 2\times(2)_k+(2)_{k-1}$ | | Repeat for all k |

PROGRAMME (1)

The programme is quite trivial in the present calculation but in later calculations programmes will be more significant because the numerical operations are more involved.

Programme (1) represents part of the calculation of the velocity on the (j+1) line from values on the j line. The suffix k in the programme means that we are calculating the velocity at (j+1,k) in terms of values $u_{j,k+1}$, $u_{j,k}$, $u_{j,k-1}$.

The computation of velocity on the (j + 1) line from the j line thus consists of repeating the programme from $k = 1$ to $k = n$, the outer edge of the boundary layer.

The value of $u_{j+1,o}$ is known from the boundary conditions. This may be made clearer by examining a representative step in the calculation as shown in Table (2,1).

| k | $\psi$ | $(1)_k = u_{j,k}$ | $(2)_k$ | $(3)_k$ | $(4)_k$ | $(5)_k = u_{j+1,k}$ |
|---|---|---|---|---|---|---|
| 0 | .00 | .0000 | | | | .0000 |
| 1 | .05 | .7543 | .5690 | .2704 | .0541 | .7002 |
| 2 | .10 | .9315 | .8676 | .1948 | .0390 | .8925 |
| 3 | .15 | .9856 | .9714 | .0792 | .0158 | .9698 |
| 4 | .20 | .9980 | .9960 | .0209 | .0042 | .9938 |
| 5 | .25 | .9998 | .9997 | .0034 | .0007 | .9991 |
| 6 | .30 | 1.0000 | 1.0000 | .0003 | .0001 | .9999 |
| 7 | .35 | 1.0000 | 1.0000 | .0000 | .0000 | 1.0000 |
| 8 | .40 | 1.0000 | | | | 1.0000 |

Calculation of velocities on $x = .0035$.

TABLE (2,1)

The velocity was calculated from $x = 0.0025$ to $x = 0.0125$ and at the latter station a check was made with the results of Howarth. There $u$ was found as a function of $\psi$ on $x = 0.0125$ and a graph of this value of $u$ plotted against $\psi$ is given in Figure (2,2). In Figure (2,2) the velocities on $x = 0.0125$ as calculated in this section, are shown to be in good agreement with Howarth's results.

As was previously stated no great stress is placed on numerical accuracy in this calculation. The agreement between the calculated results and the results of Howarth is sufficiently good to give us confidence in the method. This calculation is also useful in that it provides us with a simple model round which to build the more elaborate techniques to be used later.

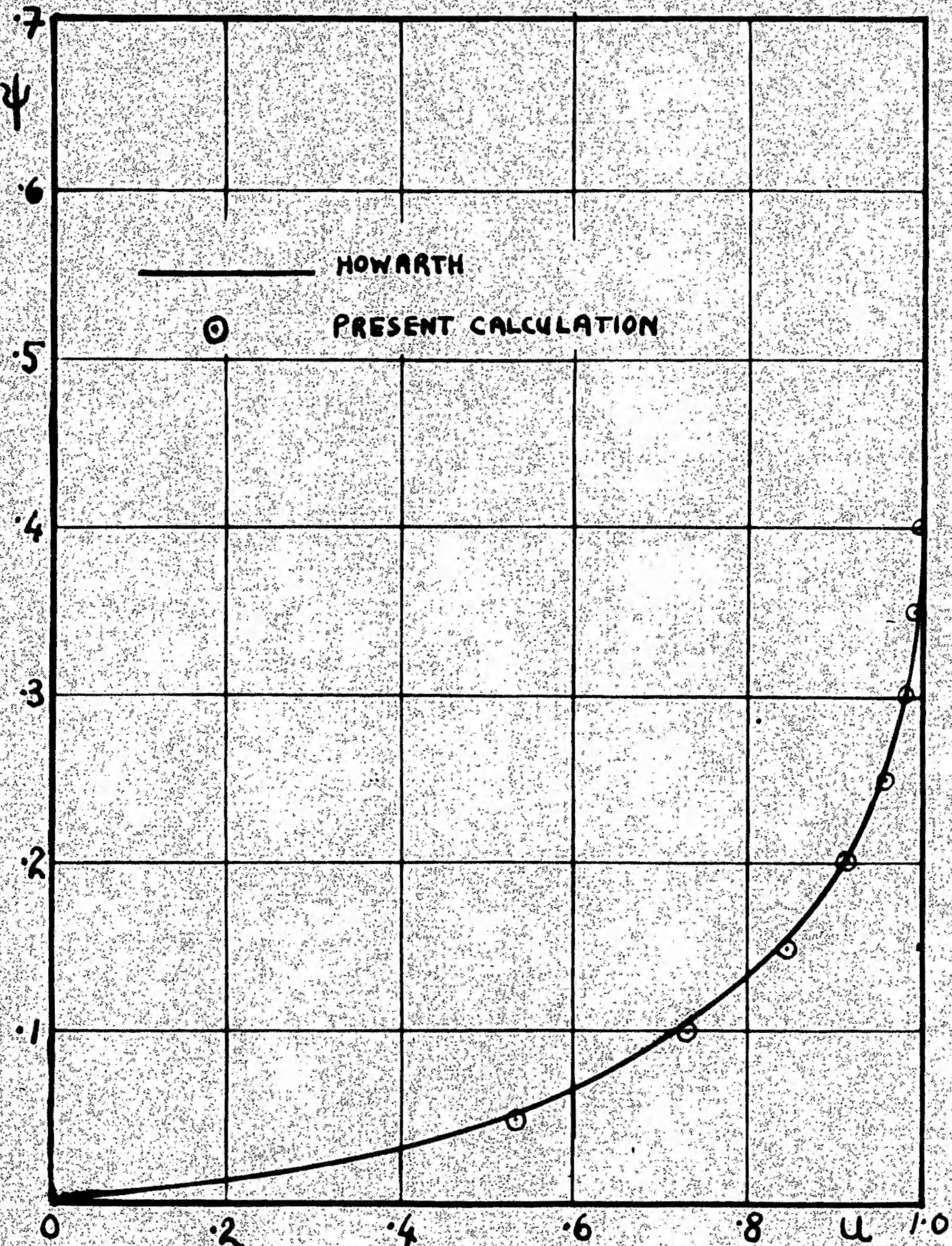


Velocity profile at x = .0125.

FIGURE (2,2).

We can now turn our attentions to the more interesting problem of flow along a flat plate against a linear adverse pressure gradient.

FLOW ALONG A FLAT PLATE AGAINST A LINEAR ADVERSE PRESSURE GRADIENT.

In section (2 B) the flow field in a boundary layer on a flat plate at zero incidence was examined, using the method of finite differences applied to the Von Mises equation. It is now intended, having justified the method to a certain extent, to compute the flow along a semi-infinite flat plate against a linear adverse pressure gradient. Particular reference will be paid to conditions in the immediate vicinity of the plate and in particular to the separation point.

Governing equation in non-dimensional form.

As was shown in section (2 A) the Von Mises equation of motion in a two dimensional steady incompressible boundary layer is,

$$\frac{\partial z}{\partial x} = \nu\sqrt{u_1^2 - z}\;\frac{\partial^2 z}{\partial \psi^2}, \qquad (2,16)$$

where $z = (u_1^2 - u^2)$, the variables being in dimensional form.

The boundary conditions for the flow are

The condition on the plate, $z = u_1^2$ when $\psi = 0$.

The condition in the free stream, $z = 0$ when $\frac{\partial z}{\partial \psi} = 0$.

The initial velocity profile, $z = z(x_o, \psi)$ when $x = x_o$, $x = x_o$ being the starting line of the calculation.

The free stream velocity $u_1(x)$ is chosen to be

$$u_1(x) = U\left(1 - \frac{x}{L}\right),$$

where $U$ is the constant value of the main stream velocity, that is the velocity of the fluid as it approaches the plate, and $L$ is a standard length. The above free stream velocity can be shown to correspond to that for flow against a linear adverse pressure gradient. Substituting the above value of velocity in the equation of motion in the free stream namely (1,13) we obtain

$$\frac{\partial p}{\partial x} = \rho \frac{U^2}{L} \left(1 - \frac{x}{L}\right) = A - Bx,$$

where $A$ and $B$ are constants, thus indicating a linear adverse pressure gradient.

As is seen from the form of the free stream velocity there is a stagnation line at the station $x = L$. This is far removed from any physical flow which we might consider, but, as will be seen later, the approximate range of the calculation is $0 \leq x \leq .1 L$ and so we are well upstream of this stagnation line.

The next step is to non-dimensionalise the differential equation (2,16). The non-dimensionalising quantities are better defined in this case than in the case of constant pressure flow since we can choose $L$ to be the characteristic length in the problem. As before we choose $U$ as the characteristic velocity and $\Psi = \frac{UL}{\sqrt{R}}$ as the characteristic stream function where $R = UL/\nu$ is the Reynolds number of the flow.

We construct the non dimensional variables $x' = {}^{x}/_{L}$, $z' = {}^{z}/_{U^2}$, $\psi' = \psi/_{\bar{\Psi}}$, in terms of which (2,16) becomes

$$\frac{\partial z'}{\partial x'} = \sqrt{(u_1')^2 - z'}\ \frac{\partial^2 z'}{\partial \psi'^2}.$$

The boundary conditions are also changed to a non dimensional form in which $u_1' = \sqrt{1 - x'}$.

<u>If we now drop the dashes for convenience</u> the non dimensional equation of motion becomes,

$$\frac{\partial z}{\partial x} = \sqrt{u_1^2 - z}\ \frac{\partial^2 z}{\partial \psi^2}, \qquad (2,17)$$

subject to the boundary conditions,

$$\begin{array}{lll} \text{(i)} & z = (1-x)^2 & \text{when } \psi = 0, \\ \text{(ii)} & z = 0 & \text{when } \frac{\partial z}{\partial \psi} \doteq 0, \\ \text{(iii)} & z = z\,(x_o, \psi) & \text{when } x = x_o, \end{array} \qquad (2,18)$$

all the variables being now in a non dimensional form.

We proceed to establish a difference replacement of (2,17).

<u>Finite difference replacement of (2,17).</u>

The $(x,\psi)$ plane is again divided by a rectangular grid with nodal points $(j,k)$. The mesh length in the x-direction is $\Delta x$, and in the $\psi$-direction is $\Delta\psi$, the mesh ratio being again $\sigma = \Delta x/(\Delta\psi)^2$.

We approximate to the derivatives of $z$ at the point $(j,k)$ in the usual manner by

$$\frac{\partial z}{\partial x} \doteq \frac{z_{j+1,k} - z_{j,k}}{\Delta x}, \quad \frac{\partial^2 z}{\partial \psi^2} \doteq \frac{z_{j,k+1} - 2z_{j,k} + z_{j,k-1}}{(\Delta\psi)^2},$$

where $z_{j,k}$ is the value of $z$ at the point corresponding to $(j,k)$, namely $(x_o + j\Delta x, k\Delta\psi)$.

Substituting the above expressions in (2,16), we derive the corresponding difference equation

$$z_{j+1,k} = z_{j,k} + \delta\sqrt{(u_1^2)_j - z_{j,k}}\,(z_{j,k+1} - 2z_{j,k} + z_{j,k-1}), \tag{2,19}$$

where the boundary conditions are now expressed in the form

$$\begin{aligned} &\text{(i)} \quad z_{j,o} = [1 - (x_o + j\Delta x)]^2, \\ &\text{(ii)} \quad z_{j,k} = 0 \text{ when } z_{j,k+1} \doteq z_{j,k}, \\ &\text{(iii)} \quad z_{o,k} \text{ is known for all } k. \end{aligned} \tag{2,20}$$

The difference equation (2,19) is only slightly more complicated than the equation (2,7) and the essential step-by-step nature of its solution is retained.

We proceed to examine the stability of (2,19).

<u>Stability of difference equation (2,19).</u>

Using the method outlined in (2 B) we form a linear error equation corresponding to (2,19) by neglecting the second and higher powers of the error function $\varepsilon_{j,k}$ in the original error equation, which is,

$$z_{j+1,k} + \varepsilon_{j+1,k} = z_{j,k} + \varepsilon_{j,k} + \delta \left[(u_1^2)_j - z_{j,k} - \varepsilon_{j,k}\right]^{1/2}$$

$$(z_{j,k+1} - 2z_{j,k} + z_{j,k-1} + \varepsilon_{j,k+1} - 2\varepsilon_{j,k} + \varepsilon_{j,k-1}),$$

$\varepsilon_{j,k}$ being the small error in the numerically calculated value of $z_{j,k}$.

By expanding $[(u_1^2)_j - z_{j,k} - \varepsilon_{j,k}]^{\frac{1}{2}}$ using the binomial theorem and neglecting all but the first power in $\varepsilon_{j,k}[(u_1^2)_j - z_{j,k}]^{-1}$, we arrive at the linear equation in the form,

$$\varepsilon_{j+1,k} = \varepsilon_{j,k} + \delta\sqrt{(u_1^2)_j - z_{j,k}}\,(\varepsilon_{j,k+1} - 2\varepsilon_{j,k} + \varepsilon_{j,k-1})$$
$$- \frac{1}{2}\,\frac{\delta\,\varepsilon_{j,k}}{\sqrt{(u_1^2)_j - z_{j,k}}}\,(z_{j,k+1} - 2z_{j,k} + z_{j,k-1}). \qquad (2,21)$$

We choose a solution of (2,21) in the form $\varepsilon_{j,k} = Ae^{\alpha j\Delta x}\, e^{i\beta k\Delta\psi}$, where $\alpha = a + ib$ and $\beta$ is real. Substituting this value for $\varepsilon_{j,k}$ in (2,21) and simplifying, we obtain,

$$e^{\alpha\Delta x} = 1 + \delta\sqrt{(u_1^2)_j - z_{j,k}}\,(e^{i\beta\Delta\psi} - 2 + e^{-i\beta\Delta\psi})$$
$$- \frac{1}{2}\,\frac{\delta}{\sqrt{(u_1^2)_j - z_{j,k}}}\,(z_{j,k+1} - 2z_{j,k} + z_{j,k-1}),$$
$$= 1 - 4\delta\sqrt{(u_1^2)_j - z_{j,k}}\,\left[\sin^2\frac{\beta\Delta\psi}{2} + \frac{1}{8[(u_1^2)_j - z_{j,k}]}\times\right.$$
$$\left.(z_{j,k+1} - 2z_{j,k} + z_{j,k-1})\right].$$

The condition for stability is that $|e^{\alpha\Delta x}| \leq 1$ and since from above, $e^{\alpha\Delta x}$ is real this becomes

$$-1 \leq 1 - 4\delta\sqrt{(u_1^2)_j - z_{j,k}}\left[\sin^2\frac{\beta\Delta\psi}{2} + \frac{z_{j,k+1} - 2z_{j,k} + z_{j,k-1}}{8[(u_1^2)_j - z_{j,k}]}\right] \leq 1. \tag{2,22}$$

The right hand condition of (2,22) can be simplified to give

$$\sin^2\frac{\beta\Delta\psi}{2} + \frac{z_{j,k+1} - 2z_{j,k} + z_{j,k-1}}{8\,u^2{}_{j,k}} \geq 0,$$

since $z_{j,k} = (u_1^2)_j - u_{j,k}^2$.

We see that this condition is satisfied for all $\beta$ if

$$z_{j,k+1} - 2z_{j,k} + z_{j,k-1} \geq 0. \tag{2,23}$$

Condition (2,23) can be shown to correspond exactly to the stability condition (2,12) of equation (2,7).

The left-hand condition of (2,23) can be simplified to yield

$$2\delta\left[(u_1^2)_j - z_{j,k}\right]^{\frac{1}{2}}\left[\sin^2\frac{\beta\Delta\psi}{2} + \frac{z_{j,k+1} - 2z_{j,k} + z_{j,k-1}}{8[(u_1^2)_j - z_{j,k}]}\right] \leq 1,$$

or

$$\delta \leq \tfrac{1}{2}\left[u_{j,k}\left(\sin^2\frac{\beta\Delta\psi}{2} + \frac{z_{j,k+1} - 2z_{j,k} + z_{j,k-1}}{8\,u_{j,k}^2}\right)\right]^{-1},$$

$$= \tfrac{1}{2}\,\frac{8u_{j,k}}{8\sin^2\frac{\beta\Delta\psi}{2}\,u_{j,k}^2 + z_{j,k+1} - 2z_{j,k} + z_{j,k-1}}.$$

We now find a lower bound for the right hand side of this inequality. The right hand side is

$$\frac{4\,u_{j,k}}{8\sin^2\frac{\beta\Delta\psi}{2}.u_{j,k}^2 + 2u_{j,k}^2 - u_{j,k+1}^2 - u_{j,k-1}^2},$$

$$\geq \frac{4u_{j,k}}{10\,u_{j,k}^2 - u_{j,k+1}^2 - u_{j,k-1}^2},$$

since $\sin^2 \frac{\beta\Delta\psi}{2} \leq 1$, and now since $u_{j,k} \leq u_{j,k+1}$, we have

$$\text{R.H.S.} \quad \geq \frac{4u_{j,k}}{9u^2_{j,k} - u^2_{j,k-1}} \geq \frac{4u_{j,k}}{9u_{j,k}{}^2} \geq \frac{4}{9} \quad .$$

It is now easily seen that if (2,23) is satisfied and $\delta \leq \frac{4}{9}$ then the stability condition (2,22) will be satisfied for all values of $\beta$.

Corresponding to the stability conditions in (2 B) we have thus established that the equation (2,19) is stable provided that

$$\begin{aligned} z_{j,k+1} - 2z_{j,k} + z_{j,k-1} &\geq 0, \\ \delta &\leq \frac{4}{9} \quad . \end{aligned} \qquad (2,24)$$

The condition (2,24) can be shown to be inherent in the differential equation and so will exist in every difference replacement of (2,16).

By a similar technique to that used in (2 B), we have corresponding to the differential equation, the result

$$\frac{\partial}{\partial x}(z + \varepsilon) = \sqrt{u_1^2 - z - \varepsilon} \left( \frac{\partial^2 z}{\partial \psi^2} + \frac{\partial^2 \varepsilon}{\partial \psi^2} \right) \quad ,$$

where $\varepsilon$ is a small error in the true solution $z$.

This equation is simplified to an equation linear in $\varepsilon$ of the form

$$\frac{\partial \varepsilon}{\partial x} = \sqrt{u_1^2 - z} \cdot \frac{\partial^2 \varepsilon}{\partial \psi^2} - \frac{\varepsilon}{2\sqrt{u_1^2 - z}} \quad \frac{\partial^2 z}{\partial \psi^2} \quad .$$

Corresponding to the error function $\varepsilon_{j,k}$ we assume that $\varepsilon$ can be expressed as $\varepsilon = Ae^{\alpha x} e^{i\beta\psi}$. Substituting this in the linear "error equation" and simplifying we obtain,

$$\alpha = -u\beta^2 - \frac{1}{2u} \frac{\partial^2 z}{\partial\psi^2} .$$

As in (2 B) the condition that $\varepsilon$ shall not increase with increasing $x$ is that

$$Rl \ \alpha \leq 0,$$

or in this case, since $\alpha$ is real,

$$u\beta^2 + \frac{1}{u} \frac{\partial^2 z}{\partial\psi^2} \geq 0.$$

This is certainly true for all $\beta$ if

$$\frac{\partial^2 z}{\partial\psi^2} \geq 0.$$

The above condition is, of course, the differential form of the condition (2,23).

The worth of the above examination of a differential equation will become more apparant in the examination of compressible flow problems where the differential and thus difference equations are more complicated. In this case it is found much more convenient to consider a differential "error equation", the results of which point the way to the more accurate examination of the difference equation for the error.

Apart from this consideration the extraction of stability criteria from a differential equation for the error yields those stability conditions which are applicable to all difference replacements of the same order as the differential equation.

Before going on to discuss the computation of the velocity field, the true significance of the stability conditions (2,24) should be examined. By the very method of derivation of these criteria, namely always considering the worst possible case, it is likely that we have been over stringent in the conditions to be applied.

In an actual calculation, the stability of the difference equation at any point should in fact be determined by applying the condition (2,22) at that point. This of course, would prove to be extremely laboxrious and for this reason the simple form (2,24) is used for all points in the field. If (2,24) is satisfied at a point then the difference equation (2,19) is certainly stable at that point, although a higher mesh ratio could be sufficient to ensure stability at most nodes.

<u>Numerical calculation of the velocity field. (primary calculation)</u>

In the evaluation of $z$ and hence $u$ inside the boundary layer the finite difference equation (2,19) is used, with $\Delta x = .0025$, $\Delta\psi = .1$ and so $\delta = .25$. This satisfies the condition $\delta \leq \frac{4}{9}$.

The calculation was started at $x = 0.05$, this particular station being chosen to promote an easy comparison with the results of Witting [20] who also started his finite difference solution of the Prandtl boundary layer equations at this station.

Like Witting we choose our initial velocity profile at $x = .05$ from Howarth [12]. In Howarth's paper the velocity $u$ and the stream function $\psi$ are expressed as power series in the variable $\eta = \frac{y}{\sqrt{x}}$. The first six terms of each series are given in tabular form as functions of $\eta$. $u$ and $\psi$ being expressed at $x = .05$ as,

$$u = .5\left\{ f_0^1(\eta) - .4\, f_1^1(\eta) + .16\, f_2^1(\eta) - .064\, f_3^1(\eta) + .0256\, f_4^1(\eta) - .01024\, f_5^1(\eta) + .004096\, f_6^1(\eta) \right\},$$

and

$$\psi = .2236\left\{ f_0(\eta) - .4\, f_1(\eta) + .16\, f_2(\eta) - .064\, f_3(\eta) + .0256\, f_4(\eta) - .01024\, f_5(\eta) + .004096\, f_6(\eta) \right\},$$

respectively.

Using Howarth's tables for $f_i(\eta)$ and $f_i^1(\eta)$ $(i = 0 \ldots 6)$, we can thus find $u$ as a function of $\psi$ at $x = .05$, and so we now have the values of $z$ at all the nodes on $x = .05$. The initial values of $z$ are given in Table (2,4).

Using (2,19) in the particular form

$$z_{j+1,k} = z_{j,k} + .25\sqrt{(u_1^2)_j - z_{j,k}}\,(z_{j,k+1} - 2z_{j,k} + z_{j,k-1}),$$

the velocity is evaluated at all nodes downstream of the station $x = 0.05$, the step-by-step nature of solution being similar to that described in (2 B).

The calculation was carried out as far downstream as the station $x = 0.13$, in all a total of 36 steps. The most economical programme for the calculation is given below in Programme (2).

| OPERATION | $z_{j+1,k} = z_{j,k} + .25\sqrt{(u_1^2)_j - z_{j,k}}\,(z_{j,k+1} - 2z_{j,k} + z_{j,k-1})$ | | |
|---|---|---|---|
| $(1)_k$ | $z_{j,k}$ | $(5)_k$ | $(4)_k \times .25$ |
| $(2)_k$ | $(u_1^2)_j - (1)_k$ | $(6)_k$ | $(5)_k \times (3)_k$ |
| $(3)_k$ | $\sqrt{(2)_k}$ | $(7)_k$ | $(1)_k + (6)_k = z_{j+1,k}$ |
| $(4)_k$ | $(1)_{k+1} - 2(1)_k + (1)_{k-1}$ | | Repeat for all k. |

PROGRAMME (2).

As before the calculation of $z$ at nodes on the $(j + 1)$ line consists of a repeated number of applications of the programme at the nodes on the j-line. As an example the particular section of the calculation in which the values of $z$ on the line $x = .0725$ are obtained from values on $x = .07$ is given in Table (2.2).

The values of the velocity arising from the above calculation are listed at selected stations of $x$ in Table (2.4) and demonstrated in Figure (2.3). The velocity at the nodes on $x = .05, .07 \ldots .12$, are displayed in the table, the corresponding velocity profiles being drawn in the figure. The growth of the boundary layer is also demonstrated in figure (2.3).

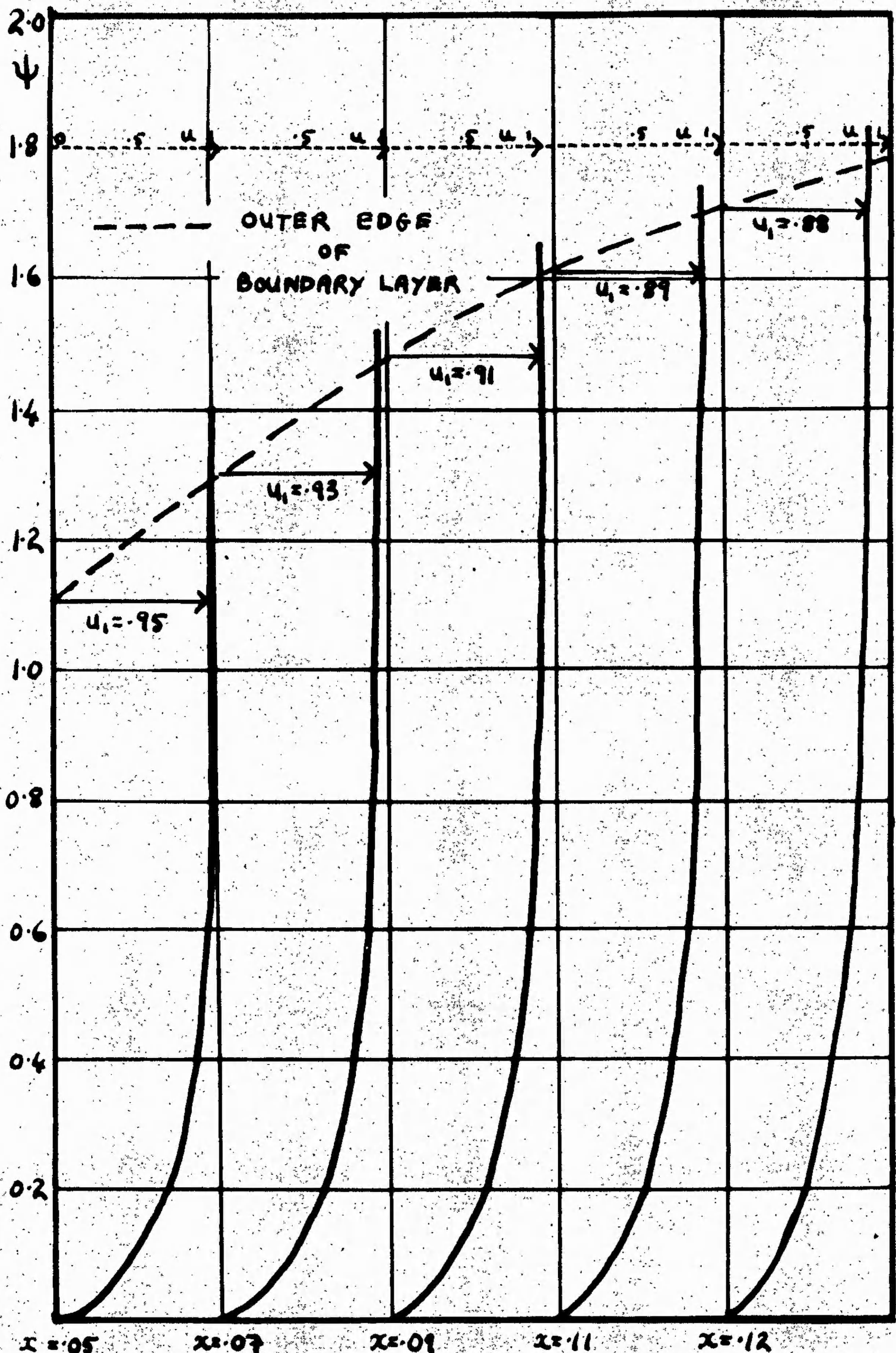


Velocity profiles

FIGURE (2,3)

| k | $\psi$ | $(1)_k = z_{j,k}$ | $(2)_k$ | $(3)_k$ | $(4)_k$ | $(5)_k$ | $(6)_k$ | $(7)_k = z_{j+1,k}$ |
|---|---|---|---|---|---|---|---|---|
| 0 | .0 | .8649 | | | | | | .8603 |
| 1 | .1 | .6801 | .1848 | .4299 | .0051 | .0013 | .0005 | .6806 |
| 2 | .2 | .5004 | .3645 | .6038 | .0275 | .0069 | .0041 | .5045 |
| 3 | .3 | .3478 | .5171 | .7191 | .0331 | .0083 | .0059 | .3537 |
| 4 | .4 | .2283 | .6366 | .7980 | .0331 | .0083 | .0066 | .2349 |
| 5 | .5 | .1419 | .7230 | .8503 | .0274 | .0068 | .0058 | .1477 |
| 6 | .6 | .0829 | .7820 | .8843 | .0215 | .0054 | .0047 | .0876 |
| 7 | .7 | .0454 | .8195 | .9053 | .0153 | .0038 | .0035 | .0489 |
| 8 | .8 | .0232 | .8417 | .9175 | .0100 | .0025 | .0023 | .0255 |
| 9 | .9 | .0110 | .8539 | .9241 | .0059 | .0015 | .0014 | .0124 |
| 10 | 1.0 | .0047 | .8602 | .9274 | .0034 | .0008 | .0008 | .0055 |
| 11 | 1.1 | .0018 | .8631 | .9285 | .0017 | .0004 | .0004 | .0022 |
| 12 | 1.2 | .0006 | .8643 | .9297 | .0008 | .0002 | .0002 | .0008 |
| 13 | 1.3 | .0002 | .8647 | .9299 | .0002 | .0000 | .0000 | .0002 |
| 14 | 1.4 | .0000 | .8649 | .9300 | .0000 | .0000 | .0000 | .0000 |

Calculation of $z$ at $x = 0.0725$

TABLE (2.2)

At this stage in the calculation we now know the value of the x-component of velocity at all the nodes in the boundary layer. The y-component of the velocity is small and is not estimated.

The biggest disadvantage of the above method is that the number of problems we can handle is restricted to those for which some velocity profile is known. This is comparable to the state of affairs in the papers of Witting [20] and Leigh [21].

In (1 A) we discussed the conditions round the nose of the plate. In the classical conception of a boundary layer the velocity profile at the leading edge $x = 0$ is $u = 0$ when $y = 0$ and $u = 1$ when $y > 0$. The existence of such a distribution has been the cause of much controversy. It is now agreed that the boundary layer starts slightly upstream of the nose of the plate and thus has a small thickness at $x = o$. It is further agreed that conditions in the immediate vicinity of the nose are not adequately represented by the boundary layer equations.

If we choose our starting station to be $x = o$ and the starting z distribution there to be $z = 1$ when $\psi = o$ and $z = o$ when $\psi = .1, .2, .3 \ldots$, we are in fact assuming a classical boundary layer. It could also be said that in such a distribution we are assuming that the boundary layer thickness at the nose of the plate is less than our nearest node.

Starting with the above distribution of z at $x = o$ the values of z are calculated in the normal fashion downstream as far as the station $x = 0.0575$. The values at $x = .05$ and $x = .0575$ are compared with the corresponding values found in the first calculation, this comparison is given in Table (2.3). It is clearly seen that the agreement is good and what is more significant the agreement is improving as the calculation proceeds.

In another calculation the starting distribution was chosen to be $z = 1$ when $\psi = o$, $z = \frac{1}{2}$ when $\psi = .1$ and $z = o$ when $\psi = .2, .3$ . The values of z calculated from this starting distribution merged rapidly with the results obtained from the calculation started with the classical distribution. This demonstrates that the initial velocity profile is not as strong a boundary condition as the free

| | x = .050 | | x = .0575 | |
|---|---|---|---|---|
| ψ | (1) | (2) | (1) | (2) |
| 0 | .9025 | .9025 | .8883 | .8883 |
| .1 | .6677 | .6704 | .6743 | .6770 |
| .2 | .4536 | .4597 | .4746 | .4808 |
| .3 | .2843 | .2926 | .3121 | .3182 |
| .4 | .1661 | .1730 | .1918 | .1972 |
| .5 | .0890 | .0950 | .1099 | .1146 |
| .6 | .0434 | .0463 | .0585 | .0628 |
| .7 | .0201 | .0221 | .0289 | .0318 |
| .8 | .0074 | .0098 | .0128 | .0146 |
| .9 | .0027 | .0033 | .0051 | .0060 |
| 1.0 | .0005 | .0009 | .0017 | .0022 |
| 1.1 | .0000 | .0002 | .0005 | .0007 |
| 1.2 | | .0000 | .0001 | .0002 |
| 1.3 | | | .0000 | .0000 |

(1) Values of z found from the primary calculation.

(2) Values of z found from the calculation started at x = o.

Comparison of starting distributions.

TABLE (2.3).

stream velocity or the stagnation line along the plate. We have thus given some justification for the use of the classical velocity distribution as a starting point for the calculation.

## Sub-division of the strip adjacent to the plate (Secondary calculation).

One of the quantities we are trying to find in this problem is the skin friction at various stations along the plate. The skin friction or shearing stress on the plate is $\tau = \mu \left(\frac{\partial u}{\partial y}\right)_o$, where the subscript o denotes conditions on the plate.

As a relative measure of the skin friction we need only calculate $(\frac{\partial u}{\partial y})_o$. A particular feature of this evaluation will be the estimation of the separation point $x_s$ the point at which $(\frac{\partial u}{\partial y})_o = 0$.

It was found, on trying to estimate the velocity gradient on the plate, that the nearest $\psi$ line on which the values of the velocity were known namely $\psi = .1$, was not sufficiently close to the plate to enable an accurate assessment of $(\frac{\partial u}{\partial y})_o$ to be made. For this reason some means of finding the velocity at nodes in the strip $0 \leq \psi \leq .1$ must be found.

The first method which was considered was that of divided differences, a difference technique in which the mesh size in the $\psi$ direction decreases as we near the plate. Since this method entails a complete change in the structure of the difference equation an alternative approach was sought.

The method used is the technique of repeated sub-division of the strip $0 \leq \psi \leq .1$. The strip was bisected by the line $\psi = .05$ and values of z calculated on this line using the difference equation (2.19). The calculation is particularly straightforward in that the value of z at $(x + \Delta x, .05)$ is obtained from the three values at $(x, 0)$, $(x, .05)$ and $(x, .1)$. The calculation started at $x = .05$ and finished at $x = .13$.

To maintain the condition $\delta = .25$ it is necessary to adjust $\Delta x$. With $\Delta\psi = .05$ we choose $\Delta x$ to be $.0025 \times .25$. We have thus sub-divided each original interval in the x direction by three points, the values of z at the new intermediate nodes on $\psi = .1$ being found by graphical interpolation. The number of steps required to reach .13 is now 144.

After this calculation the strip $0 \leq \psi \leq .05$ was further halved and values of z were found at nodes on $\psi = .025$, here again the mesh length in the x-direction is reduced by a factor of four.

A final sub-division was carried out to find the velocity at nodes on the line $\psi = .0125$, this being considered sufficiently near the plate.

The values of velocity found by the above technique are presented at selected stations of x in Table (2.4) and used to complete the velocity profiles in Figure (2,3).

The next calculation is concerned with estimating the velocity gradient accurately on the plate. In actual fact this proved extremely troublesome and much time was spent before the problem was finally resolved.

For the sake of completeness it seems advisable to give an account of some of the methods of extrapolation which were tried rather than ~~so~~ merely to reproduce the finally developed form of the method.

It must be borne in mind that the calculations in the incompressible boundary layers are not only important for their own sake, they also provide a relatively simple field in which to explore the possibilities and shortcomings

| ψ \ x | 0.05 | 0.07 | 0.09 | 0.11 | 0.12 |
|---|---|---|---|---|---|
| .0125 | .1664 | | | | |
| .025 | .2379 | .2068 | .1801 | .1554 | .1432 |
| .05 | .3415 | .2990 | .2640 | .2320 | .2172 |
| .1 | .4846 | .4289 | .3849 | .3453 | .3270 |
| .2 | .6701 | .6038 | .5497 | .5028 | .4913 |
| .3 | .7862 | .7181 | .6635 | .6146 | .5919 |
| .4 | .8581 | .7980 | .7447 | .6968 | .6745 |
| .5 | .9020 | .8503 | .8023 | .7575 | .7361 |
| .6 | .9269 | .8843 | .8422 | .8014 | .7817 |
| .7 | .9395 | .9053 | .8690 | .8327 | .8146 |
| .8 | .9461 | .9175 | .8863 | .8542 | .8378 |
| .9 | .9486 | .9241 | .8971 | .8685 | .8538 |
| .10 | .9497 | .9273 | .9034 | .8776 | .8642 |
| .11 | .9500 | .9285 | .9067 | .8831 | .8709 |
| .12 | | .9297 | .9085 | .8864 | .8750 |
| .13 | | .9299 | .9093 | .8884 | .8774 |
| .14 | | .9300 | .9096 | .8891 | .8787 |
| .15 | | | .9099 | .8897 | .8794 |
| .16 | | | .9100 | .8899 | .8798 |
| .17 | | | | .8900 | .8799 |
| .18 | | | | | .8800 |
| .19 | | | | | |

Values of velocity inside the boundary layer.

TABLE (2.4)

of the general method, with a view to the use of the Von Mises transformation in solving the compressible boundary layer equations.

We shall now examine some of the possible extrapolation techniques for calculating the velocity gradient on the plate.

Extrapolation formulae.

From the results of the primary calculation we know at any station $x$ in the range $0 \leq x \leq .13$ the values of $z$ and $u$ at nodes $\psi = .1, .2, .3 \ldots.$ The secondary calculation furnishes us with more detailed information near the plate. We have in fact calculated values of $z$ at the nodes $\psi = .05$, $\psi = .025$ and $\psi = .0125$ for any station $x$.

From the above set of values at any station $x$ we would like to derive the value of the skin friction at this station. The skin friction is given by $\left(\frac{\partial u}{\partial y}\right)_0$ or in terms of our variables $-\frac{1}{2}\left(\frac{\partial z}{\partial \psi}\right)_0$, since

$$\frac{\partial u}{\partial y} = \frac{\partial u}{\partial \psi} \cdot \frac{\partial \psi}{\partial y} = -\frac{1}{2}\frac{\partial z}{\partial \psi} .$$

We define a function $f(\Delta\psi, x)$ as

$$f(\Delta\psi, x) = \frac{z(\Delta\psi, x) - z(0,x)}{\Delta\psi} ,$$

where $f(\Delta\psi, x)$ tends to $\left(\frac{\partial z}{\partial \psi}\right)_0$ as $\Delta\psi \to 0$.

It should be pointed out that, unless otherwise stated in connection with the extrapolation techniques, all calculations are carried out on a line normal to the plate.

For the purposes of reference the extrapolation techniques will be labelled.

Method A.

Although in the problem of interpolation a graphical method may be quite accurate, the same is not true of extrapolation.

At each station of $x$ a graph of $f(\Delta\psi, x)$ can be drawn through the known values at $\Delta\psi = .0125, .025, .05, .1 \ldots$, and the value of $f(0,x)$ can be found from the graph. Since the gradient of this curve is not known at the origin the technique is too inaccurate to be of use.

Method B.

If the function $f(\Delta\psi, x)$ is expressed in the form

$$f(\Delta\psi, x) = a + b\,\Delta\psi + c\,(\Delta\psi)^2 + d\,(\Delta\psi)^3, \qquad x = \text{const},$$

then $\left(\frac{\partial u}{\partial y}\right)_0 = -\frac{1}{2}\left(\frac{\partial z}{\partial \psi}\right)_0 = -\frac{1}{2}\,a.$

Knowing the values of $f(\Delta\psi, x)$ at the four nodes $\Delta\psi = .0125$, $.025$, $.05$ and $.1$ at any station $x$ we can form four simultaneous equations to be solved for $a$, $b$, $c$ and $d$.

Using the method, $\left(\frac{\partial u}{\partial y}\right)_0$ was calculated at various stations of $x$, the results being given in Table (2,5). A graph of $\left(\frac{\partial u}{\partial y}\right)_0$, calculated by this method, against distance along the plate is shown in figure (2,4). On comparison with the values of skin friction found by Howarth [12], the method is a poor one and an alternative procedure is required.

Method C.

At any station $x$ we know the values of $f(\Delta\psi, x)$ for various points $\Delta\psi$, in particular if $f(\Delta\psi, x)$ is known at points of the form $\Delta\psi$, $2\Delta\psi$ and $4\Delta\psi$ then a well-known formula for finding $f(0,x)$ is

$$f(0,x) = \frac{f^2(2\Delta\psi,\ x) - f(\Delta\psi,\ x).\ f(4\Delta\psi,\ x)}{2f(2\Delta\psi,\ x) - f(\Delta\psi,\ x) - f(4\Delta\psi,\ x)} \quad (2,25)$$

The above formula was also arrived at independently by an intuitive process as shown below.

In the problem of incompressible flow the method is being tested and as such comparison with known results is desirable. During the two previous calculations (A) and (B) it was found that the calculated values of $(\frac{\partial u}{\partial y})_o$ were extremely high when compared with Howarth's values. This tends to suggest that the curve of $f(\Delta\psi,x)$ against $\Delta\psi$ has a large gradient at the origin, such a gradient resulting from $f(\Delta\psi, x)$ expressed in the form

$$f(\Delta\psi,\ x) = A + B\ (\Delta\psi)^n \quad ,$$

where $A$ and $B$ are constants and $0 < n < 1$ (the above expression will have more significance later). Knowing the values of $f(\Delta\psi,\ x)$ at $\Delta\psi = .0125,\ .025$ and $.05$, we can set up three simultaneous equations to be solved for $A$, $B$ and $n$. If we eliminate $B$ and $n$ from these equations we find that

$$f\ (0,\ x) = A = \frac{f^2(.025,\ x) - f(.05,\ x)\ f(.0125,\ x)}{2f(.025,\ x) - f(.05,\ x) - f(.0125,x)} \quad ,$$

which is a particular form of (2,25).

Using the above equation the values of $f(0,\ x)$ and hence $(\frac{\partial u}{\partial y})_o$ were calculated along the plate in the range $0.05 \leq x \leq 0.13$. The resulting curve of $(\frac{\partial u}{\partial y})_o$ plotted against $x$ was found to be extremely oscillatory near $x = .05$, the oscillations diminishing somewhat as $x = .13$

was approached and the curve did cross the axis of $x$, in the vicinity of $x = .125$. The curve was however insufficiently smooth to allow any accurate estimate of this zero (the separation point) being made.

It was deduced that the reason for the fluctuation in the calculated values is the fact that the formula is very sensitive to small errors in the values of $f(\Delta\psi, x)$. Because of this the values of $f(\Delta\psi, x)$ were smoothed.

At each station of $\Delta\psi$, $f(\Delta\psi, x)$ considered now as a function of $x$, was smoothed over the range $0.05 \leq x \leq .13$ by the method of least squares. The smoothed values are now used as a basis for the calculation.

Using the smoothed values the calculation was repeated in the same range $0.05 \leq x \leq 0.13$ in steps of $\Delta x = 0.0025$. The resulting values of $(\frac{\partial u}{\partial y})_o$, although still producing an undulating curve are found to be in good general agreement with the values of Howarth.

Both sets of values of $(\frac{\partial u}{\partial y})_o$ at stations along the plate are given in Table (2,5), the corresponding graphs of $(\frac{\partial u}{\partial y})_o$ plotted against $x$ being shown in figure (2,4).

With reference to Table (2,5) it should be noted that those values of $(\frac{\partial u}{\partial y})_o$ which are negative have no meaning in a physical sanse, such a negative gradient possibly implying back flow, in the region of which the boundary layer equations are not necessarily applicable. The negative values are useful however, in a mathematical sense, to enable us to

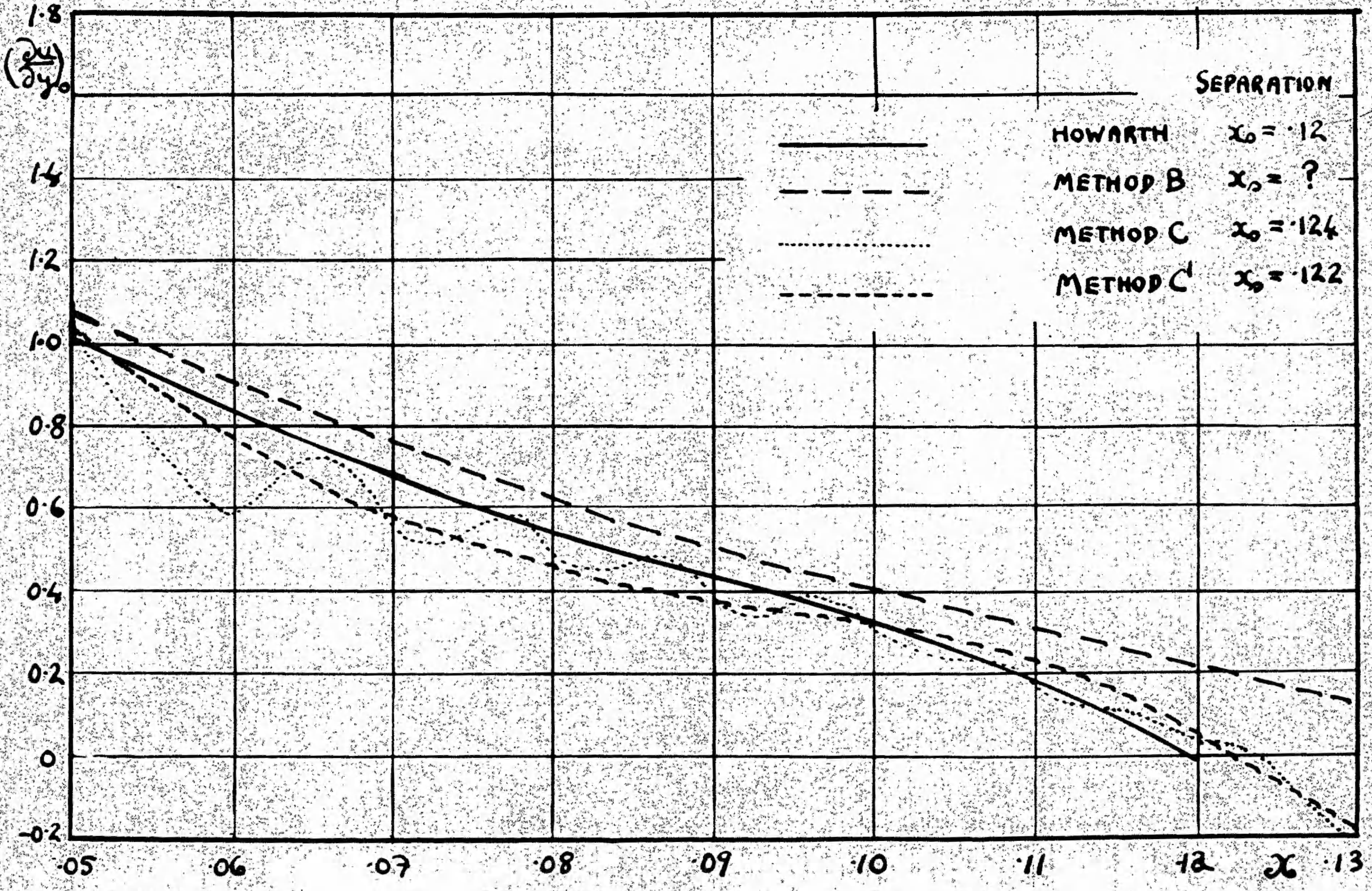


$(\frac{\partial u}{\partial y})_0$ calculated using methods (B) and (C)

FIGURE (2,4)

| x | METHOD B | METHOD C | METHOD C' | HOWARTH | x | B | C | C' | H |
|---|---|---|---|---|---|---|---|---|---|
| .05 | 1.07 | 1.03 | 1.05 | 1.00 | .10 | .407 | .29 | 0.321 | 0.320 |
| .06 | .892 | .58 | .792 | 0.835 | .11 | .319 | .17 | 0.233 | 0.190 |
| .07 | .738 | .56 | .580 | 0.681 | .12 | .230 | .05 | 0.045 | 0.000 |
| .08 | .618 | .48 | .455 | 0.555 | .125 | .182 | -.01 | -0.076 | |
| .09 | .510 | .37 | .383 | 0.435 | .13 | .147 | -.21 | -0.175 | |

METHOD C' refers to the method C using the smoothed values of $f(\Delta\psi, x)$

Velocity gradient on the plate.

TABLE (2,5)

estimate the position $x_s$ at which $(\frac{\partial u}{\partial y})_o = 0$. In a similar manner although the values of $(\frac{\partial u}{\partial y})_o$ which lie below the x-axis in figure (2,4) are useful in determining the separation point they must be discarded downstream of this separation point, once it has been estimated.

The calculated value of the separation point is $x_s = .122$ which compares favourably with the results of Howarth .120, Leigh .1198, Görtler .1198, and Witting .124. Although the method (C) yields relatively good results the reason for this was not fully understood at this stage, and so an alternative technique for exploring the region near the plate will now be given.

Method D.

It may be suggested that the mesh size $\Delta\psi = .1$ of the primary calculation is too large and because of this the truncation errors in the calculated values of the velocity may be relatively large. Whilst, as will be seen later, these errors are not big enough to cause dismay when considered over the main part of the field, they may be sufficient to markedly affect any efforts to calculate the velocity gradient on the plate.

A further point to be considered is the method of sub-division used in the secondary calculation. Since, in the first instance, the interval $0 \leq \psi \leq .1$ is halved it can be expected that any error in the value of $z$ at $\psi = .1$ will, to a large extent, be carried over to the value of $z$ at $\psi = .05$. This transfer of errors will be carried over all the sub-divisions, the error becoming more significant as the plate is approached.

If instead of reaching the station $\psi = .025$ by two sub-divisions of the interval we could reach it in one step, that is by dividing the range $0 \leq \psi \leq .1$ into four, it is safe to assume that the error in $z$ at $\psi = .1$ will influence less seriously the values of $z$ at the nodes $\psi = .075$, $.05$ and $.025$.

To carry out a process, similar to that used in the secondary calculation, with the strip $0 \leq \psi \leq 0.1$ now divided by three lines of internal nodes would take considerable time and because of this an alternative procedure was sought.

The differential equation which we are trying to solve is,

$$\frac{\partial z}{\partial x} = \sqrt{u_1^2 - z} \;\; \frac{\partial^2 z}{\partial \psi^2} \quad .$$

This equation can be reduced to an ordinary differential equation if we keep $x$ constant and assume that $(\frac{\partial z}{\partial x})$ is known as a function of $\psi$.

If we consider any station $x$ then $\frac{\partial z}{\partial x}$ is known at the nodes $\psi = 0, 0.1, 0.2 \ldots$ and we can thus interpolate to find the values of $(\frac{\partial z}{\partial x})$ at all points in the range $0 \leq \psi \leq .1$, the technique of interpolation being assumed more accurate than that of extrapolation.

On a line $x = \text{const}$, the range $0 \leq \psi \leq .1$ is divided by the five points labelled 0, 1, 2, 3, 4 as shown below. Using a difference interpolation the value of $(\frac{\partial z}{\partial x})$ is calculated at the three internal points, $\frac{\partial z}{\partial x}$ at the node 1 being labelled $(\frac{\partial z}{\partial x})_1$.

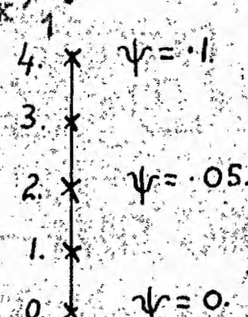


The ordinary differential equation for $z$ in terms of $\psi$ can now be solved by the method of relaxation at the nodes 1, 2, 3 or by the method outlined below.

The ordinary differential equation is replaced at the node $r$ by the difference equation,

$$\left[\frac{\partial z}{\partial x}\right]_r = \sqrt{(u_1^2) - z_r} \quad \frac{z_{r+1} - 2z_r + z_{r-1}}{(\Delta\psi)^2} \quad .$$

If this equation is rewritten in terms of $u_r$ at the nodes $r = 1, 2, 3$, we obtain the following three simultaneous equations,

$$\left[\frac{\partial z}{\partial x}\right]_3 (\Delta\psi)^2 = u_3 \left[2u_3^2 - u_2^2 - u_4^2\right],$$

$$\left[\frac{\partial z}{\partial x}\right]_2 (\Delta\psi)^2 = u_2 \left[2u_2^2 - u_1^2 - u_3^2\right],$$

$$\left[\frac{\partial z}{\partial x}\right]_1 (\Delta\psi)^2 = u_1 \left[2u_1^2 - u_2^2\right].$$

Since $u_4$ is known we have thus three equations to be solved for the three unknowns $u_1$ $u_2$ and $u_3$. The above equations can be rearranged into a form more suitable for solution, namely,

$$u_1\, u_4^2 + \frac{u_1}{u_3}\left(\frac{\partial z}{\partial x}\right)_3 (\Delta\psi)^2 = 4u_1^3 - 3\left(\frac{\partial z}{\partial x}\right)_1 (\Delta\psi)^2 - 2\,\frac{u_1}{u_2}\left(\frac{\partial z}{\partial x}\right)_2 (\Delta\psi)^2, \tag{2,26}$$

$$\frac{u_3}{u_1} = \left[3 - 2\left(\frac{\partial z}{\partial x}\right)_1 \frac{(\Delta\psi)^2}{u_1^3} - \left(\frac{\partial z}{\partial x}\right)_2 \frac{(\Delta\psi)^2}{u_1^3}\,\frac{u_1}{u_2}\right]^{\frac{1}{2}}, \tag{2,27}$$

$$\frac{u_2}{u_1} = \left[2 - \left(\frac{\partial z}{\partial x}\right)_1 \frac{(\Delta\psi)^2}{u_1^3}\right]^{\frac{1}{2}}. \tag{2,28}$$

In any specific problem a trial solution for $u_1$ is used to find $u_3/u_1$ and $u_2/u_1$ using (2,27) and (2,28). The values of $u_3/u$, $u_2/u_1$ and $u_1$ are then substituted in (2,26), the residue determing a revised value for $u_1$. The convergence of the process is quite speedy. Once an accurate value for $u_1$ is found, $u_2$ and $u_3$ are calculated from (2,27) and (2,28).

A calculation of this type was carried out at the station $x = .12$. The range $0 \leq \psi \leq .1$ was divided by the three internal points $\psi = .075$, $.05$ and $.025$ and values of the velocity obtained at these points. The range $0 \leq \psi \leq .025$ was then divided into four equal parts by the points $\psi = .01875$, $.0125$ and $.00625$. Two other sub-divisions were carried out until the velocity was known down to the station $\psi = .000390625$.

The values of velocity and $-\frac{1}{x} f(\Delta\psi, x)$ found from the above calculation are presented in Table (2,6).

From Howarth we know that at $x = .12$, $\left(\frac{\partial u}{\partial y}\right)_o = 0$. It was intended in the present calculation to find how many sub-divisions must be carried out before $-\frac{1}{x} f(\Delta\psi, x) \doteq \left(\frac{\partial u}{\partial y}\right)_o$ . As can be seen from Table (2,6) the smallest value $f(.000310625, .12) = .21$ and we are forced to the conclusion that the method does not yield accurate results.

This breakdown may be due to two reasons, the method may be incorrect or the method may be correct and the small error in the value of $z$ at $\psi = .1$ may be creating large errors in the intermediate values.

In order to test which of these is correct a second set of calculations is carried out in which the value of $u$ at $\psi = .1$ is taken from the results of Leigh [21].

In Leigh's paper, he is mainly interested in a small region upstream of the separation point. For this region $u$ is tabulated as a function of $y$ at various stations of $x$.

In order to find $u$ as a function of $\psi$ at $x = .120$ we use a form of numerical integration to find $\psi$ in terms of $y$, since

$$u = \frac{d\psi}{dy}, \quad x = \text{const},$$

we have $$\psi = \int u \, dy, \quad x = \text{const}.$$

Care is needed in the numerical integration since Leigh's non-dimensional variables differ from the ones used in the present paper, a scale factor of $\frac{1}{8}$ being used to convert a value of $\psi$ from Leigh's results into a value of $\psi$ as used in the present calculation.

For the purposes of this check calculation Leigh's values of $\psi$ are found by graphical integration, a graph of $u$ against $\psi$ being plotted from which $u$ at nodes on $x = .12$ are found.

The value of $u$ calculated by Leigh at $\psi = .1$ on $x = .12$ is $u = .320$, as compared with the value of $u = .3270$ of the present primary calculation.

Since this point (.12, .1) is the node in the primary calculation at which we can expect the greatest error, the above comparison speaks well for the accuracy of the primary calculation, considering the relatively large initial mesh lengths used.

Using this value $u = .320$ at $\psi = .1$ a calculation was carried out using Method (D) to find the values of the velocity at nodes as close to the plate as $\psi = .025$ on the line $x = .12$. Another calculation which starts with Leigh's value for $u$ at $\psi = .025$, namely $u = .1320$ is carried out to find the velocity at nodes as close to the plate as $\psi = .000390625$.

The results of these calculations are also given in Table (2,6) and on comparison with the previous set of results it can be deduced that the original error in the velocity at $\psi = .1$ leads to larger errors on the velocity at nodes nearer the plate. What is also significant is that if we compare all the above results with the values taken directly from Leigh it is seen that the divergence increases as we approach the plate, indicating that the method breaks down in some fashion as the plate is approached.

| $\psi$ | STARTING VALUE $u_1 = .3270$ | | STARTING VALUE $u_{.1} = .3200$ | | STARTING VALUE $u_{.025} = .1320$ | | LEIGH'S RESULTS | |
|---|---|---|---|---|---|---|---|---|
| | $u_{\Delta\psi}$ | $-\frac{1}{2} f_{\Delta\psi}$ | $u_{\Delta\psi}$ | $-\frac{1}{2} f_{\Delta\psi}$ | $u_{\Delta\psi}$ | $-\frac{1}{2} f_{\Delta\psi}$ | $u_{\Delta\psi}$ | $-\frac{1}{2} f_{\Delta\psi}$ |
| .1 | .3270 | .535 | .3200 | .512 | | | .3200 | .512 |
| .05 | .2180 | .475 | .2093 | .438 | | | .2075 | .431 |
| .025 | .1413 | .399 | .1364 | .372 | .1320 | .348 | .1320 | .348 |
| .0125 | .0925 | .342 | | | .0832 | .277 | .0830 | .276 |
| .00625 | .0612 | .300 | | | .0545 | .238 | .0548 | .240 |
| .003125 | .0407 | .265 | | | .0350 | .196 | .0345 | .190 |
| . | .0274 | .240 | | | .0228 | .166 | .0210 | .141 |
| . | .0186 | .221 | | | .0150 | .144 | .0125 | .100 |
| . | .0128 | .210 | | | .0100 | .128 | .0070 | .063 |

Calculation of the velocity near the plate

( TABLE (2,6).

Before going on to discuss how this difficulty was overcome we shall consider next the problem of stability with respect to the present calculation.

The unstable region.

In the primary calculation it was found that the stability condition

$$h_{j,k} = z_{j,k+1} - 2z_{j,k} + z_{j,k-1} \geq 0 , \qquad (2,23)$$

was violated at nodes on $\psi = .1$ for $x \geq 0.08$. The values of $h_{j,k}$ along the line $\psi = .1$ are given in Table (2,7).

| | | | | | | | | |
|---|---|---|---|---|---|---|---|---|
| x | .05 | .0525 | .0550 | .0575 | .06 | .0625 | .0650 | .0675 |
| $h_{j,1}$ | .0207 | .0185 | .0163 | .0143 | .0124 | .0104 | .0084 | .0066 |
| x | .07 | .0725 | .0750 | .0775 | .08 | .0825 | .0850 | .0875 |
| $h_{j,1}$ | .0051 | .0036 | .0011 | .0004 | -0009 | .0023 | -0037 | - 0048 |
| x | .09 | .0925 | .0950 | .0975 | .10 | .1025 | .1050 | .1075 |
| $h_{j,1}$ | -0060 | -.0071 | -.0083 | -.0093 | -.0103 | -.0114 | -0124 | -0133 |
| x | .11 | .1125 | .1150 | .1175 | .12 | .1225 | .1250 | .1275 |
| $h_{j,1}$ | -.0142 | -.0151 | -0160 | -0166 | -0176 | -.0185 | -0193 | -0201 |

Variation of $h_{j,k}$ along $\psi = .1$

TABLE (2,7)

Because of the regularity of the calculated values of $z$ it was assumed that the instability was mild in effect. Another reason for continuing the calculation even although the stability condition is violated is that this condition might be over stringent. We must now examine however more closely the instability in the present problem.

The inherent stability condition is violated not only along the line $\psi = .1$ but in a region near the plate. This can best be demonstrated by considering the differential equation,

$$\frac{\partial z}{\partial x} = \sqrt{u_1^2 - z}\ \frac{\partial^2 z}{\partial \psi^2}\ .$$

From the differential equation it is seen that $\frac{\partial z}{\partial x}$ has the same sign as $\frac{\partial^2 z}{\partial \psi^2}$ and since it is the sign of $\frac{\partial^2 z}{\partial \psi^2}$ which governs the instability we shall examine $\frac{\partial z}{\partial x}$ .

In the free stream $\frac{\partial z}{\partial x} = 0$ and on the plate $\frac{\partial z}{\partial x} = - 2\ (1 - x)$.

Along any station $x$ it is found that as we move in from the free stream $\frac{\partial z}{\partial x}$ increases from zero to a maximum positive value and subsequently decreases through zero to the negative value it assumes on the plate. We thus have, at any station $x$, a small interval $0 \leqq \psi \leqq \varepsilon$ in which $\frac{\partial z}{\partial x}$ and hence $\frac{\partial^2 z}{\partial \psi^2}$ is negative, with the result that at all points in this interval the stability condition (2,23) is violated.

By the above argument we have divided the boundary layer into two parts, the main body of the layer at all points of which the stability criteria (2,24) are satisfied and a thin region next to the plate at which the inherent stability condition (2,23) is violated. This, the unstable region, is bounded by the locus $\frac{\partial^2 z}{\partial \psi^2} = 0$ and gradually thickens as we move downstream until at $x = .12$ it extends to somewhere between $\psi = .1$ and $\psi = .2$.

The above division of the boundary layer is similar to the division employed in the method of inner and outer solutions of the same problems by Von Karman and Millikan [34].

It should be pointed out that the existence of a region of instability is purely a function of the free stream flow. In the present problem $u_1 = 1 - x$, which represents a decelerated flow, in which there exists a region of instability. In an accelerated flow $\frac{\partial u_1}{\partial x} \geq 0$ and so on the plate $(\frac{\partial z}{\partial x})_o \geq 0$, and hence there is no region of instability.

The effect of the instability on the calculation is a function of the mesh size. If, in the present problem, we had chosen $\Delta\psi = .2$ then the condition (2,23) would have been satisfied at all the nodes in the field (the condition may of course be violated downstream of $x = .13$). To use such a technique to overcome the difficulty would be inadvisable because any increase in mesh size impairs the accuracy of the difference replacement and also we are achieving no useful purpose since the region we are mainly interested in is near the plate. The smaller the mesh size taken however the more accurately is the region of instability defined.

It should be pointed out that the effects of instability may not be confined to the unstable region, they may in fact spread out into the boundary layer. This can be seen if we examine the node $x = .0825$, $\psi = .1$.

We assume that the calculated value of $z$ at the above node is in error due to a breakdown of condition (2,23) at $\psi = .1$ on $x = .08$. In the calculation of $z$ at nodes on $x = .0850$ the stability condition is satisfied at $\psi = .2$ but since to calculate the value of $z$ at this node we use the value of $z$ at $(.0825, .1)$, this calculated value may also be in error, regardless of the fact that it is in the stable region. By the above process errors may be introduced at stations right out toward the free stream as the calculation proceeds.

Since the stability condition violated is inherent in the differential equation it is applicable to all finite difference replacements of the same order as the differential equation. If we are searching for a new difference equation, stable over all the boundary layer it must be, if in fact it exists, of a higher order and it is thus much more complex. Rather than change the difference equation an alternative technique for calculating the velocities in the unstable region is discussed.

Calculation of velocities in the unstable region.

One method which may be used to calculate the velocity at nodes in the unstable region, in which the difference equation can only be used with reserve, is described below.

The primary calculation is interupted at the station $x = .08$, at which station condition (2,23) is violated at $\psi = .1$ and we seek an alternative procedure for finding $z\ (.0825,\ .1)$.

The values of $z$ at the nodes .2, .3, .4 ... are calculated on $x = .0825$. From the values of $z$ at the $\psi = .2$ node on $x = .0775$, .08 and .0825 an approximate value of $\left(\frac{\partial z}{\partial x}\right)_{.0825}$ is obtained in the form.

$$\left(\frac{\partial z}{\partial x}\right)_{.0825} = 200\ (z_{.0775} - 4z_{.08} + 3z_{.0825}),\quad \psi = .2.$$

The above process is repeated to estimate $\left(\frac{\partial z}{\partial x}\right)$ at $\psi = .3,\ .4,\ .5\ ...$ on $x = .0825$, the value of $\left(\frac{\partial z}{\partial x}\right)_o$ being known from the boundary conditions.

A divided difference interpolation is now used to find a value for $\left(\frac{\partial z}{\partial x}\right)$ at $\psi = .1$ on $x = .0825$. From this value of $\left(\frac{\partial z}{\partial x}\right)$ and the formula (2,29) we can find a value for $z$ at $\psi = .1$ on $x = .0825$.

Having now obtained a value for $z$ at all the nodes on $x = .0825$, we next proceed to calculate $z$ on the line $x = .0850$. The value of $z$ at (.0850, .2) must be recalculated using the revised value of $z$ at (.0825, .1). The technique just described is then used to find $z$ at (.0850, .1) all the other values remaining the same.

Bearing in mind that as the calculation proceeds more and more points in the stable region may have to be reexamined, the values of $z$ at nodes near the plate are recalculated from $x = .08$ to $x = .12$. Selected values are compared with the values of $z$ resulting from the primary calculation in Table (2,8).

| $\psi$ | $x = .08$ | | $x = .09$ | | $x = .10$ | | $x = .11$ | | $x = .12$ | |
|---|---|---|---|---|---|---|---|---|---|---|
| | $z_c$ | $z$ | $z_c$ | $z$ | $z_c$ | $z$ | $z_c$ | $z$ | $z_c$ | $z$ |
| .1 | .6812 | .6812 | .6803 | .6800 | .6776 | .6770 | .6750 | .6728 | .6700 | .6675 |
| .2 | .5151 | .5151 | .5258 | .5259 | .5338 | .5337 | .5398 | .5393 | .5440 | .5430 |
| .3 | .3699 | .3699 | .3878 | .3879 | .4025 | .4025 | .4144 | .4144 | .4243 | .4241 |
| .4 | .2529 | .2529 | .2736 | .2736 | .2913 | .2913 | .3065 | .3065 | .3195 | .3195 |
| .5 | .1643 | .1643 | .1845 | .1845 | .2025 | .2025 | .2183 | .2185 | .2325 | .2325 |

$z_c$ are values corrected for stability.

$z$ are values from primary calculation.

Correction for Stability.

<u>TABLE (2,8)</u>

From the table of results it is seen that the numerical difference between the values of $z$ is small and the differences are in fact largely concentrated in the line $\psi = .1$, little change being produced in the values of $z$ at $\psi = .2, .3 \ldots$. This tends to confirm the assumption that the instability is mild.

The change in the velocity at $x = .12$, $\psi = .1$ is small, $u_c = .3230$ as compared with $u = .3270$. This change, however, does affect the values of $z$ calculated using the method (D). If we use the method D to calculate $u$ at $\psi = .025$ on $x = .120$ starting with $u = .3230$ at $\psi = .1$

it is found that $u = .138$ as compared with $u = .1413$ from the original calculation and $u = .132$ from Leigh.

The above method which has been put forward as a means of calculating the velocity in the unstable region may be incorporated in the primary calculation, especially if this calculation is performed on an electronic computing machine.

At any stage in the calculation the sign of $h_{j,k}$ from (2,23) is tested, if the sign is positive (as will be the case in the major part of the field) the finite difference calculation is used, if the sign is negative a technique similar to that just described will be employed.

The next section was prompted by a suggestion of Professor Görtler that the singularity of the Von Mises equation at the plate might be the reason for the region of instability, as produced by a finite difference calculation. This confirming, in his view, that the Von Mises equation is unsuitable as a basis for numerical calculation.

The singularity of the Von Mises equation.

If the Von Mises equation

$$\frac{\partial z}{\partial x} = \sqrt{u_1^2 - z}\ \frac{\partial^2 z}{\partial \psi^2},$$

is examined at $\psi = 0$ it is found that $\left(\frac{\partial^2 z}{\partial \psi^2}\right)_0 = \infty$ since $\left(\frac{\partial z}{\partial x}\right)_0$ is finite and $(z)_0 = u_1^2$. Because of this singularity it is supposed that the Von Mises equation can not be used in a numerical technique for solving boundary layer problems. A discussion of this is given by Prandtl [16] and Görtler [17].

It was also pointed out that the singularity may be the reason for the region of instability. That this is not so can be readily seen by examining two different flows.

In a decelerated flow there is a singularity on the plate and a region of instability. In an accelerated flow there is still a singularity on the plate although in this case the equation is stable at all points in the boundary layer. The singularity on the plate must in some way be incorporated in the solution and this can best be done by considering the compatibility conditions on the plate.

Compatibility conditions on the plate.

In non dimensional form the Prandtl boundary layer equations are,

$$u \frac{\partial u}{\partial x} + v \frac{\partial u}{\partial y} = u_1 \frac{du_1}{dx} + \frac{\partial^2 u}{\partial y^2}, \qquad (2,29)$$

$$\frac{\partial p}{\partial y} = 0,$$

$$\frac{\partial u}{\partial x} + \frac{\partial v}{\partial y} = 0,$$

where $u = v = \frac{\partial u}{\partial x} = \frac{\partial v}{\partial y} = 0$ when $y = 0$.

If we are interested in conditions near the plate we can find from (2,29) certain relations connecting the derivations on the plate. In the manner described by Prandtl [16] we write (2,29) for $y = 0$ to obtain

$$\left(\frac{\partial^2 u}{\partial y^2}\right)_0 = - u_1 \frac{du_1}{dx} .$$

If we now repeatedly differentiate (2,29) we find certain other conditions on the plate, the first of which is that $(\frac{\partial^3 u}{\partial y^3})_o = 0$. If the equation (2,29) is to be satisfied near the plate then the particular expression for u must satisfy the above compatability conditions on the plate. In particular if we express u in the form

$$u(y) = \alpha_1 y + \alpha_2 \frac{y^2}{2!} + \alpha_3 \frac{y^3}{3!} + \dots , \qquad (2,30)$$

then all the constants $\alpha$ (constants at any station $x = \text{const}$) are not free. We can in fact show that

$$\alpha_2 = - u_1 \frac{du_1}{dx}, \ \alpha_3 = 0, \ \alpha_5 = 0, \ \alpha_6 = - 2\alpha_2(\frac{du_1}{dx})^2, \ \dots, \qquad (2,31)$$

with the remaining constants $\alpha_1, \alpha_4, \alpha_7 \dots$, free.

In the numerical solution of Witting [20] he evaluates the velocity at nodes in the (x,y) plane and to find the velocity near to the plate he expresses u in the form (2,30) including the relations (2,31). Using such a technique it is possible to calculate the free constants at any station x from the known values of velocity. This enables an accurate representation of the velocity in the neighbourhood of the plate to be achieved, along with a comrespondingly accurate value of $(\frac{\partial u}{\partial y})_o$. Leigh [21] uses a similar technique to find $(\frac{\partial u}{\partial y})_o$ and hence the separation point.

At first sight it would seem that since $(\frac{\partial^2 z}{\partial \psi^2})_o$ is infinite we are unable to find an equivalent set of compatability conditions for z. We do know, however, that on the plate

$z = u_1^2$ , $\frac{\partial z}{\partial \psi} = -2\frac{\partial u}{\partial y}$ is finite and $\frac{\partial^2 z}{\partial \psi^2}$ is infinite.

If we consider an expansion of the form

$$z = z_o + A\psi + B\psi^n, \tag{2,32}$$

to satisfy the above conditions we require $1 \angle n \angle 2$.

At this point it is interesting to compare (2,32) with the technique used to establish the formula

$$f(o,x) = \frac{f^2(.025,x) - f(.05,x)\, f(.0125,x)}{2f(.025,x) - f(.05,x) - f(.0125,x)},$$

which was used in Method (C).

The above formula resulted from considering

$$f(\psi,x) = \frac{z(\Delta\psi,x) - z(o,x)}{\Delta\psi} = A + B(\Delta\psi)^m, \quad 0 \angle m \angle 1,$$

or

$$z\ (x,\Delta\psi) = z\ (x,o) + A\Delta\psi + B(\Delta\psi)^{m+1}\ .$$

This formula is exactly equivalent to (2,32) and the accuracy of the Method (C) might well be explained by this fact.

Corresponding to (2,32) we could equally well consider an expansion for $u$ of the form,

$u = \psi^n\ (a + b\psi^{1/2} + c\psi + d\psi^{3/2} + \ldots)$ where $0 \angle n \angle 1$.

If we substitute this value for $u$ in the Von Mises equation in the form

$$-\tfrac{1}{2}\frac{\partial z}{\partial x} = u^2\ \frac{\partial^2 u}{\partial \psi^2} + u\ \left(\frac{\partial u}{\partial \psi}\right)^2\ . \tag{2,33}$$

and if we choose $\psi = 0$ we find that $n = \frac{1}{3}$ and further that

$$\frac{3}{4}\ a^2b = -\ \tfrac{1}{3}\ (\frac{\partial z}{\partial x})_o\ .$$

We can thus write $u$ in the form

$$u = a\ \psi^{\frac{1}{2}} - \frac{2}{3a^2}\ (\frac{\partial z}{\partial x})_o.\ \psi + c.\psi^{3/2} + d.\psi^2. \qquad (2,34)$$

If now we differentiate (2,33) we obtain

$$\frac{\partial u}{\partial \psi}\ \frac{\partial u}{\partial x} + u\frac{\partial^2 u}{\partial x \partial \psi} = 4u\ \frac{\partial^2 u}{\partial \psi^2} + u^2\ \frac{\partial^3 u}{\partial \psi^3} + (\frac{\partial u}{\partial \psi})^3\ ,$$

and substituting (2,34) for $u$ in the above expression and choosing $\psi = 0$ we obtain a further compatability condition

$$c = -\frac{7}{8}\ \frac{b^2}{a} = -\frac{7}{18}\ \frac{1}{a^5}\ (\frac{\partial z}{\partial x})_o^2\ .$$

We can thus further refine (2,34) to give,

$$u = a\psi^{1/2} - \frac{2}{3a^2}\ (\frac{\partial z}{\partial x})_o.\ \psi - \frac{7}{18a^5}\ (\frac{\partial z}{\partial x})_o^2.\ \psi^{3/2} + d\psi^2, \qquad (2,35)$$

In a similar fashion we can find corresponding expansions for $z$ and $\frac{\partial z}{\partial x}$ for small values of $\psi$ namely

$$z = z_o - a^2\psi - 2ab\psi^{3/2} + (b^2 + 2ac)\psi^2 - 2(bc + ad)\psi^{5/2}$$

$$- (c^2 + 2bd)\psi^3 - 2cd\psi^{7/2} - d^2\psi^4, \qquad (2,36)$$

and

$$\frac{\partial z}{\partial x} = (\frac{\partial z}{\partial x})_o - a(\frac{7}{2}\ b^2 + 4ac)\psi^{1/2} - ({}^{15}/_2\ a^2d + 2b^3 + 13abc)\psi$$

$$- (10^a c^2 + \frac{19}{2}\ b^2c + 21abd)\psi^{3/2} - (27bc^2 + 14b^2d + 29acd)\psi^2 -$$

$$\left(-\frac{9}{2}\ ad^2 + 6c^2 + 37bcd\right)\psi^{5/2} - \frac{57}{2}\ c^2d\psi^3 - \frac{11}{2}cd^2\psi^{7/2} + 12d^3\ \psi^4. \qquad (2,37)$$

In (2,36) and (2,37) a, b and c carry the same significance as in (2,35). It is obvious that to obtain the same accuracy as (2,35) terminated at $\psi^2$ we need terms in $\psi^4$ in both (2,36) and (2,37) and so the expression for the velocity will be used in the extrapolation which is to follow.

Equation (2,37) may explain why Method (D) broke down. In Method (D) the singularity in $\frac{\partial z}{\partial x}$ at $\psi = 0$ was completely ignored in the interpolation. If instead of interpolating $\frac{\partial z}{\partial x}$ we found intermediate values using (2,37) then the method might be considerably improved. This will be mentioned later.

It is interesting at this stage to compare the expression (2,35) with the formula which Leigh uses to express $u$ in terms of $y$ in the vicinity of the plate at $x = .1198$. The formula used is

$$u = Ay + .055\, y^2 + By^4, \tag{2,38}$$

and from this equation we find that,

$$\psi = \tfrac{1}{2} Ay^2 + \frac{.055}{3} y^3 + \frac{1}{5} By^5.$$

From the above expression we compute $\psi^{1/2}$, $\psi^{3/2}$ and $\psi^2$ in terms of $y$ which we substitute in

$$u = a\psi^{1/2} + b\psi^2 + c\psi^{3/2} + d\psi^2 .$$

On comparison with the value of $u$ in (2,38) we find that

$$a = 2A, \quad b = \frac{.44}{3a^2}, \quad c = -\frac{.01882}{a^5} .$$

If we now take into account the fact that $\psi_L = 8\,\psi_P$, where $\psi_L$ is the variable used in Leigh's paper and $\psi_P$ is the variable used in the present calculation we find that

$$u = A\,\psi^{1/2} + \frac{1.1736}{a^2}\,\psi - \frac{1.2052}{a^5}\,\psi^{3/2} + d\,\psi^2,$$

which is in fact the particular form of (2,35) at x = .12.

We are now in a position to use (2,34) or (2,35) as an expression for u near the plate.

Expansion of the velocity in the vicinity of the plate.

At any station x, we have shown how we can form a series expansion for the velocity in the vicinity of the plate. Three expansions which include the compatibility conditions on the plate, are considered for comparison purposes as follows,

$$u = a\psi^{1/2} - \frac{2}{3a^2}\left(\frac{\partial z}{\partial x}\right)_o \psi + c\psi^{3/2} + d\psi^2, \qquad (2,34)$$

$$u = a\psi^{1/2} - \frac{2}{3a^2}\left(\frac{\partial z}{\partial x}\right)_o \psi - \frac{7}{18a^5}\left(\frac{\partial z}{\partial x}\right)_o^2 \psi^{3/2} + d\psi^2, \qquad (2,35)$$

$$u = a\psi^{1/2} - \frac{2}{3a^2}\left(\frac{\partial z}{\partial x}\right)_o \psi - \frac{7}{18a^5}\left(\frac{\partial z}{\partial x}\right)_o \psi^{3/2} + d\psi^2 + e\psi^{5/2}, \qquad (2,39)$$

In each of the above expansions it can easily be proved that

$$\left(\frac{\partial u}{\partial y}\right)_o = \frac{1}{2}\,a^2 .$$

Expansion (2,34). (Method E).

At any station x, $\left(\frac{\partial z}{\partial x}\right)_o$ is known and if we know the values of u for three values of $\psi$ we can set up three simultaneous equations to be solved for the three unknowns a, c and d. If c and d are eliminated we can establish an equation for a.

If the three nodes are at $\psi_1$, $\psi_2$ and $\psi_3$ where $\psi_1 = 2\psi_2$, $\psi_2 = 2\psi_3$ and if the values of the velocity at these nodes are $u_1$, $u_2$ and $u_3$ respectively, then the resulting equation to be solved for a is

$$11.312\ U_3 - 6.828\ U_2 + U_1 = 3.656\ \psi_3^{1/2} a - 4.036 \left(\frac{\partial z}{\partial x_o}\right) \psi_3 . \frac{1}{a^2} .$$

(2,40)

The particular form of this equation when $\psi_3 = .0125$ (we are in fact using the three nodes .05, .025 and .0125) is

$$27.7012\ U_3 - 16.7330\ U_2 + 2.4519\ U_1 = a - .03369 \left(\frac{\partial z}{\partial x}\right)_o \frac{1}{a^2} .$$

(2,41)

An alternative equation for a is that formed from the values of u at $\psi = 0.1, 0.2, 0.3$. This equation is

$$37.04\ U_3 - 120.28\ U_2 + 147.76\ U_1 = 13.2193a - 1.221 \left(\frac{\partial z}{\partial x}\right)_o \frac{1}{a^2} .$$

(2,42)

Both of the equations (2,41) and (2,42) are cubic equations with one negative and two positive roots, if all the roots are real. The root which we require is the smallest positive root, since u must be less than unity and positive for all values of $\psi$.

Using (2,42) with the particular values of $(\frac{\partial z}{\partial x})_o$, we calculate a and hence $(\frac{\partial u}{\partial y})_o$ at the stations $x = .05, .06 \dots$ It was found however that at the stations $x = .11$ and $x = .12$, no positive root for a existed. The value of a at $x = .10$ is positive and therefore a must have a zero at $x_\rho$ in the range $.10 < x_\rho < .11$. This zero is the estimated position of the separation point. In order to define the separation point more accurately a is calculated at $x = .105, .1075$ and it is discovered that $.1075 < x_\rho < .11$. The values of a and $(\frac{\partial u}{\partial y})_o$ calculated using (2,42) are given in Table (2,9), a graph of a plotted against x is shown in figure (2,5) and a graph of $(\frac{\partial u}{\partial y})_o$ against x is shown in figure (2,6). In table (2,9) these results are listed under (42).

It must be stressed again that no physical significance should be attached to the negative values of a, they only in fact serve to yield upper bounds for the separation point $x_\rho$.

The above calculation of a and $(\frac{\partial u}{\partial y})_o$ was repeated from $x = .08$ using the values of velocity at $\psi = .1$, $.2$ and $.3$ corrected for instability. The results of this calculation (labelled $42_c$) are shown in Table (2,9) and figures (2,5) and (2,6). In this case it is found that $.1025 < x_\rho < .105$. In other words the correction for stability has moved forward the separation point estimate.

Turning our attention now to equation (2,41) which makes use of the values of velocity calculated in the secondary calculation at $\psi$ = .0125, .025 and .05, we can evaluate a and hence $(\frac{\partial u}{\partial y})_o$ at stations of x along the plate using the equation (2,41). The calculated values of a and $(\frac{\partial u}{\partial y})_o$ are listed as (41) in Table (2,9) and a graph of a against x is given in figure (2,5) and of $(\frac{\partial u}{\partial y})_o$ against x in figure (2,6).

| x | | .05 | .06 | .07 | .08 | .09 | .10 | .11 | .12 | .13 |
|---|---|---|---|---|---|---|---|---|---|---|
| a | 42 | 1.44 | 1.32 | 1.21 | 1.13 | .987 | .856 | -.350 | -.361 | – |
| | $42_c$ | 1.44 | 1.32 | 1.21 | 1.13 | .976 | .838 | -.352 | -.359 | – |
| | 41 | 1.435 | 1.307 | 1.202 | 1.092 | .989 | .876 | .755 | .580 | -.255 |
| | Howarth | 1.42 | 1.29 | 1.17 | 1.05 | .933 | .800 | .616 | .000 | – |
| $\frac{\partial u}{\partial y_o}$ | 42 | 1.03 | .87 | .73 | .60 | .49 | .37 | – | – | – |
| | $42_c$ | 1.03 | .87 | .73 | .60 | .48 | .35 | – | – | – |
| | 41 | 1.03 | .85 | .72 | .60 | .49 | .38 | .28 | .17 | – |
| | Howarth | 1.0 | .83 | .68 | .55 | .435 | .32 | .19 | .00 | – |

a and $(\frac{\partial u}{\partial y})_o$ at stations along the plate.

TABLE (2,9)

In this calculation $x_s$ is found to be in the range $.12 \angle x_s \angle .13$ and on a closer examination the range is reduced to $.121253 \angle x_s \angle .121875$.

The values of a calculated to produce this refinement are given in Table (2,10) and illustrated in Figure (2,7).

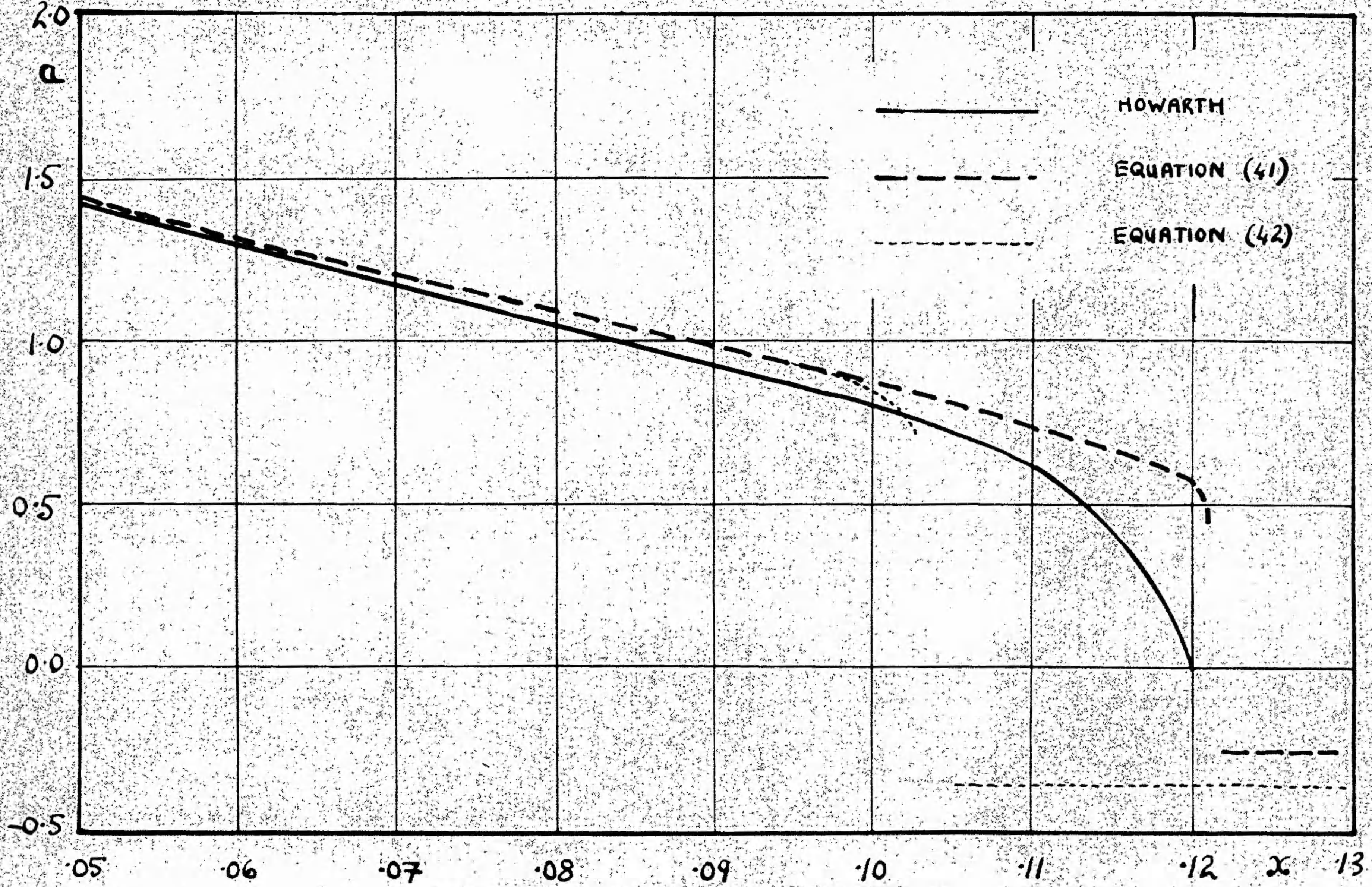


a at stations along the plate

FIGURE (2,5)

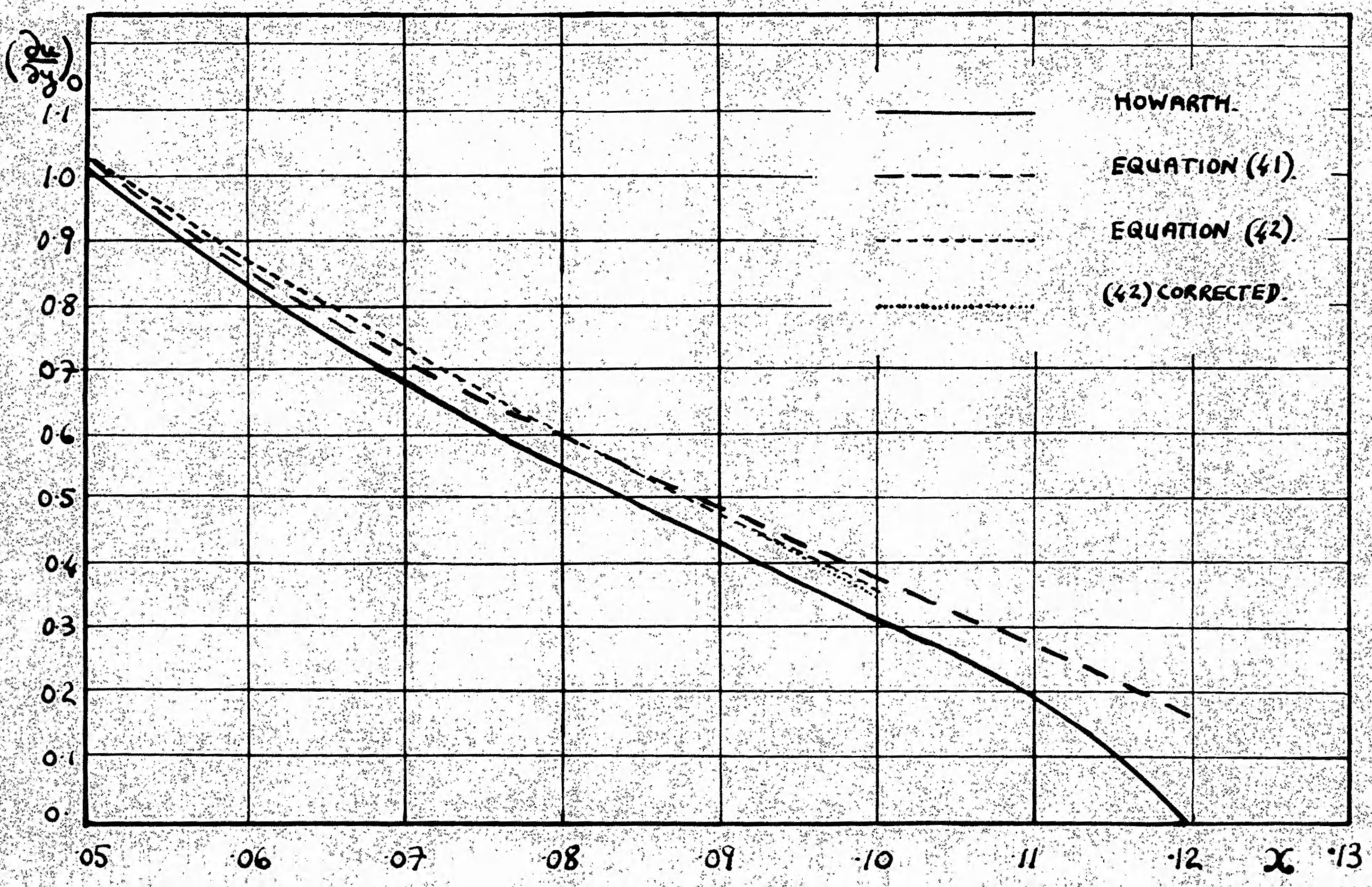


$(\frac{\partial u}{\partial y})_0$ at stations along the plate

<u>FIGURE (2,6)</u>

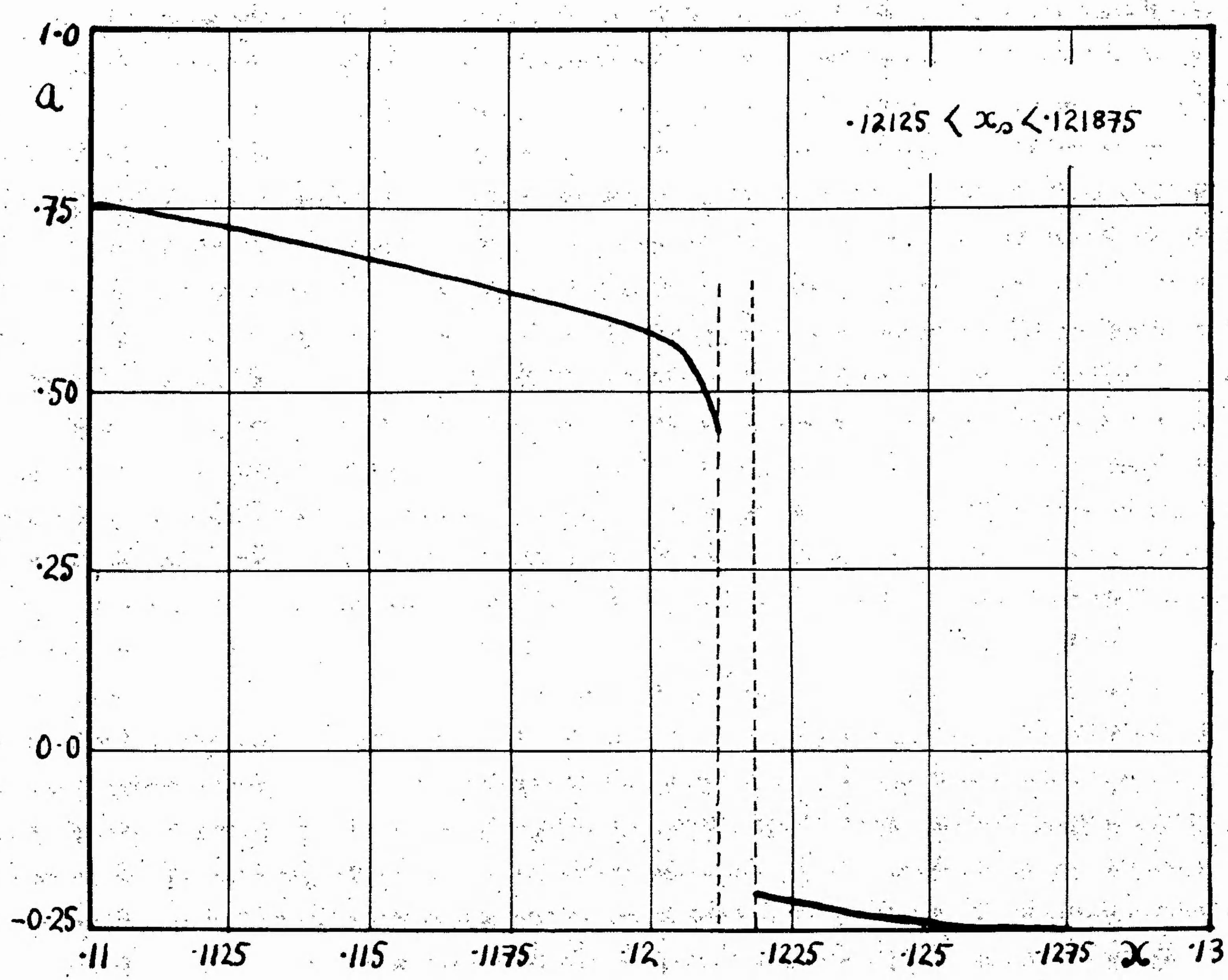


a calculated between x = .11 and x = .13

FIGURE (2,7)

| | | | | | |
|---|---|---|---|---|---|
| x | .11 | .1150 | .1175 | .120 | .120625 |
| a | .755 | .680 | .633 | .58 | .565 |
| $(\frac{\partial u}{\partial y})_o$ | .28 | .231 | .200 | .168 | .159 |
| x | .12125 | .121875 | .1225 | .125 | .13 |
| a | .45 | -.245 | -.2465 | -.250 | -.255 |
| $(\frac{\partial u}{\partial y})_o$ | .101 | — | — | — | — |

a and $(\frac{\partial u}{\partial y})_o$ using (2,41) in $.11 < x < .13$.

TABLE (2,10)

It seems safe to assume that if the values of $u$ at the nodes $\psi = .0125$, $.025$ and $.05$ were corrected for stability a shift forward of the separation point would result. As it is, the above value of $x_s$ agrees favourably with the now generally accepted value of $x_s = .1198$, obtained by Leigh.

It should be noted that in figures (2,5) and (2,6) and (2,7) the singular nature of the separation point is ably demonstrated.

We shall now discuss the expansions (2,35) and (2,36).

Expansions (2,35) and (2,36). (Method F).

In expansion (2,35), we require to know the values of $u$ at two stations of $\psi$ (on any line $x$ = const) in order to find an equation for $a$. If we let the values of $u$ at $\psi_2$ and $\psi_3$ be $u_2$ and $u_3$ respectively and if $\psi_2 = 2\psi_3$ the equation to be solved for $a$ is

$$4U_3 - U_2 = 2.586\ \psi_3^{1/2}\ a - 1.333\left(\frac{\partial z}{\partial x}\right)_o \frac{\psi_3}{a^2} - .4557\left(\frac{\partial z}{\partial x}\right)_o \frac{\psi_3^{3/2}}{a^5}, \tag{2,43}$$

a sextic equation.

In a similar manner if $u_1$, $u_2$ and $u_3$ are the values of velocity at $\psi_1$, $\psi_2$ and $\psi_3$ where $\psi_1 = 2\psi_2 = 4\psi_3$, then we can use these values of the velocity to eliminate d and e from three equations of the form (2,36) and so produce a more accurate sextic equation for a of the form

$$22.624\ U_3 - 9.656\ U_2 + U_1 = 10.9698\ \psi_3^{1/2}\ a$$

$$- 4.8747\left(\frac{\partial z}{\partial x}\right)_o \frac{\psi_3}{a^2} - 1.288\left(\frac{\partial z}{\partial x}\right)_o^2 \psi_3^{3/2}\ \frac{1}{a^5}\ . \tag{2,44}$$

Using the particular forms of (2,43) and (2,44) corresponding to $x = .11$ the values of a and $\left(\frac{\partial u}{\partial y}\right)_o$ were calculated for varying values of $\psi_3$. The values of velocity at the nodes $\psi = .2, .1, .05, .025, .0125$ are taken from the primary and secondary calculations. The calculated values are given in Table (2,11), the nomenclature being the same as in Table (2,9). The values of velocity corrected for stability at $x = .11$, $\psi = .2$ and $.1$ are also used to produce a value of a and $\left(\frac{\partial u}{\partial y}\right)_o$ as shown in Table (2,11).

| $(\partial u/\partial y)_o$ | | | | | | | | |
|---|---|---|---|---|---|---|---|---|
| $\psi_3$ | 43 | 44 | 43c | 44c | 42 | 42c | 41 | HOWARTH |
| .1 | .377 | .373 | .372 | .366 | .366 | .351 | | .320 |
| .05 | .375 | .371 | | | | | | |
| .025 | .377 | .378 | | | | | | |
| .0125 | .380 | .381 | | | | | .380 | |

Calculation of $(\frac{\partial u}{\partial y})_o$ on $x = .11$

TABLE (2.11)

From the close similarity between the values of $(\frac{\partial u}{\partial y})_o$ calculated from (2,43) and (2,44) it was decided that a and $(\frac{\partial u}{\partial y})_o$ should be calculated at $x = .12$ using (2,43) for convenience.

At the station $x = .12$ the values of a and $(\frac{\partial u}{\partial y})_o$ are calculated in a similar manner using (2,43) with $\frac{\partial z}{\partial x} = - 1.76$. The result of this calculation is given in Table (2,12).

| | 43 | | 43c | | 41, 42c | | HOWARTH |
|---|---|---|---|---|---|---|---|
| $\psi_3$ | a | $(\partial u/\partial y)_o$ | a | $(\partial u/\partial y)_o$ | a | $(\partial u/\partial y)_o$ | $(\partial u/\partial y)_o$ |
| .1 | .725 | .263 | .721 | .260 | .580 | .17 | 0.0. |
| .05 | .649 | .211 | | | | | |
| .025 | .638 | .203 | | | | | |
| .0125 | .627 | .174 | | | -.359 | - | |

$(\frac{\partial u}{\partial y})_o$ at $x = .120$

TABLE (2,12).

From table (2,12) it is seen that the method (F) produces different results from the method (E), the latter producing good results while the former, although a more accurate formula, does not.

In order to discover why this should be so we shall apply both methods to Leigh's results.

METHOD (E) and (F) applied to Leigh's results.

From Leigh [21] at $x = .1198$ $u$ is known as a function of $y$. From this we numerically integrate, using Sutherland's law, to find $\psi$ in terms of $u$, and from this we can find $u$ at $\psi$ nodes on $x = .1198 \doteqdot .12$.

| | | | | | |
|---|---|---|---|---|---|
| $\psi$ | .2 | .1 | .05 | .025 | .0125 |
| $u_L$ | .4780 | .3200 | .2075 | .1325 | .0830 |
| $\psi$ | .00625 | .003125 | .0015625 | .00078125 | |
| $u_L$ | .0548 | .0345 | .0210 | .0125 | |

Values of $u$ from Leigh's results at $x = .120$

TABLE (2,13).

A table of values of $u_L$ against $\psi$ is given in Table (2,13). The first thing to be noticed from Table (2,13) is that Leigh's primary calculation, which stops at $y_L = .1$ (as opposed to $\psi = .1$ of the present paper) is much nearer the plate. This is an obvious disadvantage of the present method since a much smaller mesh size in the $\psi$ - direction is required to find the conditions on the plate.

Two/

Two calculations are carried out to find $a$ and $(\frac{\partial u}{\partial y})_o$ from Leigh's results.

Using (2,40) with the particular value of $(\frac{\partial z}{\partial x})_o$ we calculate $a$ and $(\frac{\partial u}{\partial y})_o$. The results, given as functions of $\psi_3$, are shown in Table (2,14) and the values of $a$ are illustrated in Figure (2,8).

Using (2,43) $a$ and $(\frac{\partial u}{\partial y})_o$ are calculated for decreasing values of $\psi_3$, again the results being given in Table (2,14) and illustrated in Figure (2,8).

| $\psi_3$ | (40) | | (43) | |
|---|---|---|---|---|
| | $a$ | $(\partial u/\partial y)_o$ | $a$ | $(\partial u/\partial y)_o$ |
| .1 | -.923 | | .713 | .254 |
| .05 | -.820 | | .611 | .187 |
| .025 | -.710 | | .573 | .164 |
| .0125 | -.710 | | .502 | .126 |
| .00625 | -.570 | | .485 | .118 |
| .003125 | -.480 | | .420 | .088 |
| .0015625 | -.480 | | .360 | .065 |
| .00078125 | -.405 | | .300 | .045 |

$a$ and $(\frac{\partial u}{\partial y})$, calculated from Leigh's result.

<u>TABLE (2,14)</u>.

From the table and figure it is seen that as $\psi_3$ tends to zero, $(\frac{\partial u}{\partial y})_o$ tends to zero, indicating that $x_s = .120$ from Leigh's results. To illustrate the fact that $(\frac{\partial u}{\partial y})_o$ does markedly decrease with $\psi_3$ we need only compare Table (2,14) with Table (2,11).

From/

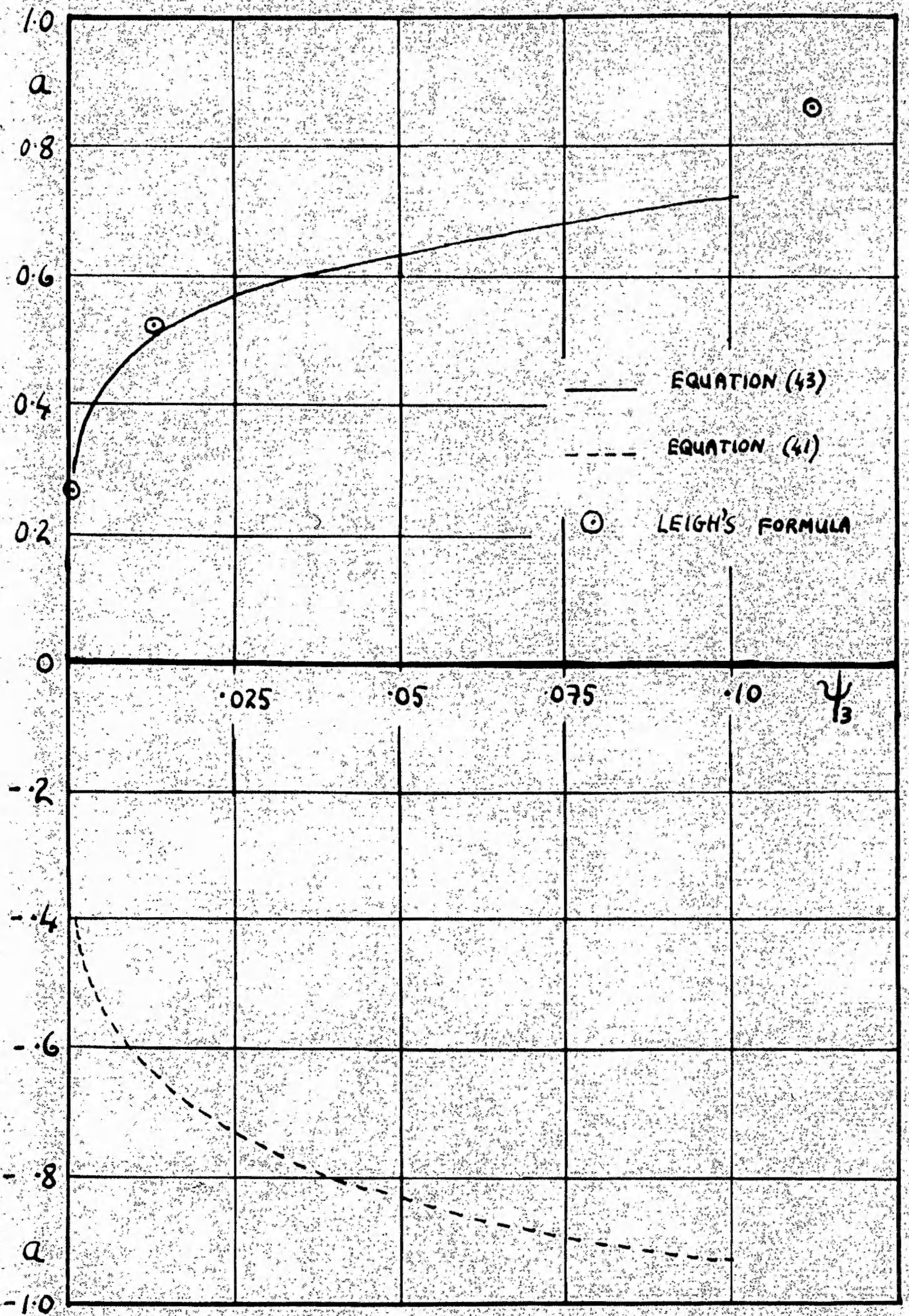


a calculated at x = .120 from Leigh's values

<u>FIGURE (2,8)</u>

From Table (2,11) we see that at $x = .11$, the value of $(\frac{\partial u}{\partial y})_o$ remains nearly constant as we decrease $\psi_3$ .

Another feature of figure (2,8) is that whereas the value of $a$ using (2,43) approaches $o$ from above, the value using (2,40) approaches $o$ from below.

If we consider the picture of $(\frac{\partial u}{\partial y})_o$ along the plate it is obvious that the calculated value of separation from (2,43) will approach the true value from the right as $\psi_3 \rightarrow 0$ and using (2,40) the calculated value will approach the true value from the left. This latter shift is confirmed in figure (2,5).

As a final check on the methods of extrapolation $(\frac{\partial u}{\partial y})_o$ is calculated at stations $y$ using Leigh's formula (2,38). The values are given in Table (2,15) and shown in figure (2,8). For reference in Table (2,15) the corresponding value of $\psi_3$ to the lower value of $y$ is listed.

| $\div\psi_3$ | $y$ | $(\partial u/\partial y)_o$ |
|---|---|---|
| | .1, .2 | .017 |
| .0005 | .4, .8 | .040 |
| .0130 | 1.2, 1.6 | .126 |
| .1012 | 2.4, 2.8 | .239 |

$(\frac{\partial u}{\partial y})_o$ calculated using Leigh's method.

<u>TABLE (2,15)</u>.

From/

From figure (2,8) it is obvious that at any equivalent station of $\psi_3$ the calculation of $(\frac{\partial u}{\partial y})_0$ in terms of $\psi$ is just as accurate as the corresponding calculation in terms of $y$ and so the singularity on the plate does not prevent us from accurately assessing conditions on and near the plate.

## 2.D.

## SUMMARY.

In section (2) the application of a finite difference technique for solving the incompressible boundary layer equations has been examined. From the work carried out we deduce that there are two parts to the problem, (a) the calculation of the velocity in the boundary layer and (b) the determination of the conditions near the plate from the results of (a). It would appear that in the present calculations, the mesh size $\Delta\psi = .1$ is on the large side. The use of a smaller mesh size would probably require the use of an electronic computer.

The velocity is calculated at the majority of nodes in the boundary layer using the finite difference equation but an alternative procedure may be used to find the velocity at nodes in the unstable region. Several methods of finding conditions near the plate have been discussed. The method (C) furnishes a simple and relatively accurate means of finding the velocity gradient on the plate and hence locating the separation point.

An alternative approach for finding the velocity near the plate (at all points in the unstable region) is to use method (D) in which $\frac{\partial z}{\partial x}$ is expressed in the form of (2,37) which incorporates the singularity on the plate.

Perhaps the most accurate determination of

$(\frac{\partial u}{\partial y})_o$ stems from the methods (E) and (F). Using either of these methods we find an expression for $u$ in the vicinity of the plate and from this expansion $(\frac{\partial u}{\partial y})_o$ is determined. With a smaller initial mesh size the two calculated values for $x_\rho$ although still on either side of the true value, will be almost coincident. Thus the separation point can be accurately determined.

The velocity is obtained in terms of $y$ by evaluating numerically $y = \int_0^\psi \frac{d\psi}{u}$ at each station $x$. The integrand is infinite at the lower limit and so it is necessary to evaluate $y$ in the form

$$y = \int_0^{u'} \frac{du}{u\frac{du}{d\psi}} + \int_{\psi'}^{\psi} \frac{d\psi}{u}$$

where $u'$ is the velocity corresponding to $\psi'$ an arbitrary small value of $\psi$ and $u\frac{\partial u}{\partial \psi}$ takes the value $\frac{1}{2}a^2$ on the plate.

In conclusion, we may say that the method produces satisfactory results, which will be improved by a reduction in mesh size. The value of the separation point found is $x_\rho = .122$, compared with the true value of $x_\rho = .1198$.

The method used by Leigh produces a more accurate value for the separation point in the incompressible case, but the present method which does not necessarily require the velocity to be given at a starting station $x$, is also applicable to compressible flow problems for which it is primarily intended.

# SECTION III.

## COMPRESSIBLE BOUNDARY LAYER.

3 A

GENERAL METHOD OF SOLVING THE BOUNDARY LAYER EQUATIONS.

In section (2) the Von Mises form of the boundary layer equations was tested as a means of evaluating the velocity field in an incompressible boundary layer adjacent to a flat plate. We have shown that, although there are certain difficulties to be overcome, the numerical technique based on the Von Mises equation is particularly straightforward to apply.

The results of section (2) are in good agreement with known results, derived by more complex methods, and the accuracy can be improved by refining the mesh sizes.

Having justified numerical methods based on the Von Mises transformation in incompressible flow problems we shall now proceed to the problem for which it is primarily intended, that of compressible boundary layer flow.

We are now concerned with the steady, two dimensional flow of a compressible fluid past a semi infinite flat plate placed lengthwise to the stream (as far as possible conditions used in section (2) will be maintained for the sake of comparison). In the particular computations carried out in this section the fluid we are considering is air, and it is assumed that air is a perfect gas.

Although supersonic regions exist in parts of the field, the interaction of shock waves and boundary layer will be ignored.

Governing Equations.

In the $(x, \psi)$ plane we assume that the plate is lying along the positive part of the x-axis and that the fluid is approaching the plate with a constant velocity in the positive x-direction.

It is adviseable to make a slight change in notation. We shall denote the mainstream velocity by $U_M$ and all other variables shall bear the subscript $M$ when applied to conditions in the main stream.

The subscript 1 shall denote conditions in the free stream, in which all variables are functions of $x$ only. The relation between the subscripted variables can be illustrated by the result $U_1 = U_M$ at $x = 0$. The subscript o refers to conditions on the plate.

In section (1 A) the existence of thermal and velocity boundary layers (of comparable thickness if $\sigma$ the Prandtl number is of the order of unity) has been proved and we are now set the problem of finding the velocity and temperature inside the boundary layer. For discussion purposes, it is convenient to imagine a single boundary layer, this is not grievously in error since the outer edge of both layers is almost coincident, as will be seen in the results to follow.

In order to evaluate the velocity and temperature (in actual fact it is more convenient to evaluate velocity and enthalpy) inside the boundary layer we use a finite difference technique to solve the compressible boundary layer equations in Von Mises form.

The governing equations, in the usual notation, which were established in (1 B) are

$$\frac{\partial q}{\partial x} = \left[\frac{1}{i_1}\frac{dq_1}{dx}\right] i + \left[\frac{\gamma p}{\gamma - 1}\right] q^{\frac{1}{2}} \frac{\partial}{\partial \psi}\left(\frac{\mu}{i}\frac{\partial q}{\partial \psi}\right), \qquad (3,1)$$

$$\frac{\partial p}{\partial \psi} = 0, \qquad (3,2)$$

$$\frac{\partial i}{\partial x} = -\left[\frac{1}{2i_1}\frac{dq_1}{dx}\right] i + \left[\frac{\gamma p}{\sigma(\gamma-1)}\right] \frac{\partial}{\partial \psi}\left(\frac{\mu q^{\frac{1}{2}}}{i}\frac{\partial i}{\partial \psi}\right)$$

$$+ \left[\frac{\gamma p}{4(\gamma-1)}\right] \frac{\mu}{i q^{\frac{1}{2}}}\left(\frac{\partial q}{\partial \psi}\right)^2. \qquad (3,3)$$

In the above equations $q = u^2$, $i = c_p T$ is the enthalpy and $\sigma = \frac{\mu c_p}{k}$ is the Prandtl number. The viscosity $\mu$ is a function of the enthalpy and from (3,2) we see that the pressure is a function of $x$ only.

Since $p = p(x)$ and all the variables in the free stream are functions of $x$ only all the quantities in square brackets depend solely on $x$.

Before going on to discuss the boundary conditions we will establish two relations connecting the velocity and the enthalpy.

<u>Relations between the velocity and the enthalpy in the main stream.</u>

In the main stream the velocity and enthalpy are constant. If, in the main stream, the velocity of sound is $C_M$ then

$M_M = \dfrac{U_M}{C_M}$ is the Mach number at all points there. $M_M$ is called the initial mach number.

We are assuming that the fluid is a perfect gas and also that in the main and free streams (regions in which the effects of viscosity are neglected) all changes are adiabatic.

It must be noted that no calculation is required in the main stream. Because of the adiabatic property of the main stream we know that

$$C_M^2 = \frac{\gamma p_M}{\rho_M},$$

and since the fluid is a perfect gas we also have

$$\frac{p_M}{\rho_M T_M} = R = C_p - C_v,$$

thus $\quad C_M^2 = \gamma T_M(C_p - C_v) = \gamma i_M(1 - \frac{Cv}{Cp}) = i_M\ (\gamma - 1).$

We can thus deduce that,

$$i_M = \frac{U_M^2}{M_M^2\ (\gamma - 1)}.$$

It is found convenient to define a constant $r$ to be

$$r = \frac{2}{(\gamma - 1)\ M_M^2}. \tag{3,4}$$

In terms of $r$ the relation between $i_M$ and $q_M$ becomes,

$$i_M = \frac{r}{2}\ q_M. \tag{3,5}$$

Relation between the velocity and the enthalpy in the free stream.

For conditions in the free stream equation (3,3) becomes

$$\frac{di_1}{dx} = -\frac{1}{2i_1}\frac{dq_1}{dx}\quad i_1 ,$$

or
$$\frac{di_1}{dx} + \frac{1}{2}\frac{dq_1}{dx} = 0,$$

which integrates to give,

$$i_1(x) + \frac{1}{2}\, q_1(x) = \text{const.}$$

By choosing $x = o$ we find that the constant is $i_M + \frac{1}{2}\, q_M$ and so the free stream enthalpy can be expressed as,

$$i_1(x) = i_M + \frac{1}{2}\, q_M - \frac{1}{2}\, q_1(x) ,$$

$$i_1(x) = \frac{1}{2}\,[q_M(1+r) - q_1(x)\,]. \qquad (3,6).$$

Boundary conditions.

We next consider the boundary conditions which must be specified for a unique solution.

Conditions on the plate.

On the plate the velocity is zero. The condition on the enthalpy however, depends on the nature of the problem. In the thermometer problem the fluid is flowing over a plate on which the temperature distribution is known, whereas in the problem of no heat transfer there is no flow of heat between the plate and the fluid, and so the enthalpy gradient normal to the plate is zero on the plate.

We shall in fact be examining thermometer problems and so on the plate we must specify the temperature or enthalpy distribution. We shall further assume a constant enthalpy distribution on the plate, the particular value of which will be discussed later.

On the plate then, we have the following two conditions

$$q = 0, \quad i = i_o \text{ a known quantity.}$$

Conditions in the free stream.

As discussed in previous sections, the thickness of the velocity boundary layer at any station $x$ is defined as the smallest value of $\psi$ at which $\frac{\partial u}{\partial \psi} \doteqdot 0$, to the degree of accuracy required. In a similar fashion the outer edge of the temperature boundary layer is the locus of points at which $\frac{\partial i}{\partial \psi} \doteqdot 0$. The fact that the two boundary layers are not entirely coincident does not trouble us at all in the calculation.

To be consistent with the work done in section (2 C) we choose the free stream velocity to be,

$$u_1(x) = U_M\left(1 - \frac{x}{L}\right), \text{ when } \frac{\partial q}{\partial \psi} \doteqdot 0.$$

From (3,6) we can see that the corresponding free stream enthalpy is

$$i_1(x) = \frac{q_M}{2}\left[(1 + r) - \left(1 - \frac{x}{L}\right)^2\right] \text{ when } \frac{\partial i}{\partial \psi} \doteqdot 0.$$

Initial condition.

From the evidence gathered in section (2 C) we are justified in starting our calculation at the leading edge of the plate with the classical velocity and enthalpy distributions.

The boundary conditions at $x = 0$ are thus

$$q = q_M \text{ when } \psi > 0, \quad q = 0 \text{ when } \psi = 0,$$

$$i = i_M \text{ when } \psi > 0, \quad i = i_o \text{ when } \psi = 0.$$

We must remember that $q_M$ and $i_M$ are related by (3,5).

A picture of the boundary conditions is given in figure (3,1).

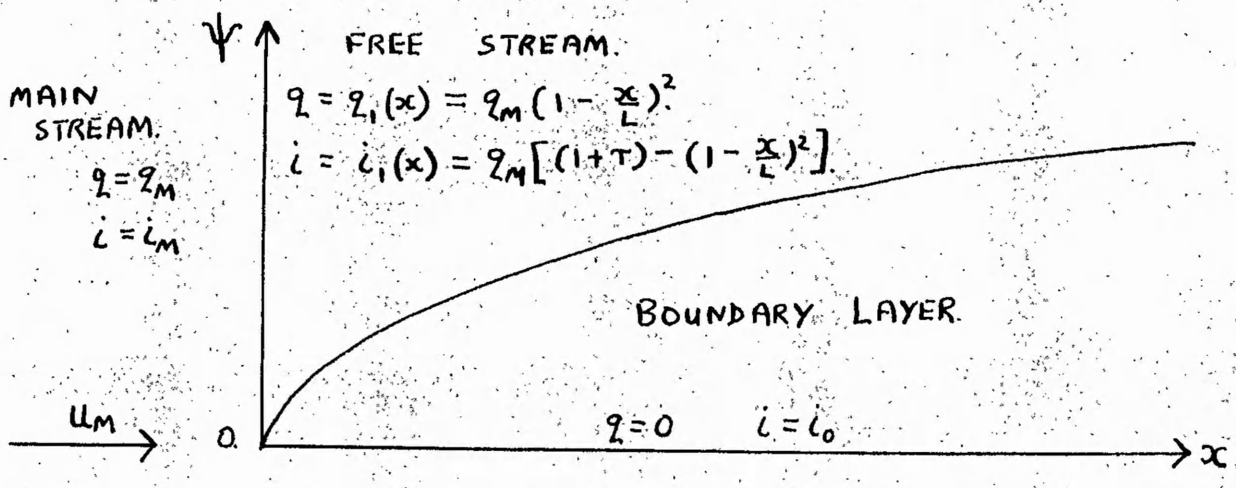


FIGURE (3,1).

Relation between pressure and enthalpy.

We know from equation (3,2) that along any line normal to the plate the pressure is constant, in other words,

$p = p_1(x)$, at all points in the boundary layer.

In/

In the free stream we have an adiabatic perfect gas flow and so

$$\frac{p_1}{(\rho_1)^\gamma} = \text{const} = \frac{p_M}{(\rho_M)^\gamma} ,$$

from which we get

$$\frac{p_1}{p_M} = \left(\frac{\rho_1}{\rho_M}\right)^\gamma .$$

We also know that

$$\frac{p_1}{\rho_1 \, i_1} = \frac{p_M}{\rho_M i_M} ,$$

or

$$\frac{p_1}{p_M} = \frac{i_1}{i_M} \left(\frac{p_1}{p_M}\right)^{1/\gamma} ,$$

and so

$$p = p_1(x) = p_M \left[\frac{i_1(x)}{i_M}\right]^{\gamma/\gamma-1} .$$

We have thus established a formula which enables us to specify the pressure at any point in the boundary layer in the form

$$p = p_M \left[\frac{i_1(x)}{i_M}\right]^{\gamma/\gamma-1} , \qquad (3,7).$$

Relations between viscosity and enthalpy.

As discussed in section (1 A) it is generally accepted that the most accurate representation of the variation of viscosity with temperature is Sutherland's law,

$$\mu = A \, \frac{T^{1.5}}{T + C} , \qquad (3,8)$$

where A and C are constants, and T is the absolute temperature measured in degrees Kelvin.

Many attempts have been made to express $\mu$ in the form

$$\mu = B\,T^{\omega} \tag{3,9}$$

where $B$ and $\omega$ are constants chosen to make (3,9) fit (3,8) as closely as possible over the required range of temperature. For air it is found that over a large range of temperature $\omega \doteq 1$, in other words an alternative approximation for the variation of $\mu$ with $T$ is

$$\mu = CT \tag{3,10}$$

One of the aims of this section is to test the validity of (3,10).

<u>Non Dimensionalising the equations.</u>

The values of velocity, enthalpy, density, viscosity and pressure in the main stream are chosen as the characteristic values of these quantities for the purposes of non dimensionalising the equations. The characteristic length is $L$ and the characteristic stream function $\Psi$ will be determined later.

We construct the non dimensional variables,

$$x' = x/L,\; q' = q/U_M^2\;,\; i' = i/i_M,\; \rho' = \rho/\rho_M\;,\; \mu' = \mu/\mu_M$$

$$p' = p/p_M \text{ and } \psi' = \psi/\Psi\;.$$

The characteristic variables satisfy certain relations, namely

$$i_M = \frac{r}{2}\,U_M^2\;, \text{ and } \frac{p_M}{\rho_M\, i_M} = \frac{\gamma}{\gamma - 1} \tag{3,11}$$

In terms of the non dimensional variables equation (3,1) becomes

$$\frac{\partial q'}{\partial x'} = \left[\frac{1}{i_1'}\ \frac{dq_1'}{dx'}\right] i' + p'(q')^{\frac{1}{2}}\ \frac{\partial}{\partial \psi'}\left(\frac{\mu'}{i'}\ \frac{\partial q'}{\partial \psi'}\right) \frac{\gamma}{\gamma - 1}\left[\frac{p_M \mu_M\ U_M L}{i_M\ \Psi^2}\right].$$

We choose $\frac{\gamma}{\gamma - 1}\left[\frac{p_M \mu_M\ U_M L}{i_M\ \Psi^2}\right] = 1,$

and using (3,11) this reduces to

$$\frac{\mu_M \rho_M U_M L}{\Psi^2} = 1,$$

or $\Psi = \frac{\rho_M U_M L}{\sqrt{R}}$, where the Reynolds number $R = \frac{U_M \rho_M\ L}{\mu_M}$.

We now rewrite equation (3,3) in terms of the non dimensional variables, as

$$\frac{\partial i'}{\partial x'} = -\left[\frac{1}{i_1'}\ \frac{dq_1'}{dx'}\right] i'\ \frac{U_M^2}{2i_M} + \frac{p'}{\sigma}\ \frac{\partial}{\partial \psi'}\left(\frac{(q')^{\frac{1}{2}}\mu'}{i'}\ \frac{\partial i'}{\partial \psi'}\right)\left[\frac{\gamma}{\gamma - 1}\ \frac{p_M \mu_M U_M L}{\Psi^2\ i_M}\right] + \frac{p'\mu'}{i_1'}\ \frac{1}{(q')^{\frac{1}{2}}}\left(\frac{\partial q'}{\partial \psi'}\right)^2 \frac{\gamma}{4(\gamma-1)}\ \frac{p_M \mu_M U_M^3}{i_M^2\ \Psi^2}.$$

Using (3,11) and the value found for $\Psi$ this reduces to

$$\frac{\partial i'}{\partial x'} = -\left[\frac{1}{ri_1'}\ \frac{dq_1'}{dx'}\right] i' + \left[\frac{p'}{\sigma}\right]\ \frac{\partial}{\partial \psi'}\left(\frac{(q')^{\frac{1}{2}}\mu'}{i'}\ \frac{\partial i'}{\partial \psi'}\right) + \left[\frac{p'}{2r}\right]\ \frac{\mu'(q')^{\frac{1}{2}}}{i'}\ \left(\frac{\partial q'}{\partial \psi'}\right)^2.$$

Turning our attention now to the boundary conditions, it it easily verified that in terms of the non dimensional variables the free stream values are,

$$q_1' = (1-x')^2, \quad i_1' = 1 + \frac{1}{r}\,(2x' - (x')^2),$$

and the initial conditions are

$$q' = 1, \quad i' = 1, \text{ when } x = o,$$

whilst the conditions on the plate are

$$q' = o, \quad i' = i_o', \text{when } \psi = o.$$

The relation (3,7) connecting the pressure and the free stream enthalpy now becomes

$$p' = (i_1')^{\gamma/\gamma-1} = \left[1 + \frac{1}{r}\,(2x' - x'^2)\right]^{\gamma/\gamma-1}.$$

The variation between viscosity and enthalpy can be written as

$$\mu' = (i')^{1.5} \quad \frac{1+C'}{i'+C'},$$

where $C' = {}^{C}/T_M$. The approximate forms (3,9) and (3,10) are now

$$\mu' = (i')^{\omega} \text{ and } \mu' = i'.$$

<u>It is found convenient to drop the dashes</u>, and so we arrive at the equations in their final form.

<u>Final form of the equations</u>.

In terms of non dimensional variables the Von Mises boundary layer equations for compressible flow are,

$$\frac{\partial q}{\partial x} = \left[\frac{1}{i_1} \quad \frac{dq_1}{dx}\right] \; i + [p]\, q^{\frac{1}{2}} \; \frac{\partial}{\partial \psi}\left(\frac{\mu}{i} \; \frac{\partial q}{\partial \psi}\right), \qquad (3,12)$$

and

$$\frac{\partial i}{\partial x} = -\left[\frac{1}{ri_1}\quad\frac{dq_1}{dx}\right] i + \left[\frac{p}{\sigma}\right] \frac{\partial}{\partial\psi}\left(\frac{q^{\frac{1}{2}}\mu}{i}\quad\frac{\partial i}{\partial\psi}\right)$$

$$+ \left[\frac{p}{2r}\right] \frac{\mu}{iq^{\frac{1}{2}}}\left(\frac{\partial q}{\partial\psi}\right)^2, \qquad (3,13)$$

where $p = i_1^{\gamma/\gamma-1}$, (3,14)

and $\mu = i^{1.5}\quad\frac{1+C}{1+C}$, (3,15)

The boundary conditions are,

(i) $q = o,\ i = i_o$, when $\psi = o$,

(ii) $q = (1-x)^2$ when $\frac{\partial q}{\partial\psi} = o$, (3,16)

$i = [1 + \frac{1}{r}(2x - x^2)]$ when $\frac{\partial i}{\partial\psi} = o$,

(iii) $\left.\begin{array}{l} q = 1 \text{ when } \psi > o,\ q = o \text{ when } \psi = o, \\ i = 1 \text{ when } \psi > o,\ i = i_o \text{ when } \psi = o \end{array}\right\}\ x = o.$

If we substitute for $\mu$ according to (3,15) in the equations (3,12) and (3,13) we arrive at the full equations of motion in a compressible boundary layer, namely,

$$\frac{\partial q}{\partial x} = \left[\frac{1}{i_1}\quad\frac{\partial q_1}{dx}\right] i + \frac{1}{2}\left(\frac{114 + T_M}{114 + iT_M}\right) p(qi)^{\frac{1}{2}}\left[2\ \frac{\partial^2 q}{\partial\psi^2} + \right.$$

$$\left.\frac{114 - i\,T_M}{i(114 + i\,T_M)}\cdot\frac{\partial i}{\partial\psi}\cdot\frac{\partial q}{\partial\psi}\right], \qquad (3,17)$$

$$\frac{\partial i}{\partial x} = -\left[\frac{1}{ri_1}\quad\frac{dq_1}{dx}\right] i + \frac{p}{2\sigma}\left(\frac{114 + T_M}{114 + iT_M}\right)\cdot(qi)^{\frac{1}{2}}\left[\frac{114 - iT_M}{i(114 + iT_M}\cdot\left(\frac{\partial i}{\partial\psi}\right)^2\right.$$

$$\left. + \frac{1}{q}\frac{\partial i}{\partial\psi}\frac{\partial q}{\partial\psi} + 2\ \frac{\partial^2 i}{\partial\psi^2} + \frac{\sigma}{r}\cdot\frac{1}{q}\cdot\left(\frac{\partial q}{\partial\psi}\right)^2\right]. \qquad (3,18).$$

In the above equations $114/T_M$ is the particular value for air, where $T_M$ is the temperature (in dimensional form) of the main stream.

In any particular problem we must specify $M_M$ and hence $r$, $T_M$, $\sigma$ and $\gamma$ and substitute the appropriate values in (3,16), (3,17) and (3,18).

Approximate form of the equations.

Because of the complexity of equations (3,17) and (3,18) analytical solutions can only be found if approximations are made to the equations. For air the Prandtl number $\sigma = 0.72$ and if we write $\mu = i^{\omega}$, $\omega \doteq 1$. Thus two approximations which can be used are $\sigma = 1$ and $\omega = 1$. The reason for choosing these values will now be shown.

If we turn to equations (3,12) and (3,13), multiply (3,13) by $r$ and add to (3,12), we obtain,

$$\frac{\partial q}{\partial x} + r\frac{\partial i}{\partial x} = pq^{\frac{1}{2}}\frac{\partial}{\partial\psi}\left(\frac{\mu}{i}\frac{\partial q}{\partial\psi}\right) + p\frac{\mu}{i}\frac{\partial q}{\partial\psi}\cdot\frac{1}{2q^{\frac{1}{2}}}\frac{\partial q}{\partial\psi}$$

$$+ p\frac{r}{\sigma}\frac{\partial}{\partial\psi}\left(\frac{q^{\frac{1}{2}}\mu}{i}\frac{\partial i}{\partial\psi}\right),$$

$$= p\left[\frac{\partial}{\partial\psi}\left(\frac{q^{\frac{1}{2}}\mu}{i}\frac{\partial q}{\partial\psi}\right) + \frac{\partial}{\partial\psi}\left(\frac{q^{\frac{1}{2}}\mu}{i}\frac{\partial}{\partial\psi}\frac{ri}{\sigma}\right)\right],$$

or

$$\frac{\partial}{\partial x}(q+ri) = p\frac{\partial}{\partial\psi}\left[\frac{q^{\frac{1}{2}}\mu}{i}\frac{\partial}{\partial\psi}\left(q + \frac{r}{\sigma}i\right)\right]. \qquad (3,19)$$

The two equations now to be solved are (3,12) and (3,19)

If $\sigma = 1$ the equation (3,19) reduces to

$$\frac{\partial}{\partial x}(q+ri) = \frac{\partial}{\partial \psi}\left[\frac{q^{\frac{1}{2}}\mu}{i}\;\frac{\partial}{\partial \psi}(q+ri)\right],$$

which has a solution

$$q + ri = \text{const.}$$

Choosing $\sigma = 1$ has thus reduced the number of differential equations to be solved from two to one.

If in addition we now choose $\omega = 1$, that is $\mu = 1$, we can simplify the equation (3,12) to be

$$\frac{\partial q}{\partial x} = \frac{i}{i_1}\cdot\frac{dq_1}{dx} + pq^{\frac{1}{2}}\cdot\frac{\partial^2 q}{\partial \psi^2},$$

where $q + ri = \text{const} = 1+r$.

Substituting for $i$ in terms of $q$ in the above equation we obtain

$$\frac{\partial q}{\partial x} = \frac{1+r-q}{1+r-q_1}\cdot\frac{dq_1}{dx} + pq^{\frac{1}{2}}\cdot\frac{\partial^2 q}{\partial \psi^2}. \tag{3,20}$$

Once $q$ has been found from (3,20) we can obtain $i$ from,

$$i = \frac{1}{r}\left[1+r-q\right]. \tag{3,21}$$

We have thus shown that by choosing $\omega = \sigma = 1$ we can reduce the equations (3,17) and (3,18) to the equation (3,20) together with the relation (3,21).

In each of the particular problems tackled, that is, for each set of parameters $M_M$, $T_M$, we shall perform two computations. The first computation will be carried out using the full equations (3,17) and (3,18), the second using (3,20) and (3,21). In the above fashion we hope to test the validity of the simplifying assumptions for two values of the parameters $M_M$ and $T_M$.

It should be noted that by using the approximate form of the equations we have made the velocity and thermal boundary layers coincident. Since $q + ri = \text{const}$ there can be no heat transfer across the plate. This can be seen by differentiating (3,21) with respect to $y$, to obtain

$$\frac{\partial i}{\partial y} = - 2u \frac{\partial u}{\partial y} ,$$

and on the plate $u = o$ and hence $(\frac{\partial i}{\partial y})_o = 0$.

Not only does the solution of the approximate equations yield the conditions of no heat transfer, it also specifies the enthalpy distribution on the plate. If we use equation (3,21) on the plate we have

$$i_o = \frac{1}{r}[1+r] = 1 + \frac{1}{r} . \qquad (3,22)$$

The above value of the enthalpy on the plate, if the approximations $\omega = \sigma = 1$ are valid, corresponds to conditions of no heat transfer. For the purposes of comparison the distribution (3,22) is used as a boundary condition even when we are solving the full equations.

We shall now set up the finite difference replacements of (3,17), (3,18), (3,20) and (3,21).

Finite difference replacements.

As described in section (1,C) the $(x,\psi)$ field is divided by a square net and the points labelled $(j,k)$. The mesh length in the x-direction is $\Delta x$ and in the $\psi$-direction is $\Delta\psi$, the mesh ratio $\delta$ being defined as before to be

$\delta = \Delta x/(\Delta\psi)^2$ .

Since the calculation is started at the leading edge, the point $(j,k)$ corresponds to the point $(j\Delta x,\ k\Delta\psi)$. The value of $q$ at the point $(j,k)$ is denoted by $q_{j,k}$ and the value of $i$ there by $i_{j,k}$ . If a variable is independent of $\psi$, for example $i_1$, its value at the station $x = j\Delta x$, for all $k$, is denoted by $(i_1)_j$.

The customary approximations for the derivatives will be used, namely

$$\left(\frac{\partial q}{\partial x}\right)_{j,k} \doteq \frac{q_{j+1,k} - q_{j,k}}{\Delta x} ,$$

$$\left(\frac{\partial^2 q}{\partial \psi^2}\right)_{j,k} \doteq \frac{q_{j,k+1} - 2q_{j,k} + q_{j,k-1}}{(\Delta\psi)^2} , \qquad (3,23)$$

$$\left(\frac{\partial q}{\partial \psi}\right)_{j,k} \doteq \frac{q_{j,k+1} - q_{j,k-1}}{2\Delta\psi} .$$

As before, these approximations (and a similar set for the enthalpy derivatives) will yield a four point forward difference equation involving the four nodes given below.

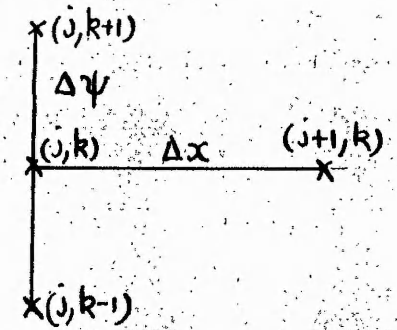

Using the approximations (3,22) and similar approximations for $\frac{\partial i}{\partial x}$, $\frac{\partial i}{\partial \psi}$ and $\frac{\partial^2 i}{\partial \psi^2}$ we can replace (3,17) and (3,18) by the following two finite difference equations,

$$q_{j+1,k} = q_{j,k} + \left[\frac{\Delta x}{i_1} \quad \frac{dq_1}{dx}\right]_j i_{j,k} + \left[\frac{\delta p}{8}\right]_j \left(\frac{114+T_M}{114+i_{j,k}T_M}\right)(qi)^{\frac{1}{2}}_{j,k} \Bigg\{$$

$$8(q_{j,k+1} - 2q_{j,k} + q_{j,k-1}) + \frac{114 - i_{j,k}T_M}{i_{j,k}(114+i_{j,k}T_M)} \cdot$$

$$(i_{j,k+1} - i_{j,k-1})(q_{j,k+1} - q_{j,k-1}) \Bigg\}, \qquad (3,24)$$

and

$$i_{j+1,k} = i_{j,k} - \left[\frac{\Delta x}{ri_1} \quad \frac{dq_1}{dx}\right]_j i_{j,k} + \left[\frac{p\delta}{8\sigma}\right]_j \frac{114+T_M}{114+i_{j,k}T_M} \quad (qi)^{\frac{1}{2}}_{j,k} \Bigg\{$$

$$\frac{114 - i_{j,k}T_M}{i_{j,k}(114+i_{j,k}T_M)}(i_{j,k+1} - i_{j,k-1})^2 + \frac{1}{q_{j,k}}$$

$$(i_{j,k+1} - i_{j,k-1})(q_{j,k+1} - q_{j,k-1})$$

$$+ 8(i_{j,k+1} + i_{j,k-1} - 2i_{j,k}) \quad \frac{\sigma}{rq_{j,k}}(q_{j,k+1} - q_{j,k-1})^2 \Bigg\}. \qquad (3,25)$$

In the above equations the quantities in square brackets are independent of k, and all the terms on the right hand sides of (3,24) and (3,25) are known on the j-line.

In a similar manner, we can replace the approximate equations (3,20) and (3,21) by,

$$q_{j+1,k} = q_{j,k} + \left[\frac{\Delta x}{1+r - q_1}\right]_j (1 + r - q_{j,k})$$
$$+[\delta p]_j \; (q)^{\frac{1}{2}}_{j,k}(q_{j,k+1} - 2q_{j,k} + q_{j,k-1}), \quad (3,26)$$

and

$$i_{j,k} = \frac{1}{r}\,(1 + r - q_{j,k}).$$

The simplifications produced by the assumptions $\omega = \sigma = 1$ are even more apparent in the difference equations.

The boundary conditions (3,15) and (3,22) for both sets of equations are now given in the form,

(i) $q_{j,o} = 0$, $i_{j,o} = 1 + \frac{1}{r}$ , for all j.

(ii) $q_{j,k+1} = [1 - j\Delta x]^2$ when $q_{j,k} = [1 - j\Delta x]^2$ .

$i_{j,k+1} = [1 + \frac{1}{r}(2j\Delta x -(j\Delta x)^2)]$ when $i_{j,k} = [1 + \frac{1}{r}\,(2j\Delta x - (j\Delta x)^2)\,]$.

(iii) $q_{o,k} = 1$, $q_{o,o} = 0$ for all k.

$i_{o,k} = 1$, $i_{o,o} = 1 + \frac{1}{r}$ for all k.

Before going on to discuss how the above sets of equations are best programmed for calculation we must make some mention of the stability conditions.

## Stability conditions.

In section (2) we have demonstrated that for each of the non linear finite difference equations considered there are two stability conditions. The first condition imposes a restriction on the size of the mesh ratio, whilst the second is a condition which is inherent in the differential equation. In section (1,c) it is seen that for a linear differential equation there is only one condition, that which exerts the restriction on the mesh size.

No knowledge is at present available concerning the accurate establishment of the stability conditions for a non linear difference equation. Because of this the method used here to establish the error equation is approximate in that, as in section (2), we construct a linear error equation.

In this section we propose to establish the stability conditions only for the approximate forms of the differential and difference equations, (3,20) and (3,26). This is done because the analysis involved in the estimation of error growth in the full equations is too lengthy. It is also felt that the restrictions obtained from considering the approximate form of the equations will prove adequate for the full equations.

We shall first construct the error equation corresponding to the differential equation (3,20). We rewrite equation (3,20) in the form,

$$\frac{\partial q}{\partial x} = \left[\frac{dq_1/dx}{1+r-q_1}\right](1+r) - \left[\frac{dq_1/dx}{1+r-q_1}\right] q + p\, q^{\frac{1}{2}} \cdot \frac{\partial^2 q}{\partial \psi^2} \;.$$

In a similar fashion to that described in section (2) we construct a linear error equation corresponding to the above equation. The linear error equation can easily be shown to be,

$$\frac{\partial \varepsilon}{\partial x} = -\left[\frac{dq_1/dx}{1+r-q_1}\right]\varepsilon + pq^{\frac{1}{2}} \cdot \frac{\partial^2 \varepsilon}{\partial \psi^2} + \frac{p}{2q^{\frac{1}{2}}} \cdot \frac{\partial^2 q}{\partial \psi^2}\, \varepsilon\,,$$

$$= \varepsilon \left\{ \frac{p}{2q^{\frac{1}{2}}} \cdot \frac{\partial^2 q}{\partial \psi^2} - \frac{dq_1}{dx} \cdot \frac{1}{1+r-q_1} \right\} + pq^{\frac{1}{2}} \cdot \frac{\partial^2 \varepsilon}{\partial \psi^2}\,. \qquad (3,27)$$

As a solution of (3,27) we choose $\varepsilon = Ae^{\alpha x}\, e^{i\beta\psi}$, where $\alpha = a+ib$ and $\beta$ is real. Substituting this value of $\varepsilon$ in (3,27) we obtain

$$\alpha = \left\{ \frac{p}{2q^{\frac{1}{2}}} \cdot \frac{\partial^2 q}{\partial \psi^2} - \frac{dq_1}{dx} \cdot \frac{1}{1+r-q_1} \right\} - pq^{\frac{1}{2}} \cdot \beta^2 \,.$$

We thus see that $\alpha$ is real and since the condition that $\varepsilon$ shall not increase as $x$ increases is $Rl\alpha \leq 0$, we obtain

$$\left\{ \frac{p}{2q^{\frac{1}{2}}} \cdot \frac{\partial^2 q}{\partial \psi^2} - \frac{dq_1}{dx} \cdot \frac{1}{1+r-q_1} \right\} - pq^{\frac{1}{2}} \cdot \beta^2 \leq 0. \qquad (3,28)$$

The above condition must be satisfied for all $\beta$ and in particular if we choose the worst possible case $\beta = 0$ we obtain the particular condition,

$$pq^{\frac{1}{2}} \cdot \frac{\partial^2 q}{\partial \psi^2} - 2q \cdot \frac{dq_1}{dx} \cdot \frac{1}{1+r-q_1} \leq 0.$$

If the above condition is satisfied then (3,28) is satisfied for all values of $\beta$.

We can rewrite this condition using (3,20) as

$$pq^{\frac{1}{2}} \cdot \frac{\partial^2 q}{\partial\psi^2} - 2q\frac{dq_1}{dx} \cdot \frac{1}{1+r-q_1} \leqq 0,$$

or

$$\frac{\partial q}{\partial x} - \frac{1+r-q}{1+r-q_1} \cdot \frac{dq_1}{dx} - 2q \cdot \frac{dq_1}{dx} \cdot \frac{1}{1+r-q_1} \leqq 0,$$

that is

$$\frac{\partial q}{\partial x} \leqq \frac{1+r+q}{1+r-q_1} \cdot \frac{dq_1}{dx} \qquad (3,29)$$

The condition (3,29) forms a useful guide in the determination of the stability conditions for (3,26). We shall now examine the stability of theddifference equation (3,26).

The error equation associated with (3,26) is,

$$q_{j+1,k} + \varepsilon_{j+1,k} = q_{j,k} + \varepsilon_{j,k} + \left[\frac{\Delta x}{1+r-q_1} \quad \frac{dq_1}{dx}\right](1+r-q_{j,k}-\varepsilon_{j,k})$$
$$+[\delta p_j](q_{j,k}+\varepsilon_{j,k})^{\frac{1}{2}}(q_{j,k+1} - 2q_{j,k} + q_{j,k-1} + \varepsilon_{j,k+1} -$$
$$2\varepsilon_{j,k} + \varepsilon_{j,k-1}),$$

where $\varepsilon_{j,k}$ is the small error in $q_{j,k}$ for all $j$ and $k$.

We now simplify the error equation for neglecting all but the first power of $\varepsilon_{j,k}$. This produces a linear error equation of the form,

$$\varepsilon_{j,k+1} = \varepsilon_{j,k} - \left[\frac{\Delta x}{1+r-q_1} \quad \frac{dq_1}{dx}\right]_j \cdot \varepsilon_{j,k} + [\delta p]_j \frac{\varepsilon_{j,k}}{2(q_{j,k})^{\frac{1}{2}}} (q_{j,k+1}$$
$$-2q_{j,k}+ q_{j,k-1})+[\delta p]_j(q_{j,k})^{\frac{1}{2}}(\varepsilon_{j,k+1} - 2\varepsilon_{j,k} + \varepsilon_{j,k-1}). \quad (3,30)$$

As a solution of (3,30) we chose $\varepsilon_{j,k}$ in the customary form, $\varepsilon_{j,k} = Ae^{\alpha j\Delta x} e^{i\beta k\Delta\psi}$ . Substiuting this value for

$\varepsilon_{j,k}$ in (3,30) we obtain,

$$e^{\alpha\Delta x} = 1 - \left[\frac{\Delta x}{1+r-q_1} \frac{dq_1}{dx}\right]_j + [\delta p]_j \frac{1}{2(q)^{\frac{1}{2}}_{j,k}} (q_{j,k+1} - 2q_{j,k} + q_{j,k-1}) - 4[\delta p]_j (q)^{\frac{1}{2}}_{j,k} \sin^2 \frac{\beta\Delta\psi}{2} . \qquad (3,31)$$

The condition for stability is

$$\left| e^{\alpha\Delta x} \right| \leq 1 \quad .$$

From (3,31) we see that $e^{\alpha\Delta x}$ is real and hence the condition for stability is,

$$-1 \leq 1 - \left[\frac{\Delta x}{1+r-q_1} \frac{dq_1}{dx}\right]_j + [\delta p]_j \frac{1}{2(q)^{\frac{1}{2}}_{j,k}} (q_{j,k+1} - 2q_{j,k} + q_{j,k-1}) - 4[\delta p]_j (q)^{\frac{1}{2}}_{j,k} \sin^2 (\beta \frac{\Delta\psi}{2}) \leq 1 \qquad (3,32)$$

Result (3,32) is therefore the stability condition which must be satisfied for all values of $\beta$ at all nodes in the field.

In order to obtain the stability conditions in a more practical form we shall examine the upper and lower conditions of (3,32) separately. The upper condition is

$$-\left[\frac{\Delta x}{1+r-q_1} \frac{dq_1}{dx}\right]_j + [\delta p]_j \frac{1}{2(q)^{\frac{1}{2}}_{j,k}} (q_{j,k+1} - 2q_{j,k} + q_{j,k-1}) - 4[\delta p]_j (q_{j,k})^{\frac{1}{2}} \sin^2 \frac{\beta\Delta\psi}{2} \leq 0.$$

Choosing the worst possible value of $\beta$ it can readily be shown that the above condition is satisfied for all $\beta$ if,

$$- 2\left[\frac{\Delta x}{1+r-q_1}\;\frac{dq_1}{dx}\right]_j q_{j,k} + [\delta p]_j (q_{j,k})^{\frac{1}{2}} (q_{j,k+1} - 2q_{j,k} + q_{j,k-1}) \leq 0.$$

Using (3,26), this can be rearranged to yield,

$$q_{j+1,k} - q_{j,k} \leq \left[\frac{\Delta x}{1+r-q_1}\;\frac{dq_1}{dx}\right]_j (1+r+q_{j,k}), \qquad (3,33)$$

which is of course the difference form of the condition (3,29).

We shall now examine the lower condition of (3,32). This can be rearranged as,

$$\left[\frac{\Delta x}{1+r-q_1}\;\frac{dq_1}{dx}\right]_j - [\delta p]_j \frac{1}{2(q)^{\frac{1}{2}}_{j,k}} (q_{j,k+1} - 2q_{j,k} + q_{j,k-1})$$

$$+ 4[\delta p]_j (q)^{\frac{1}{2}}_{j,k} \sin^2 \frac{\beta\Delta\psi}{2} \leq 2,$$

which will be satisfied for all $\beta$ if,

$$\frac{[\delta p]_j}{2(q)^{\frac{1}{2}}_{j,k}} (10\, q_{j,k} - q_{j,k+1} - q_{j,k-1}) \leq 2 - \left[\frac{x}{1+r-q_1}\;\frac{dq_1}{dx}\right]_j ,$$

that is if

$$\delta \leq \frac{2(q)^{\frac{1}{2}}_{j,k}\left(2 - \left[\frac{x}{1+r-q_1}\;\frac{dq_1}{dx}\right]_j\right)}{p_j\;(10\, q_{j,k} - q_{j,k+1} - q_{j,k-1})}. \qquad (3,34)$$

We have thus established the two stability conditions (3,33) and (3,34). We shall make the condition (3,34) more stringent by finding a lower bound for the right hand side and choosing $\delta$ less than this lower bound.

Now

$$\frac{2(q)^{\frac{1}{3}}_{j,k}\left(2-\left[\frac{\Delta x}{1+r-q_1}\ \frac{dq_1}{dx}\right]_j\right),}{p_j\ (10\ q_{j,k}-q_{j,k+1}-q_{j,k-1})}$$

$$\leq \frac{4(q_{j,k})^{\frac{1}{3}}\ \left(1+\frac{\Delta x}{1+r-q_1}\right),}{9\ p_j\ q_{j,k}}$$

$$\leq \frac{4}{9}\ \frac{\left(1+\frac{\Delta x}{1+r-q_1}\right)}{\left\{\frac{(1+r-q_1)}{r}\right\}^{\gamma/\gamma-1}},$$

$$\leq \frac{4}{9}\ \left(\frac{r}{1+r-q_1}\right)^{\gamma/\gamma-1},$$

$$\leq \frac{4}{9}\ \left(\frac{r}{r-2x+x^2}\right)^{\gamma/\gamma-1}, \qquad (3,35)$$

and so it is obvious that as the Mach number $M_M$ increases (and hence $r$ decreases) the size of this lower bound decreases for any given value of $x$. It is known however that in the actual calculation the range of $x$ is very small $0 \leq x \leq .1$ and so we can choose $x = 0$ in the above lower bound. In fact if we choose

$$\delta \angle \frac{4}{9},$$

it seems certain that we shall satisfy the condition (3,34). In the actual computation, $\delta = \frac{1}{4}$ .

It is of interest to examine the conditions (3,29) and (3,33). In the case of incompressible boundary layer flow, two similar conditions were obtained. These conditions were not satisfied in a region in the vicinity of the plate. It is safe to expect that in compressible boundary layer flow a similar region will exist in which the condition (3,29) [or equally the condition (3,33)] will not be satisfied.

If we examine condition (3,29),

$$\frac{\partial q}{\partial x} \leq \left(\frac{1+r+q}{1+r-q_1}\right) \frac{dq_1}{dx} \quad ,$$

first at the plate, where $q = \frac{\partial q}{\partial x} = 0$ we see that since $\frac{dq_1}{dx} \leq 0$ the condition is not satisfied. However, if we also examine the condition in the free stream where $q = q_1$ we find that it reduces

to $1 + r - q_1 \geq 1 + r + q_1$ ,

which again is not satisfied.

If we now examine the difference dondition (3,33) we find, from the results of the calculation to follow that, as in the incompressible case, the condition is not satisfied at nodes on $\psi = .1$ after some value of $x$; and also that at every station $x$ there are some nodes near the free stream where the condition is not satisfied. This shall be demonstrated in the section dealing with the actual computation.

The violation of the condition (3,33) in the calculation will be ignored for two reasons. First of all from the results of the incompressible flow calculation it was seen that the instability in the region next to the plate was very mild indeed. Secondly, the condition is violated in and near the free stream and in this region the numerical changes involved in the step-by-step calculation are so small that it is impossible to conceive any growth of error.

As was mentioned earlier little is known at present on non linear error equations. It is believed that there are certain regions in a field in which the violation of an inherent stability condition may result in large growth of errors but there are also regions in which this is not necessarily so. The above argument provides a very interesting topic for future research.

As was stated previously no estimation of error growth of the full equations will be presented. The considerations arrived at above will be assumed to be relevant to the full equations and so we shall choose $\delta = .25$ in both sets of calculations. We shall now programme the calculation for a desk calculating machine.

<u>Programme for the computation.</u>

With the increase in the number of numerical operations involved [as can be seen from the complexity of (3,24) and (3,25)] it is now essential to find the most efficient method of carrying out these operations. For example, as the equations stand there are several divisions involved. On a desk calculating machine the operation of division takes the longest time and so it is worthwhile to rearrange the terms in the difference equations in order to have a minimum number of divisions.

The calculations before us are the evaluations of the velocity and enthalpy at nodes in the compressible boundary layer adjacent to a flat plate. The velocity and enthalpy fields are calculated in the first case using the full finite difference equations and in the second case using the approximate form of these equations. The step-by-step nature of solution of each set of equations is comparable with that found in Section (2) although the number of individual operations is increased.

We can write the equations (3,24) and (3,25) in the form

$$q_{j+1,k} = q_{j,k} + f_{1j}\, i_{j,k} + f_{3j}\, \frac{1}{(qi)^{\frac{1}{2}}_{j,k}}\, \frac{1}{114 + T_M i_{j,k}} \Big\{ 8(qi)_{j,k}\,(q_{j,k+1} - 2q_{j,k} + q_{j,k-1}) + q_{j,k}\left(\frac{114 - T_M\, i_{j,k}}{114 + T_M\, i_{j,k}}\right) \left(i_{j,k+1} - i_{j,k-1}\right)\left(q_{j,k+1} - q_{j,k-1}\right)\Big\}, \quad (3,36)$$

and

$$i_{j+1,k} = (1 - f_{2j})\, i_{j,k} + f_{4j}\left(\frac{1}{(qi)^{\frac{1}{2}}_{j,k}}\right)\frac{1}{114 + i_{j,k}T_M} \Big\{ 8(qi)_{j,k}\,(i_{j,k+1} - 2i_{j,k} + i_{j,k-1})$$

$$+ i_{j,k}(i_{j,k+1} - i_{j,k-1})(q_{j,k+1} - q_{j,k-1}) + \frac{\sigma}{r} i_{j,k}(q_{j,k+1} - q_{j,k-1})^2$$

$$+ \left(\frac{114 - i_{j,k} T_M}{114 + i_{j,k} T_M}\right)(i_{j,k+1} - i_{j,k-1})^2 q_{j,k} \Bigg\} . \qquad (3,37)$$

In the above equations the quantities $f_{nj}$ $(n = 1,2,3,4)$ are functions of $x$ alone. They are in fact

$$f_{1j} = \left[\frac{\Delta x}{i_1} \quad \frac{dq_1}{dx}\right]_j = \frac{-2\Delta x\,[1 - j\Delta x]}{1 + \frac{1}{r}[2j\Delta x - (j\Delta x)^2]},$$

$$f_{2j} = \frac{1}{r}\, f_{1j},$$

$$f_{3j} = \frac{114 + T_M\, p_j}{8}\,\delta = \frac{114 + T_M}{8}\,\delta\left[1 + \frac{1}{r}\,(2j\Delta x - [j\Delta x]^2)\right]^{\gamma/\gamma-1},$$

$$f_{4j} = \frac{1}{\sigma}\, f_{3j} .$$

The quantities $f_j$ along with $(q_1)_j = (1 - j\Delta x)^2$ and $(i_1)_j = [1 + \frac{1}{r}(2j\Delta x - [j\Delta x]^2)$ are tabulated for values of $j$ from $j = 0$ (that is at stations of $x$ along the plate) before the actual computation commences. The programme of operations by means of which $q_{j+1,k}$ and $i_{j+1,k}$ are found from the values of $q$ and $i$ at the nodes $(j,k-1)$, $(j,k)$ and $(j,k+1)$ is given below inprogramme (3).

| OPERATION | EQUATIONS (3,36) AND (3,37) | | |
|---|---|---|---|
| $(1)_k$ | $q_{j,k}$ | $(19)_k$ | $(17)_k^2$ |
| $(2)_k$ | $i_{j,k}$ | $(20)_k$ | $(17)_k \times (18)_k$ |
| $(3)_k$ | $\frac{\mathcal{L}}{r}(2)_k$ | $(21)_k$ | $(18)_k^2$ |
| $(4)_k$ | $f_{1j}(2)_k$ | $(22)_k$ | $(1)_{j,k+1} - 2\ (1)_{j,k} + (1)_{j,k-1}$ |
| $(5)_k$ | $(1 - f_{2j})(2)_k$ | $(23)_k$ | $(2)_{j,k+1} - 2\ (2)_{j,k} + (2)_{j,k-1}$ |
| $(6)_k$ | $(1)_k \times (2)_k$ | $(24)_k$ | $(7)_k \times (22)_k$ |
| $(7)_k$ | $8 \times (6)_k$ | $(25)_k$ | $(7)_k \times (23)_k$ |
| $(8)_k$ | $\sqrt{(6)}_k$ | $(26)_k$ | $(3)_k \times (18)_k$ |
| $(9)_k$ | $T_M \times (2)_k$ | $(27)_k$ | $(2)_k \times (20)_k$ |
| $(10)_k$ | $114 + (9)_k$ | $(28)_k$ | $(13)_k \times (20)_k$ |
| $(11)_k$ | $114 - (9)_k$ | $(29)_k$ | $(13)_k \times (21)_k$ |
| $(12)_k$ | $(11)_k \times (10)_k^{-1}$ * | $(30)_k$ | $(24)_k + (28)_k$ |
| $(13)_k$ | $(12)_k \times (1)_k$ | $(31)_k$ | $(25)_k + (26)_k + (27)_k + (29)_k$ |
| $(14)_k$ | $(8)_k \times (10)_k$ | $(32)_k$ | $(15)_k \times (30)_k$ |
| $(15)_k$ | $f_{3j}/(14)_k$ * | $(33)_k$ | $(16)_k \times (31)_k$ |
| $(16)_k$ | $f_{4j}/(14)_k$ * | $(34)_k$ | $(1)_k + (4)_k + (32)_k = q_{j+1,k}$ |
| $(17)_k$ | $(1)_{j,k+1} - (1)_{j,k-1}$ | $(35)_k$ | $(5)_k + (33)_k = i_{j+1,k}$ |
| $(18)_k$ | $(2)_{j,k+1} - (2)_{j,k-1}$ | $(36)_k$ | Repeat |

PROGRAMME (3).

We can now turn our attention to the approximate equation (3,26). This equation can be written as

$$q_{j+1,k} \doteq q_{j,k} + f_{2j}(1 + r - q_{j,k}) +$$

$$f_{5j}\ (q)^{\frac{1}{2}}_{j,k} \quad (q_{j,k+1} - 2q_{j,k} + q_{j,k-1}), \tag{3,38}$$

and we have,

$$i_{j,k} = \frac{1}{r}\,(1 + r - q_{j,k}), \tag{3,39}$$

where $f_{2j}$ has the value previously given and

$$f_{5j} = \delta p_j = \delta(i_1)^{\gamma/\gamma-1} = \delta[1 + \frac{1}{r}\,(2j\Delta x - [j\Delta x]^2)^{\gamma/\gamma-1}\ .$$

As before $f_{2j}$, $f_{5,j}$, $(q_1)_j$ and $(i_1)_j$ are tabulated from $x = o$ in steps of $\Delta x$.

The programme of calculations using (3,38) and (3,39) is given below in programme (4). The divisions in the programmes are marked with asterisks.

| OPERATION | EQUATIONS (3,38) and (3,39) | | |
|---|---|---|---|
| $(1)_k$ | $q_{j,k}$ | $(6)_k$ | $(4)_k \times (3)_k$ |
| $(2)_k$ | $1 + r - (1)_k$ | $(7)_k$ | $f_{5j} \times (6)_k$ |
| $(3)_k$ | $\frac{1}{r}(2)_k = i_{j,k}$ | $(8)_k$ | $f_{2j} \times (2)_k$ |
| $(4)_k$ | $\sqrt{(1)_k}$ | $(9)_k$ | $(1)_k + (7)_k + (8)_k = q_{j+1,k}$ |
| $(5)_k$ | $(1)_{k+1} - 2\times(1)_k + (1)_{k-1}$ | $(10)_k$ | Repeat. |

PROGRAMME (4).

A comparison of programmes(3) and (4) illustrates the great simplification brought about by the assumption $\omega = \sigma = 1$. Before a calculation commences, using either of the above programmes, we must specify certain constants. The mesh sizes $\Delta x$, $\Delta\psi$ and hence $\delta$ must be given. The Prandtl number $\sigma$ and the ratio of the specific heats $\gamma$ must be specified; for air $\sigma = 0.72$ and $\gamma = 1.4$. The temperature of the main stream is taken to be $15^{\circ}C$ and so $T_M = 288^{\circ}K$. The initial Mach number must be specified and once $M_M$ is known, $r$ and hence $i_1$ and $i_0$ are known. We shall choose two particular values of initial Mach number; $M_M = 1$ and $M_M = \sqrt{10}$ .

We are now ready to start the numerical calculation of the velocity and enthalpy profiles in the boundary layer. Particular attention will be paid to the comparison of values found using the equations (3,36) and (3,37) with those obtained using (3,38) and (3,39).

3.B

NUMERICAL CALCULATIONS.

Using the method outlined in section (3 A), we shall now proceed to the numerical calculation of the velocity and the enthalpy at nodes in the boundary layer.

As can be seen from Programme (3), the time taken to complete the calculation for a compressible boundary layer is much greater than that required for a similar calculation of an incompressible boundary layer. Because of this it is only possible, at this stage, to evaluate the velocity and enthalpy at the primary nodes. No detailed calculations near the plate are carried out, and so it is not possible to make an accurate assessment of the separation point in a compressible boundary layer. It is however possible to make an estimate of the position of separation by a comparison with the results of section (2)

Near the plate, the flow is slow and so it can be regarded as incompressible for quite large values of the initial Mach number. As a result, conditions near the plate will be similar to those in an incompressible boundary layer.

In particular in the incompressible boundary layer we know that separation occurs at $x = .12$, at which station $q$ takes the value $.1069$ at $\psi = .1$.

It seems reasonable to assume that the station $x_{\rho}$ in the compressible boundary layer at which $q \doteq .1069$ at

$\psi = .1$ will be an approximate value of the separation point. This is the assumption made in estimating separation in a compressible boundary layer.

In all the calculations to follow the mesh size is $\Delta x = .0025$, $\Delta\psi = .1$ and so $\delta = .25$ For air, the fluid we are considering, the Prandtl number is $\sigma = 0.72$ and the ratio of the specific heats is $\gamma = 1.4$. We choose the main stream temperature to be $T_M = 288^\circ K$.

Two sets of calculations are carried out, the first with an initial Mach number of unity and the second with $M_M = \sqrt{10}$.

<u>Mach number $M_M = 1$</u>

With $M_M = 1$ we know that $r = \dfrac{2}{(\gamma-1)M_M^2} = 5$ and so

$$i_1(x) = 1 + 4x - .2x^2,$$

and $\quad i_o = 1.2.$

It must be remembered that the value $i_o = 1.2$ is chosen because it is the value of enthalpy on the plate which corresponds to no heat transfer if the assumptions $\omega = \sigma = 1$ are made.

It is interesting from physical considerations, to determine the temperature on the plate. $\dfrac{T_o}{T_M} = \dfrac{i_o}{i_M} = 1.2$ where the variables are now dimensional. From the above we deduce that

$$T_o = 1.2 \times 288 = 335.6^\circ K = 62.6^\circ C.$$

This means that if a missile is travelling with a Mach number of unity through air at $15^\circ C$, then when the state of no heat transfer is reached the skin temperature of the missile will be of the order of 62°C.

First calculation.

Using the equations (3,36) and (3,37) together with programme (3) and the suitable boundary conditions the velocity and enthalpy were calculated at nodes of the form ($j \times .0025$, $k \times .1$) from $x = 0$ to $x = .1125$.

Calculated values of velocity and enthalpy at selected nodes in the field are given in Tables (3,1) and (3,2) respectively. The velocity and enthalpy profiles [and hence the shape of the boundary layer] are given in figures (3,2) and (3,3) respectively.

| $\psi$ \ x | .01 | .03 | .05 | .07 | .09 | .11 |
|---|---|---|---|---|---|---|
| .0 | .0000 | .0000 | .0000 | .0000 | .0000 | .0000 |
| .1 | .7160 | .5604 | .4793 | .4212 | .3736 | .3317 |
| .2 | .9037 | .7533 | .6621 | .5939 | .5377 | .4882 |
| .3 | .9713 | .8616 | .7770 | .7092 | .6516 | .6002 |
| .4 | .9880 | .9208 | .8505 | .7886 | .7336 | .6834 |
| .5 | .9900 | .9504 | .8962 | .8427 | .7925 | .7454 |
| .6 | .9900 | .9633 | .9229 | .8785 | .8342 | .7911 |
| .7 | | .9681 | .9374 | .9010 | .8628 | .8242 |
| .8 | | .9697 | .9447 | .9147 | .8818 | .8475 |
| .9 | | .9700 | .9479 | .9224 | .8939 | .8635 |
| 1.0 | | .9700 | .9493 | .9265 | .9013 | .8741 |
| 1.1 | | | .9498 | .9285 | .9056 | .8808 |
| 1.2 | | | .9499 | .9295 | .9080 | .8849 |
| 1.3 | | | .9500 | .9298 | .9092 | .8875 |
| 1.4 | | | .9500 | .9300 | .9098 | .8887 |
| 1.5 | | | | .9300 | .9100 | .8894 |
| 1.6 | | | | | .9100 | .8898 |
| 1.7 | | | | | | .8899 |
| 1.8 | | | | | | .8900 |
| 1.9 | | | | | | .8900 |

Velocity calculated using (3,36) and (3,37), $M_M = 1$

TABLE (3,1)

The value of $q$ found from this calculation at $x = .1125$, $\psi = .1$ is $q = .1066$ and so we assert that using the full equations separation occurs in the neighbourhood of $x_s = .1125$.

| $\psi$ \ $x$ | .01 | .03 | .05 | .07 | .09 | .11 |
|---|---|---|---|---|---|---|
| .0 | 1.2000 | 1.2000 | 1.2000 | 1.2000 | 1.2000 | 1.2000 |
| .1 | 1.1078 | 1.1428 | 1.1571 | 1.1660 | 1.1725 | 1.1783 |
| .2 | 1.0489 | 1.0973 | 1.1202 | 1.1352 | 1.1464 | 1.1556 |
| .3 | 1.0182 | 1.0635 | 1.0899 | 1.1083 | 1.1226 | 1.1344 |
| .4 | 1.0067 | 1.0405 | 1.0663 | 1.0860 | 1.1019 | 1.1153 |
| .5 | 1.0040 | 1.0262 | 1.0489 | 1.0682 | 1.0846 | 1.0988 |
| .6 | 1.0040 | 1.0183 | 1.0370 | 1.0544 | 1.0704 | 1.0734 |
| .7 | | 1.0144 | 1.0291 | 1.0445 | 1.0592 | 1.0642 |
| .8 | | 1.0127 | 1.0244 | 1.0376 | 1.0511 | 1.0571 |
| .9 | | 1.0121 | 1.0217 | 1.0331 | 1.0450 | 1.0520 |
| 1.0 | | 1.0119 | 1.0203 | 1.0302 | 1.0409 | 1.0483 |
| 1.1 | | 1.0118 | 1.0198 | 1.0285 | 1.0381 | 1.0457 |
| 1.2 | | 1.0118 | 1.0195 | 1.0276 | 1.0364 | 1.0440 |
| 1.3 | | | 1.0195 | 1.0272 | 1.0354 | 1.0430 |
| 1.4 | | | | 1.0270 | 1.0348 | 1.0423 |
| 1.5 | | | | 1.0270 | 1.0345 | 1.0419 |
| 1.6 | | | | | 1.0344 | 1.0417 |
| 1.7 | | | | | 1.0344 | 1.0416 |
| 1.8 | | | | | | 1.0416 |

Enthalpy calculated using (3,36) and (3,37) $M_M = 1$

TABLE (3,2)

From the tables and the graphs it is seen that the velocity and thermal boundary layers are almost coincident and that on comparison with the incompressible boundary layer (for flow with a similar adverse pressure gradient) the compressible boundary layer is thicker and separation occurs earlier. This is shown in Figure (3,13).

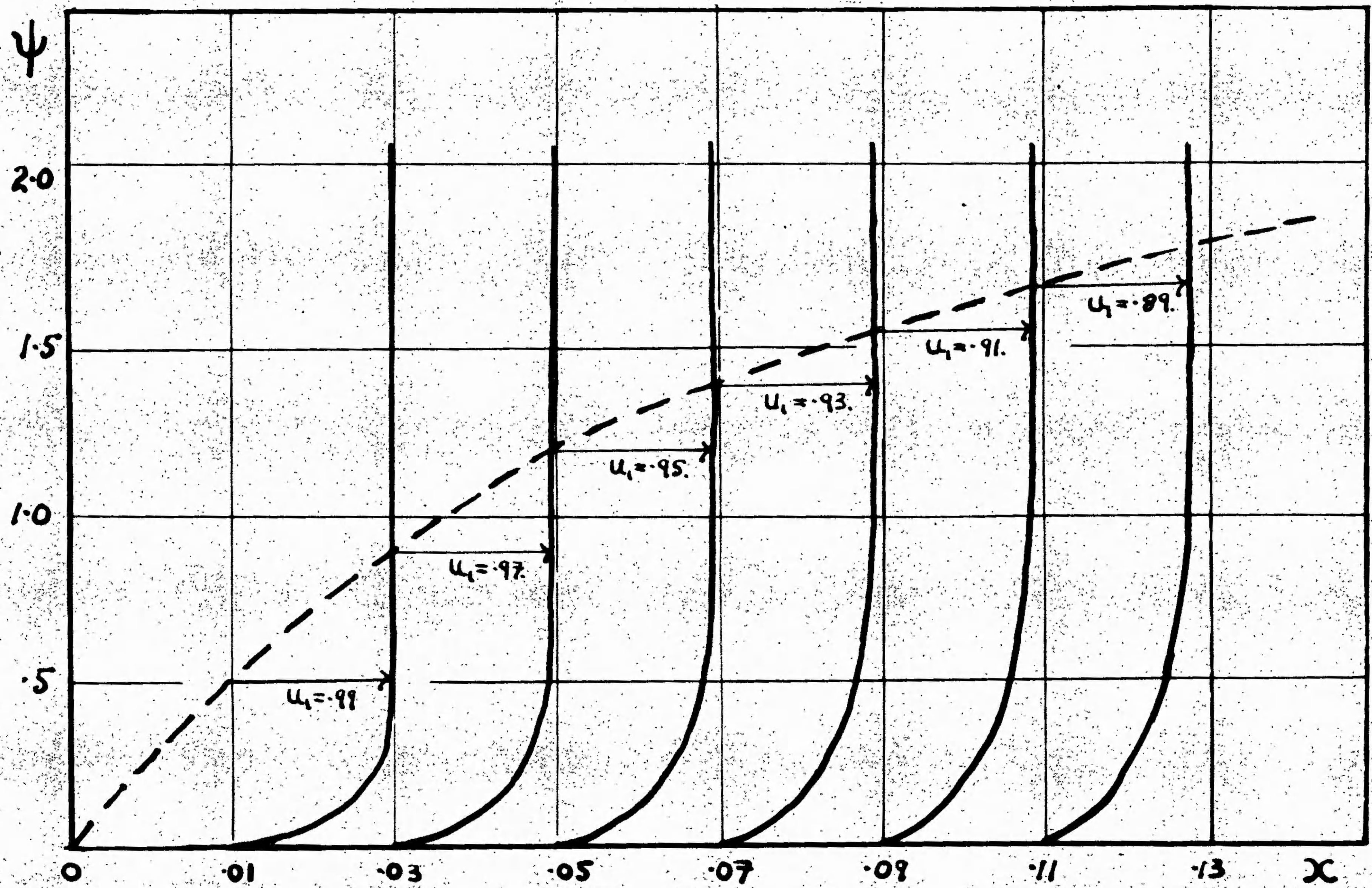


Velocity on the plate zero
Velocity Profiles (Mach number $M_M = 1$)
FIGURE (5,2)

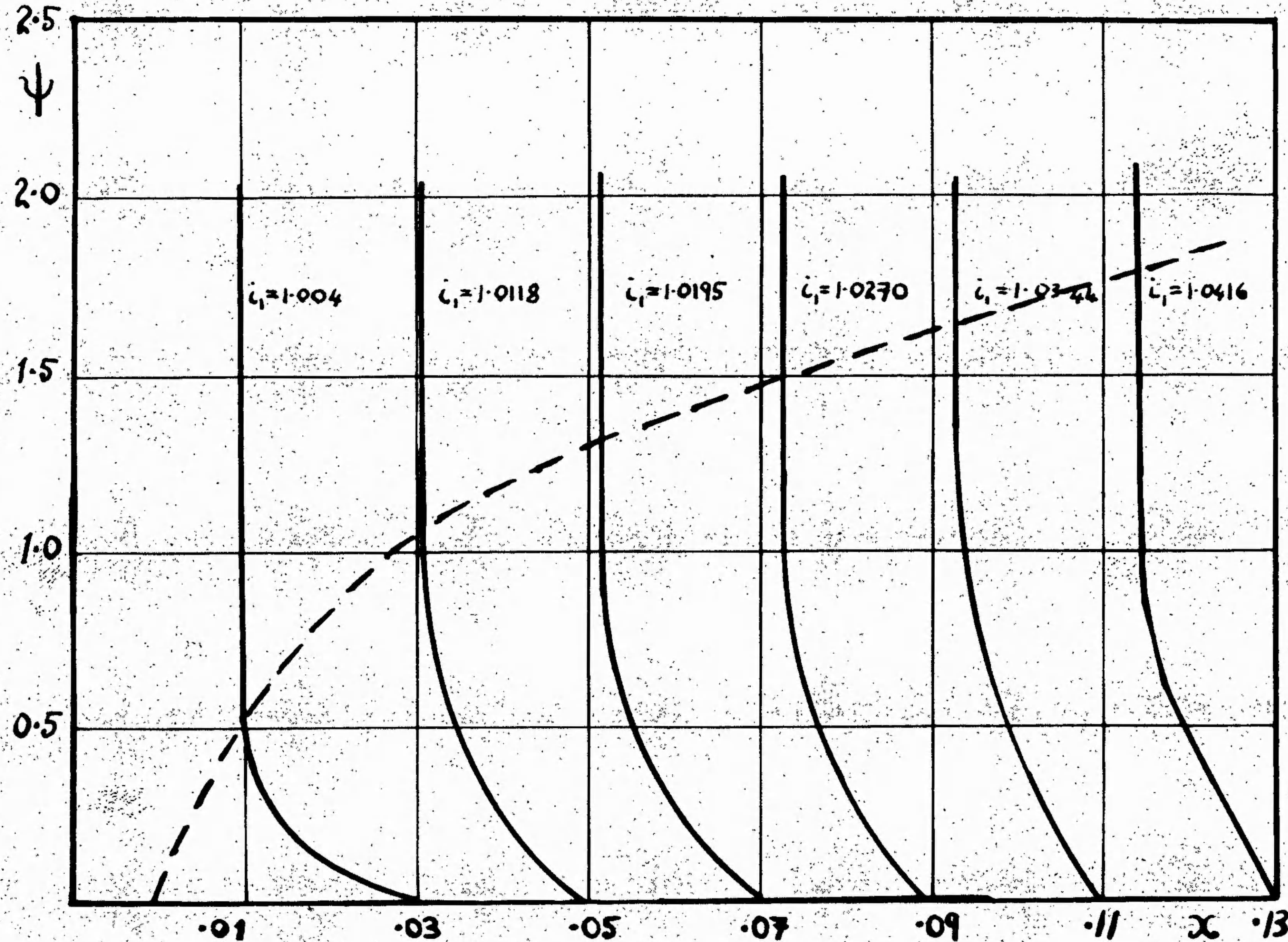


Enthalpy on the plate $i_o = 1.2$.
Enthalpy profiles (Mach number $M_M = 1$)

FIGURE (3,3)

Second calculation.

We shall now calculate the velocity and enthalpy at the same nodes using equations (3,38) and (3,39) modified to include our choice of initial Mach number. The boundary conditions are the same as those in the first calculation.

The actual values of $q$ and $i$ are not tabulated but table (3,3) contains the differences between the results of the first and second calculations.

| $\psi$ | $x = .02$ | | $x = .04$ | | $x = .06$ | |
|---|---|---|---|---|---|---|
| | $d_1\,°/_o$ | $d_2\,°/_o$ | $d_1\,°/_o$ | $d_2\,°/_o$ | $d_1\,°/_o$ | $d_2\,°/_o$ |
| .1 | 1.430 | .531 | 1.881 | .278 | 2.188 | .103 |
| .2 | .811 | 1.020 | 1.272 | .730 | 1.531 | .487 |
| .3 | .348 | 1.015 | .780 | .983 | 1.054 | .782 |
| .4 | .109 | .703 | .434 | .977 | .686 | .919 |
| .6 | .010 | .119 | .101 | .564 | .259 | .748 |
| .8 | .000 | .000 | .022 | .133 | .081 | .369 |
| 1.0 | | | .000 | .020 | .011 | .107 |
| 1.2 | | | .000 | .000 | .011 | .010 |
| 1.4 | | | | | .000 | .000 |

| $\psi$ | $x = .08$ | | $x = .10$ | | $x = .11$ | |
|---|---|---|---|---|---|---|
| | $d_1\,°/_o$ | $d_2\,°/_o$ | $d_1\,°/_o$ | $d_2\,°/_o$ | $d_1\,°/_o$ | $d_2\,°/_o$ |
| .1 | 2.291 | .017 | 2.500 | -.025 | 3.000 | -.034 |
| .2 | 1.788 | .324 | 2.057 | .226 | 2.182 | .190 |
| .3 | 1.321 | .627 | 1.560 | .505 | 1.666 | .958 |
| .4 | .917 | .813 | 1.137 | .721 | 1.263 | .672 |
| .6 | .382 | .819 | .560 | .844 | .655 | .838 |
| .8 | .161 | .536 | .254 | .614 | .306 | .695 |
| 1.0 | .060 | .251 | .076 | .392 | .117 | .437 |
| 1.2 | .035 | .077 | .025 | .163 | .076 | .258 |
| 1.4 | .012 | .000 | .037 | .048 | .013 | .086 |
| 1.6 | .000 | .000 | .025 | .000 | .025 | .019 |
| 1.8 | | | .000 | .000 | .013 | .000 |
| 2.0 | | | | | .000 | .000 |

Percentage differences ($M_M = 1$)

TABLE (3,3)

We denote the value of $q$ in the first calculation by $(q_{j,k})_1$ and the value of the enthalpy by $(i_{j,k})_1$. In the second calculation the values are $(q_{j,k})_2$ and $(i_{j,k})_2$ respectively. The percentage differences between the values are $d_1$ and $d_2$ where

$$d_1 = \frac{(q_{j,k})_1 - (q_{j,k})_2}{(q_{j,k})_1} \times 100\,^o/_o \,, \quad d_2 = \frac{(i_{j,k})_1 - (i_{j,k})_2}{(i_{j,k})_1} \times 100\,^o/_o.$$

The values of $d_1$ and $d_2$ are calculated from $x = o$ to $x = .1125$ and the values of $d_1$ and $d_2$ at selected nodes are given in Table (3,3). A graph of $d_1$ and $d_2$ against $\psi$ at various stations of $x$ is given in figures (3,4) and (3,5) respectively.

From Table (3,3) it is seen that the largest percentage differences are $d_1 \doteq 2.5\,^o/_o$ and $d_2 \doteq 1.1\,^o/_o$. This indicates that the assumption $\omega = \sigma = 1$ is reasonable when $M_M = 1$.

In this calculation it was found that the value of $q$ at $x = .1100$ was $q = .1067$ and so we can say that the separation point ~~is~~ in the vicinity of $x_\rho = .1100$ indicating that the calculation based on $\omega = \sigma = 1$ predicts separation to occur earlier than the estimate found using the full equations.

It is interesting to see from Figure (3,5) how the maximum error in $i$ appears to move towards the centre of the boundary layer as the calculation proceeds. Eventually

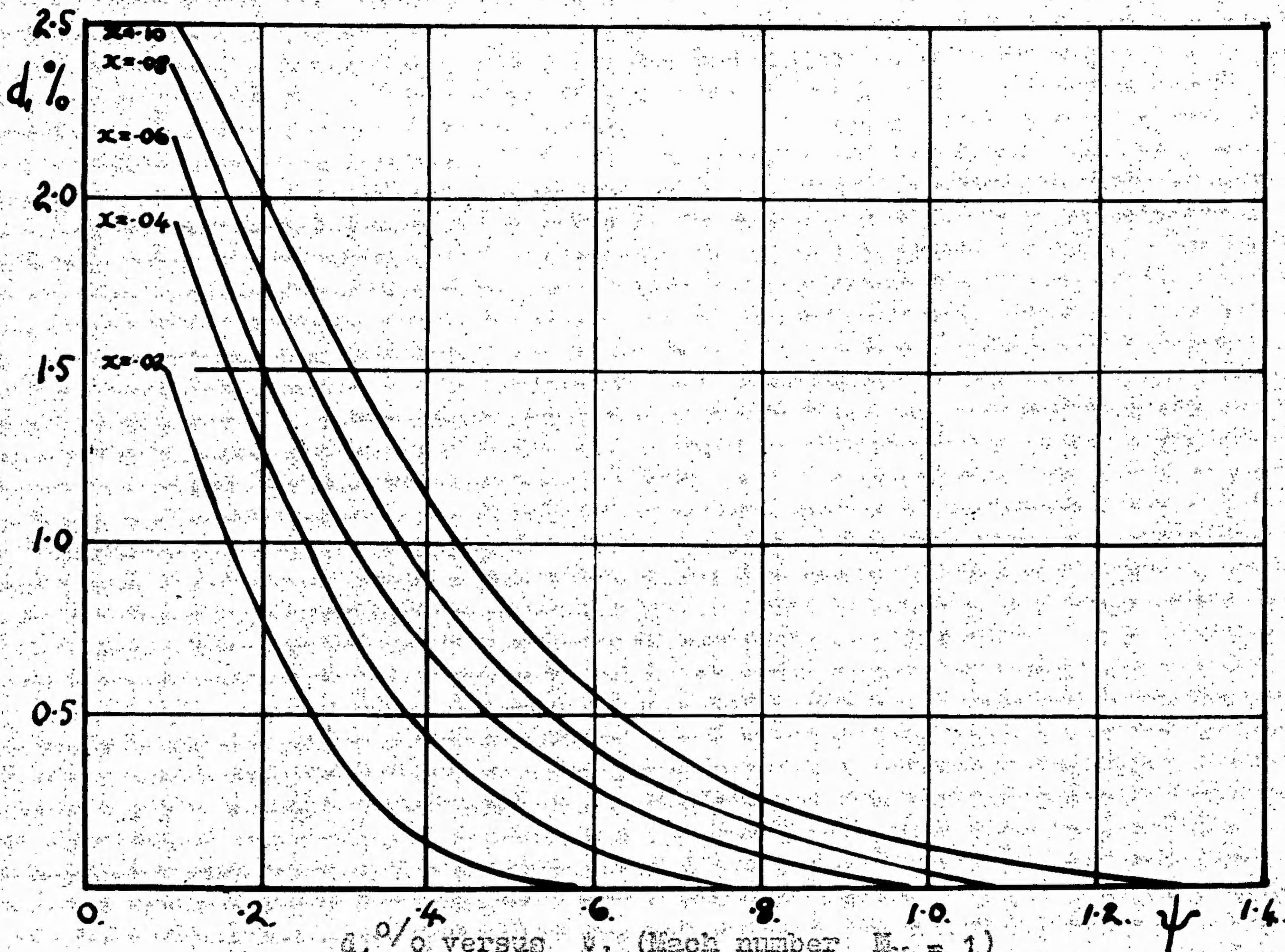


$d_1$ o/o versus $\psi$, (Mach number $M_M = 1$)

FIGURE (5,4)

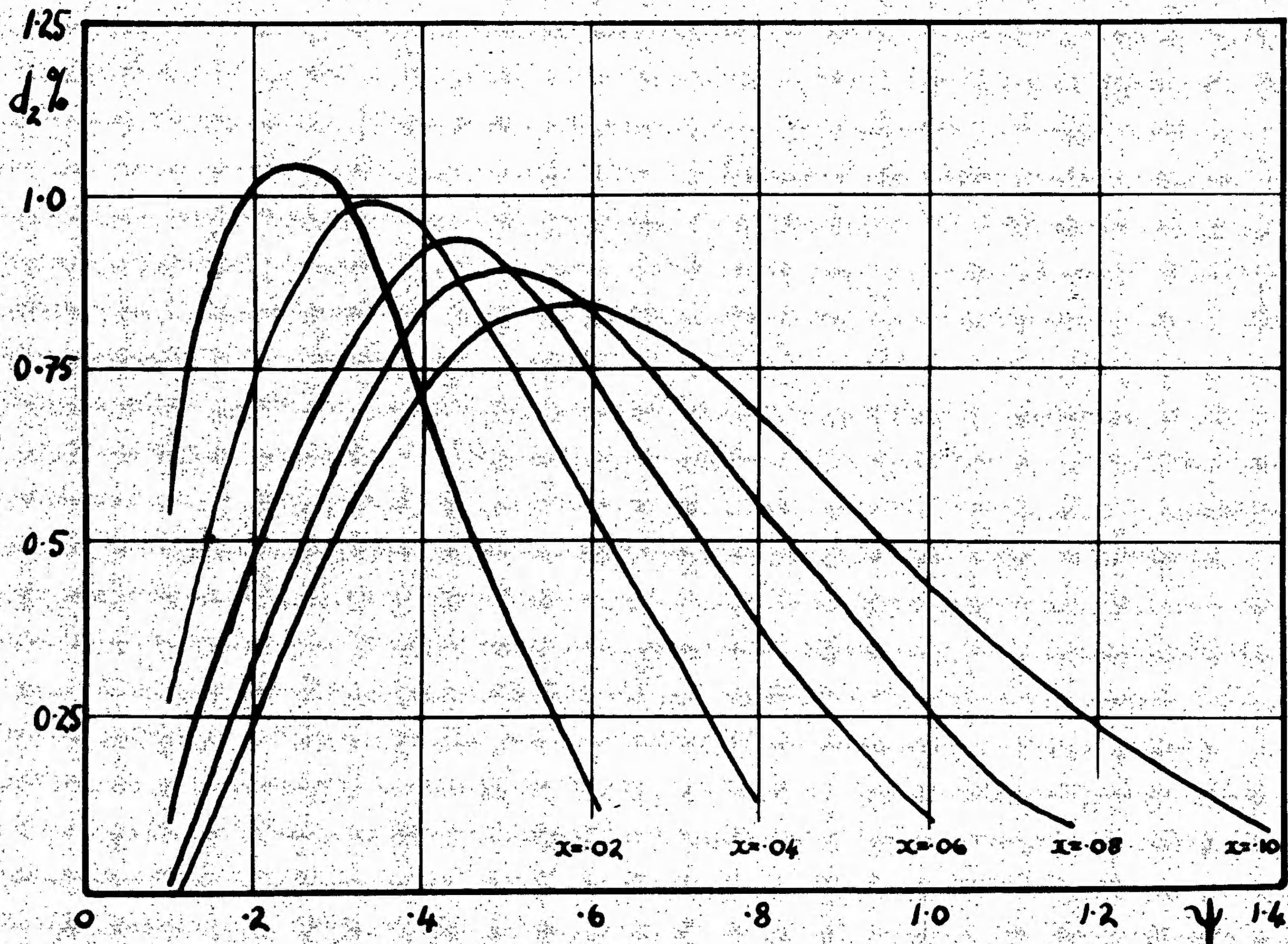


$d_2$ % versus $\psi$ (Mach number $M_M = 1$)

<u>FIGURE (3,5)</u>

the error near the plate becomes negative. With $q$ the largest error is always at the node nearest the plate.

At this stage the stability condition (3,33) was examined at the station $x = .10$. At this position the condition is

$$q_{j+1,k} - q_{j,k} \leq - .000867 \times (6 + q_{j,k}).$$

On examination it is found that the above condition is violated at $\psi = .1$ and at nodes from $\psi = .9$ to $\psi = 1.7$ (the free stream). In fact there are two regions in which the condition is violated as shown in Figure (3,6). It is felt that this violation is unimportant at nodes near the free stream and it is possible in view of the condition being over stringent, that the same might be true for the region near the plate.

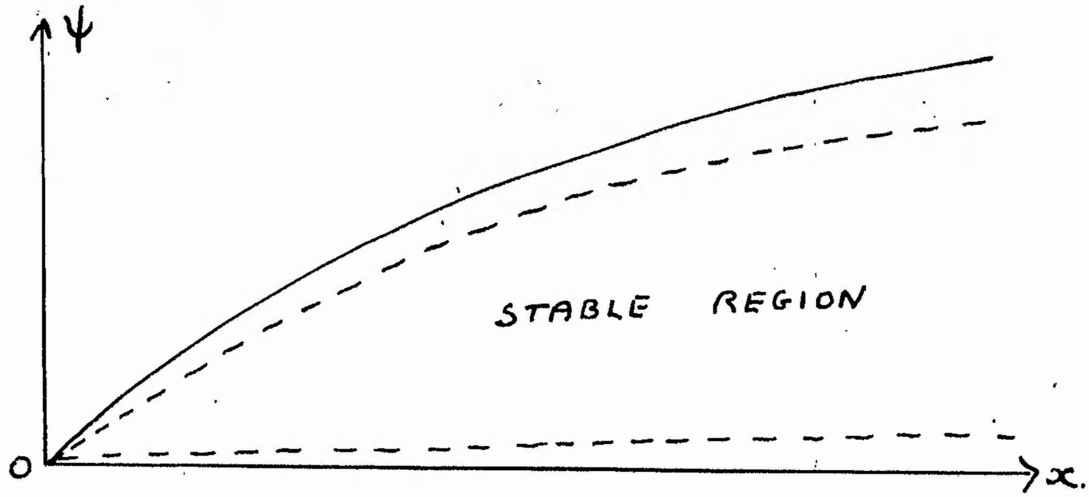


FIGURE (3,6)

Mach number $M_M = \sqrt{10}$.

The velocity and enthalpy will now be calculated in the boundary layer on a flat plate when the initial Mach number of the flow is $M_M = \sqrt{10}$.

In the equations (3,36), (3,37) and (3,38), (3,39) are substituted the appropriate values of the numerical constants, consistent with $M_M = \sqrt{10}$. The boundary conditions are also recalculated with $M_M = \sqrt{10}$, $r = .5$, and so

$$i_1(x) = 1 + 4x - 2x^2.$$
$$i_o = 3.$$

First calculation.

Using the revised forms of (3,36) and (3,37) together with Programme (3), the velocity and enthalpy are calculated in the boundary layer from $x = o$ to $x = .0825$. The calculated values of velocity and enthalpy at selected nodes are given below in tables (3,4) and (3,5). The velocity and temperature profiles are drawn at various stations $x$ in figures (3,7) and (3,8).

In this case the skin temperature is $T_o = 591^0C$, indicating the phenomenal rise in the temperature of a missile as the Mach number is increased.

In this calculation it was found that the value of $q$ at the station $x = .0825$ at $\psi = .1$ is $q = .1088$ and so we estimate that the separation point is in the neighbourhood of $x_s = .0825$.

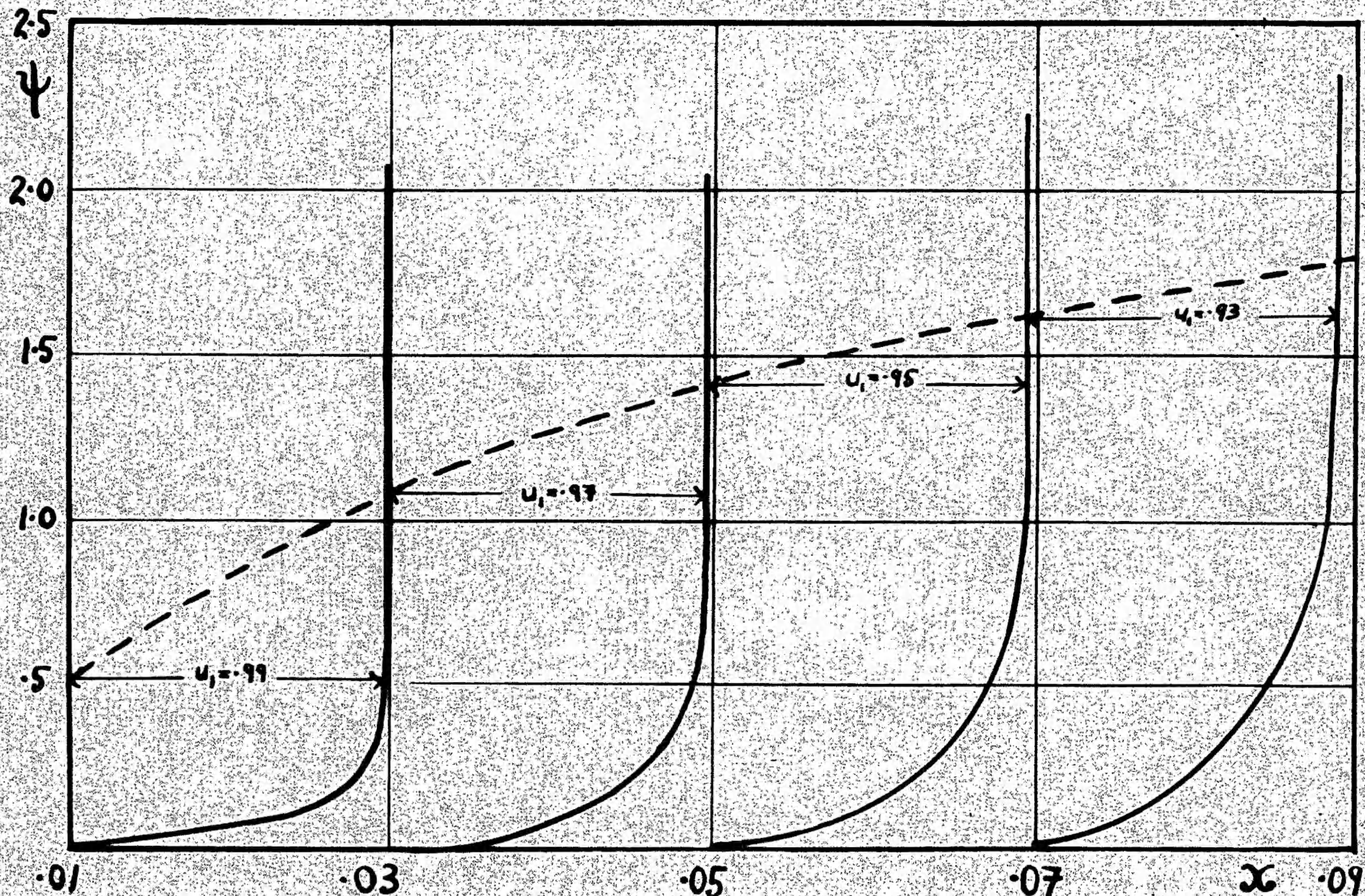


Velocity on the plate zero
Velocity profiles (Mach number $M_M = \sqrt{10}$

<u>FIGURE (5,7)</u>

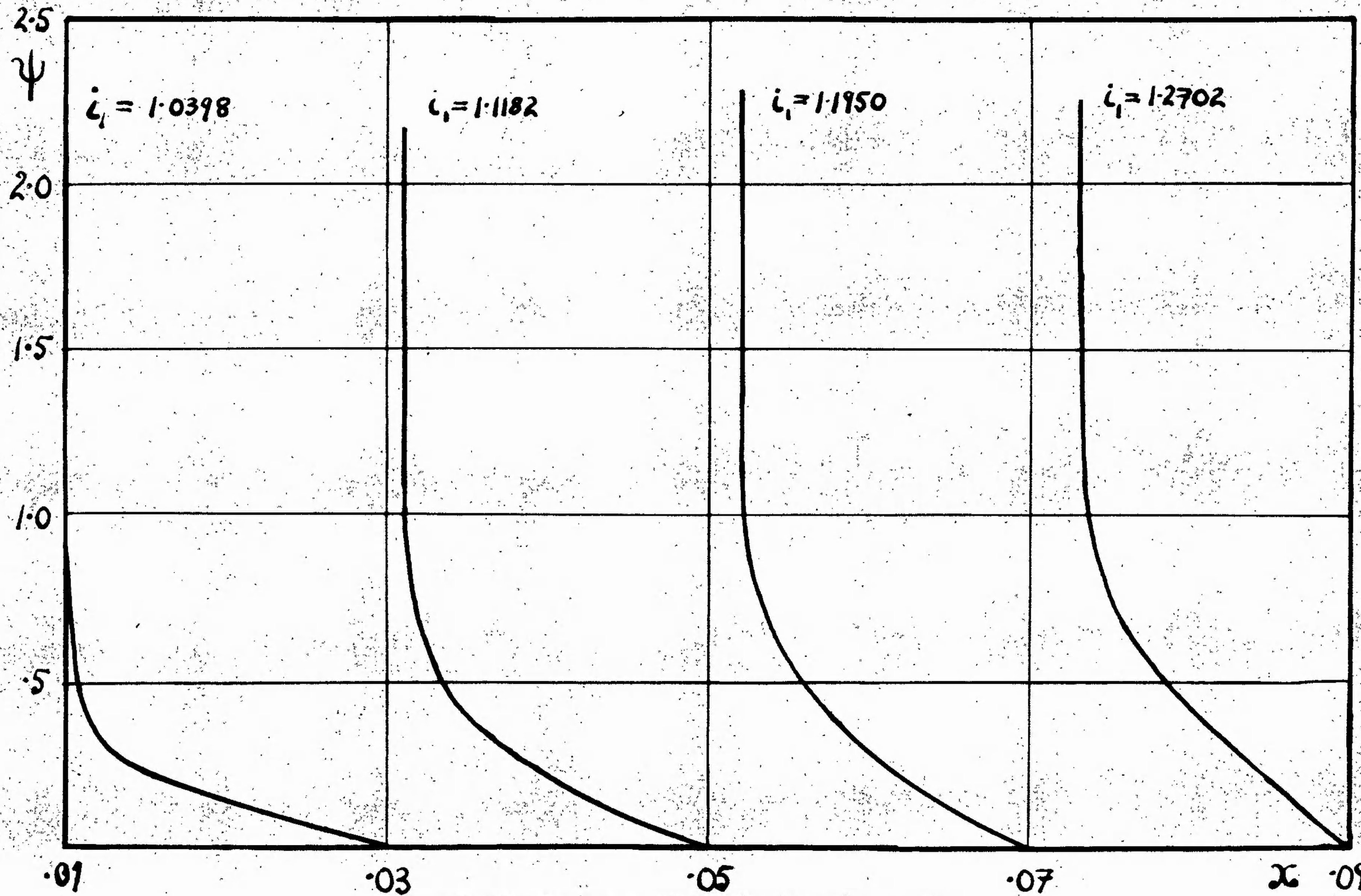


Enthalpy on the plate $i_o = 3$

Enthalpy profiles ($M_M = \sqrt{10}$)

<u>FIGURE (3,8)</u>

| $\psi$ \ x | .01 | .03 | .05 | .07 | .08 |
|---|---|---|---|---|---|
| 0 | .0000 | .0000 | .0000 | .0000 | .0000 |
| .1 | .7382 | .5585 | .4536 | .3736 | .3358 |
| .2 | .9153 | .7519 | .6365 | .5439 | .4799 |
| .3 | .9758 | .8581 | .7529 | .6612 | .5904 |
| .4 | .9897 | .9167 | .8290 | .7449 | .6746 |
| .5 | .9900 | .9470 | .8783 | .8047 | .7490 |
| .6 | .9900 | .9613 | .9093 | .8470 | .8065 |
| .7 | | .9674 | .9282 | .8765 | .8415 |
| .8 | | .9693 | .9390 | .8965 | .8673 |
| .9 | | .9698 | .9449 | .9099 | .8854 |
| 1.0 | | .9699 | .9478 | .9183 | .8973 |
| 1.1 | | .9700 | .9492 | .9235 | .9057 |
| 1.2 | | .9700 | .9497 | .9266 | .9108 |
| 1.3 | | | .9499 | .9283 | .9145 |
| 1.4 | | | .9500 | .9292 | .9172 |
| 1.5 | | | .9500 | .9297 | .9185 |
| 1.6 | | | | .9299 | .9193 |
| 1.7 | | | | .9830 | .9197 |
| 1.8 | | | | .9830 | .9199 |
| 1.9 | | | | | .9200 |
| 2.0 | | | | | .9200 |

Velocity calculated using (3,36) and (3,37) $M_M = \sqrt{10}$.

TABLE (3.4)

From the tables and the graph it is seen that the boundary layer is much thicker than the corresponding layer when the initial Mach number is unity. It is also noted that separation occurs much earlier.

| $\psi$ \ x | .01 | .03 | .05 | .07 | .08 |
|---|---|---|---|---|---|
| 0 | 3.0000 | 3.0000 | 3.0000 | 3.0000 | 3.0000 |
| .1 | 2.2014 | 2.4671 | 2.6294 | 2.7361 | 2.7755 |
| .2 | 1.5740 | 2.0228 | 2.2852 | 2.4668 | 2.5347 |
| .3 | 1.2238 | 1.6909 | 2.9954 | 2.2200 | 2.3188 |
| .4 | 1.0649 | 1.4591 | 1.7627 | 2.0061 | 2.1081 |
| .5 | 1.0398 | 1.3068 | 1.5855 | 2.6832 | 1.9370 |
| .6 | 1.0398 | 1.2135 | 1.4530 | 1.5697 | 1.7908 |
| .7 | | 1.1614 | 1.3587 | 1.4809 | 1.6747 |
| .8 | | 1.1353 | 1.2943 | 1.4157 | 1.5772 |
| .9 | | 1.1240 | 1.2521 | 1.3664 | 1.5069 |
| 1.0 | | 1.1198 | 1.2261 | 1.3317 | 1.4475 |
| 1.1 | | 1.1186 | 1.2110 | 1.3090 | 1.4024 |
| 1.2 | | 1.1182 | 1.2024 | 1.2940 | 1.3731 |
| 1.3 | | 1.1182 | 1.1982 | 1.2834 | 1.3507 |
| 1.4 | | | 1.1963 | 1.2780 | 1.3338 |
| 1.5 | | | 1.1952 | 1.2735 | 1.3254 |
| 1.6 | | | 1.1951 | 1.2719 | 1.3193 |
| 1.7 | | | 1.1950 | 1.2710 | 1.3151 |
| 1.8 | | | 1.1950 | 1.2705 | 1.3125 |
| 1.9 | | | | 1.2703 | 1.3101 |
| 2.0 | | | | 1.2702 | 1.3088 |
| 2.1 | | | | 1.2702 | 1.3079 |
| 2.2 | | | | | 1.0375 |
| 2.3 | | | | | 1.3073 |
| 2.4 | | | | | 1.3072 |

Enthalpy calculated from (3,36) and (3,37),

$$M_M = \sqrt{10}$$

TABLE (3,5)

Second calculation.

Using the particular forms of the approximate equations (3,38) and (3,39) the velocity and enthalpy were recalculated from $x = o$ to $x = .0725$.

In this case it can be seen that the approximate equations yield values which are far removed from the values calculated using the full equations. It is found that at $x = .0725$ and $\psi = .1$ the value of $q$ is $q = .1078$ and so we estimate that separation occurs in the vicinity of $x_s = .0725$, as compared with $x_s = .0825$ in the first calculation.

The percentage differences $d_1$ and $d_2$ are given in Table (3,6) and it is seen from the table that the differences cannot be neglected. The largest value of $d_1 \doteq 18\%$ and of $d_2 \doteq 11\%$. This indicates that the simplifying assumptions are much less accurate for this flow.

The graphs of $d_1$ and $d_2$ plotted against $\psi$ at various stations of $x$ along the plate are given in Figures (3,9) and (3,10). The increase in error with Mach number is readily seen from these graphs. Again in this calculation regions in which the condition (3,33) is violated are found.

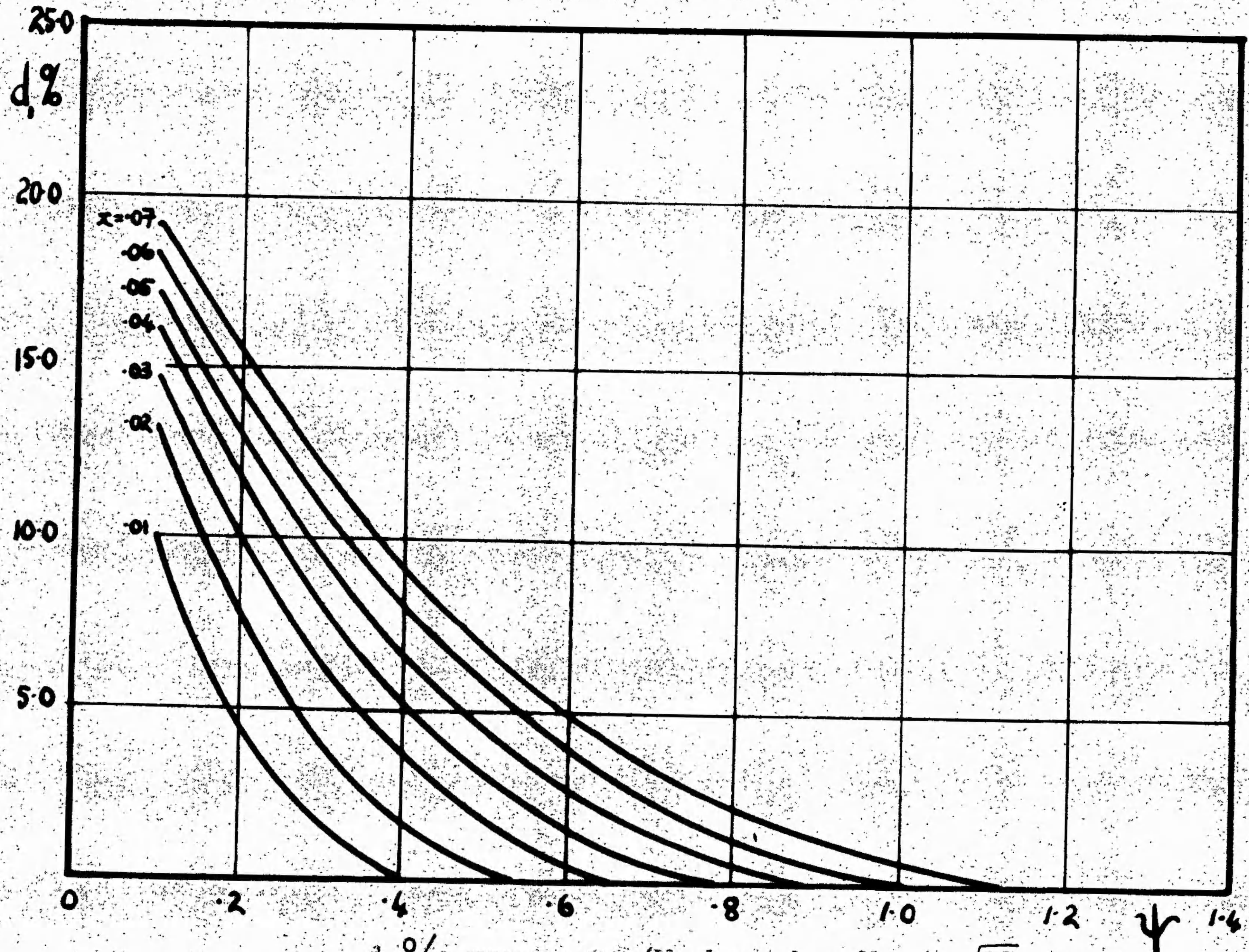


$d_1$ o/o versus $\psi$, (Mach number $M_M = \sqrt{10}$

<u>FIGURE (3,9)</u>

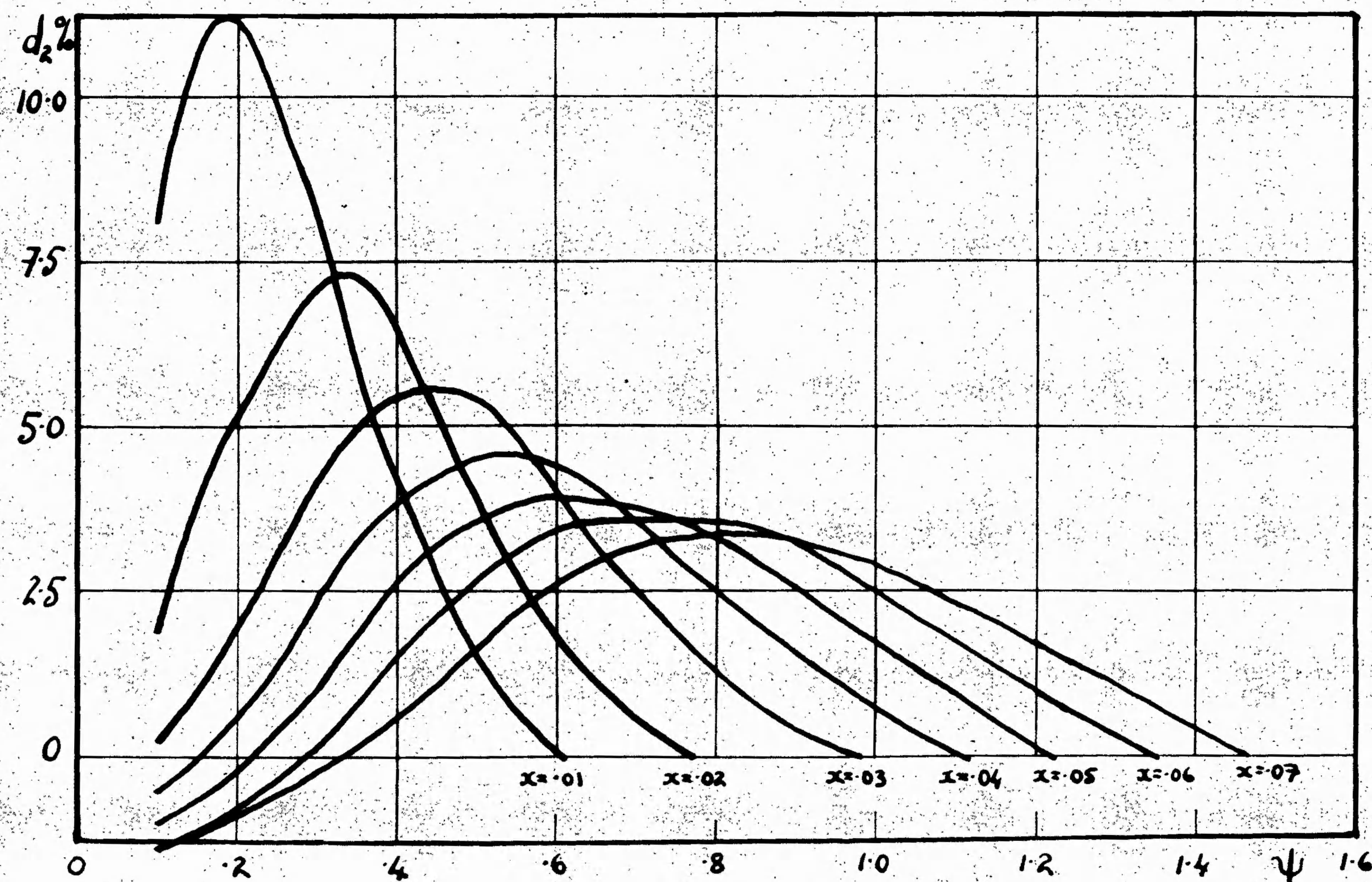


$d_2$ °/o versus ψ, (Mach number $M_M = \sqrt{10}$)

<u>FIGURE (3,10)</u>

| $\psi$ | $x = .01$ $d_1$ °/o | $d_2$ °/o | $x = .02$ $d_1$ °/o | $d_2$ °/o | $x = .03$ $d_1$ °/o | $d_2$ °/o |
|---|---|---|---|---|---|---|
| .1 | 9.836 | 8.358 | 13.002 | 1.892 | 14.363 | 0.052 |
| .2 | 4.308 | 11.271 | 7.793 | 5.109 | 10.047 | 1.967 |
| .3 | 1.491 | 8.138 | 3.953 | 3.119 | 6.205 | 4.276 |
| .4 | 0.439 | 1.455 | 1.700 | 6.461 | 3.486 | 5.572 |
| .6 | | | 0.156 | 1.682 | 0.725 | 3.980 |
| .8 | | | 0.010 | 0.037 | 0.095 | 1.101 |
| 1.0 | | | | | | 0.125 |
| 1.2 | | | | | | |

| $\psi$ | $x = .04$ $d_1$ °/o | $d_2$ °/o | $x = .05$ $d_1$ °/o | $d_2$ °/o | $x = .07$ $d_1$ °/o | $d_2$ °/o |
|---|---|---|---|---|---|---|
| .1 | 15.571 | -0.558 | 17.152 | -1.125 | 18.839 | - 1.363 |
| .2 | 11.986 | 0.447 | 13.055 | -0.446 | 15.200 | - 1.297 |
| .3 | 8.108 | 2.423 | 9.490 | 1.082 | 11.299 | - 0.198 |
| .4 | 5.145 | 4,048 | 6,591 | 2.649 | 9.298 | 0.632 |
| .6 | 1.593 | 4.623 | 2.636 | 4.349 | 4.919 | 2.828 |
| .8 | 0.350 | 2.473 | 0.793 | 3.392 | 2.202 | 3.585 |
| 1.0 | 0.062 | 0.719 | 0.166 | 1.606 | 0.806 | 2.883 |
| 1.2 | 0.010 | 0.112 | 0.033 | 0.482 | 0.244 | 2.681 |
| 1.4 | | 0.008 | 0.011 | 0.092 | 0.069 | 0.717 |
| 1.6 | | | | 0.008 | 0.022 | 0.196 |
| 1.8 | | | | | | 0.062 |
| 2.0 | | | | | | 0.012 |

Percentage differences $M_M = \sqrt{10}$

TABLE (3.6)

Comparison with incompressible boundary layer.

To determine the effect of an increase in Mach number we shall compare certain parameters.

It has already been stated that the boundary layer thickness increases as the Mach number increases and this is demonstrated in Figure (3,11). In Figure (3,11) the outer edge of the various boundary layers is shown and it can be seen that the outer edges of the velocity and thermal boundary layers for the flow in which $M_M = \sqrt{10}$ are not in fact coincident. In the figure the incompressible flow is labelled $M_M = 0$.

In Figure (3,12) the values of $q$ plotted against $\psi$ at the station $x = .08$ are given for the three boundary layers examined, incompressible, $M_M = 1$ and $M_M = \sqrt{10}$. It can readily be seen that at a given station $x$ the velocity profile becomes more linear as the Mach number is increased.

Finally in figure (3,13) the values of $q$ plotted against $x$ at the station $\psi = .1$ are shown for the three boundary layers considered. This graph demonstrates the fact that as the Mach number increases so the separation point moves forward.

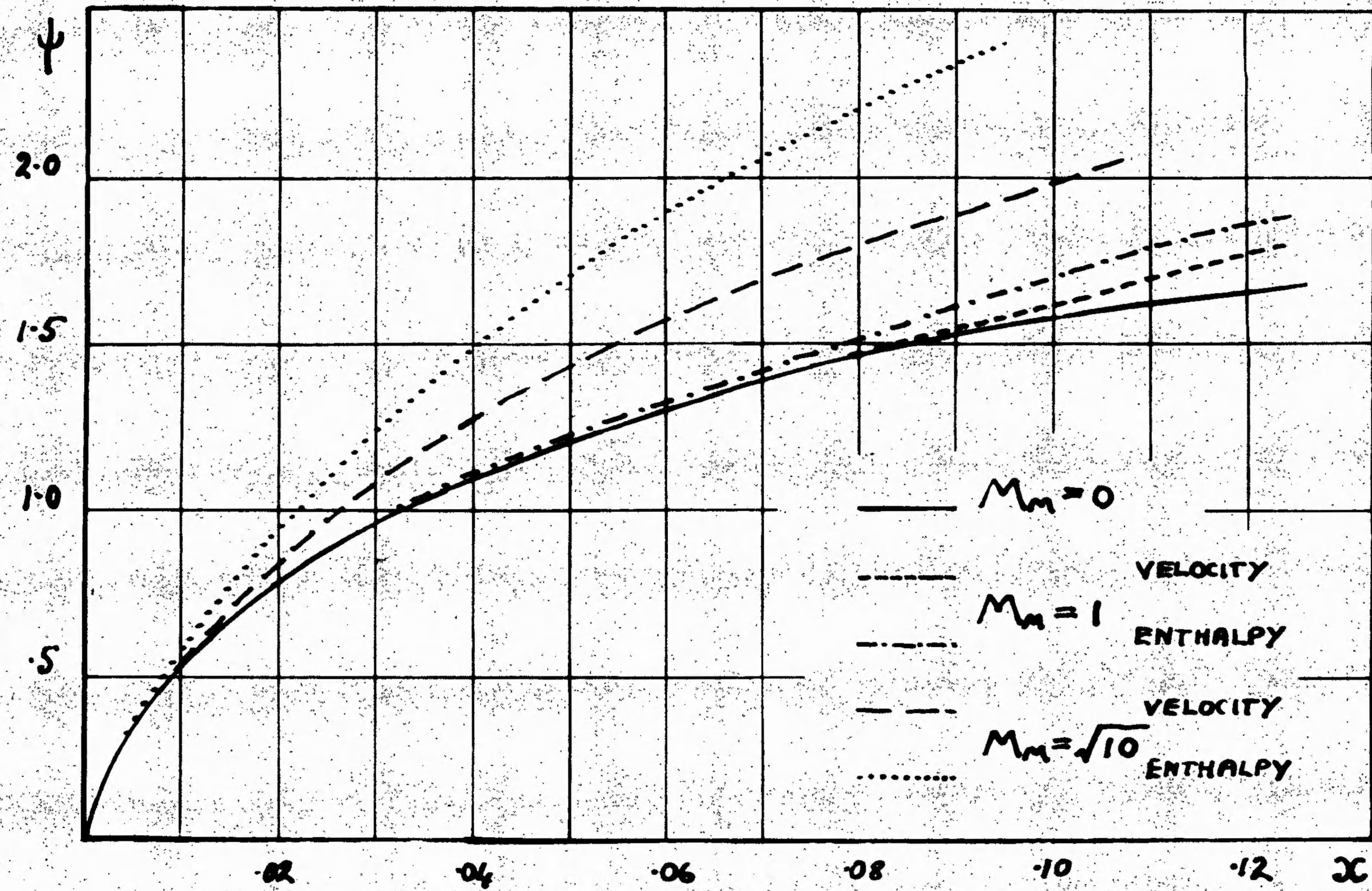


Comparison of boundary layer thickness.

FIGURE (5,11)

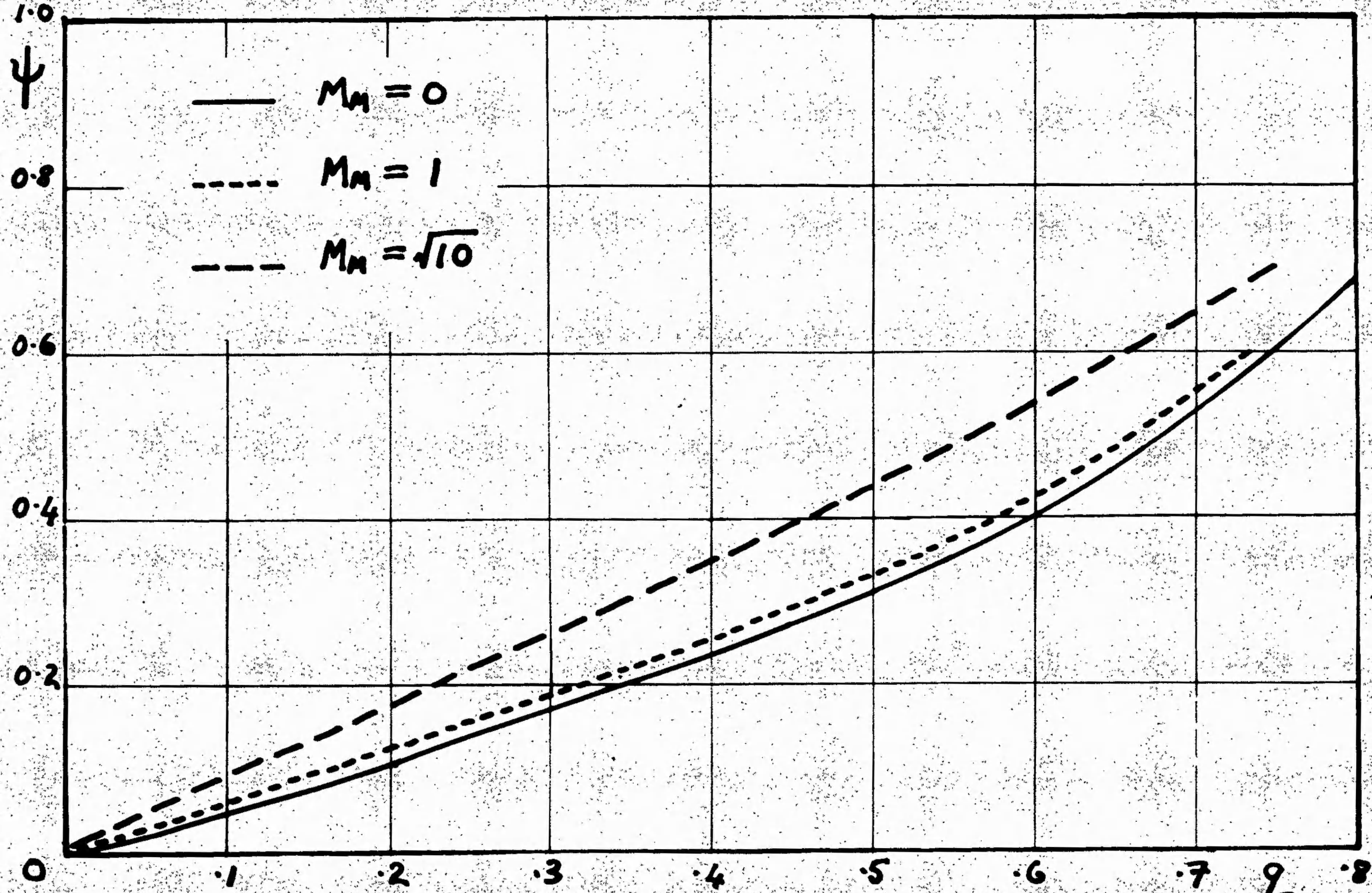


Comparison of velocity profiles at x = .08

FIGURE (3,12)

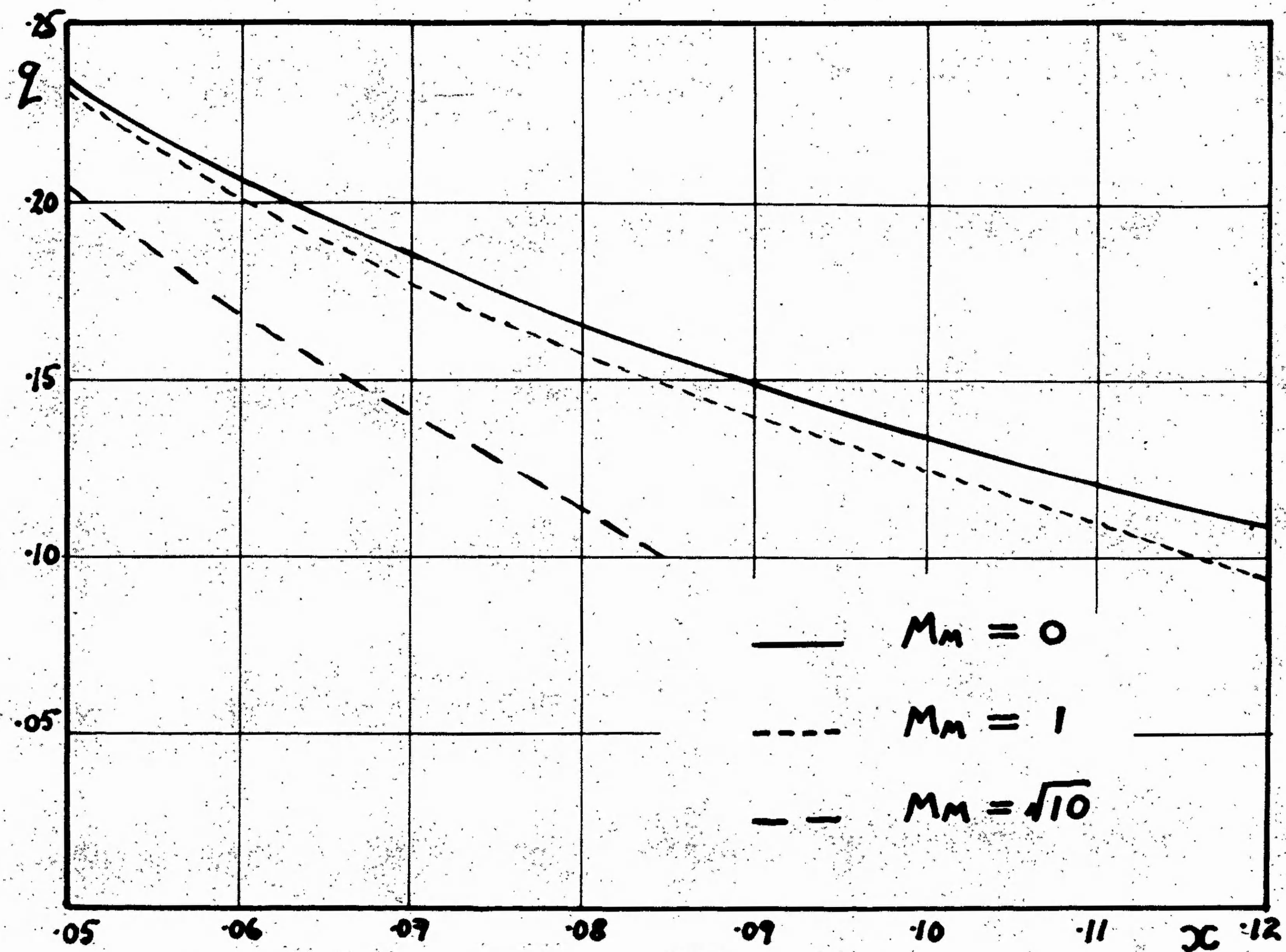


Comparison of q at $\psi$ = ·1.

FIGURE (3,15).

## 3.C.

## SUMMARY.

The calculated velocity and enthalpy profiles in two compressible boundary layers have been listed in the previous section. From these results certain interesting conclusions may be drawn.

It is evident that as the Mach number increases the boundary layers thicken (the enthalpy layer is actually thicker than the velocity layer) and the separation point moves toward the nose of the plate. In a practical sense this means that as the Mach number increases it is much more difficult to maintain fully laminar conditions of flow.

The estimated values of the separation point are compared with the results of Illingworth [27] and Stewartson [23], who used the simplifying assumptions to obtain solutions.

| $M_M$ | No Approximations | $\omega = \sigma = 1$ Approximations | Illingworth | Stewartson |
|---|---|---|---|---|
| 1 | .1125 | .1100 | .101 | .110 |
| $\sqrt{10}$ | .0825 | .0725 | .060 | .074 |

If we examine the results of the calculations in which the full equations are used, as compared with the results derived from the approximate equations, it is evident that as the Mach number increases the validity of the assumptions $\omega = 1, \sigma = 1$ decreases.

It is unfortunate at this stage that we can make no accurate assessment of the heat transfer on the plate. It is hoped, however, that this will be done at a later date.

The inherent stability condition and regions in which it is violated are also points of interest in this section. The condition is violated at nodes in and near the free stream and so it is to be expected that errors may grow at such nodes. Contradictory to this we know that as the free stream values are specified before the calculation is started there can be no growth of error.

From the above argument it would seem that a violation of the inherent stability condition may or may not produce error growth. Until more is known about non linear partial difference equations this question cannot be discussed further.

In conclusion we may say that the method is extremely simple (if labourious) in its application to compressible flow problems. With the use of electronic computing machinery much of the labour will be removed.

## CONCLUSION.

The essential features of this thesis are (1) the use of the Von Mises form of the boundary layer equations and (2) the use of finite difference methods.

Some remarks concerning the thesis in general are listed below.

(a) The singularity on the plate which prevented many Authors from using numerical techniques based on the Von Mises equation, has been incorporated in the present method of solution. We have shown, in fact, that at a given distance from the plate the extrapolation formula derived in the present thesis is comparable in accuracy with the formula in terms of $y$ used by Leigh.

(b) A disadvantage of the method is that a small mesh size is required in the primary calculation. It is felt that the initial mesh size used in this thesis is rather large. As stated previously this difficulty can be overcome by the use of an electronic computer.

(c) Concerning the stability and stability conditions many interesting facts have been discovered. From the incompressible flow calculation it is seen that in the unstable region near the plate the instability is mild. From the compressible flow calculations it is seen that the inherent stability condition is violated at nodes in or near the free stream. However, at such nodes we do not expect any marked error growth.

Both of these facts tend to suggest that the inherent stability is not vital. If this is so, the method of solution is even easier to apply, since no correction for stability is required. This must however, be left open until more is known about the stability of non linear partial difference equations.

(d) The main advantages of the method are, (1) applicability to both incompressible and compressible boundary layer flow, no major change being required in the method of calculation and, (2) the great simplicity of the actual numerical calculations.

(e) Both in the incompressible and compressible boundary layer problems the results of the present calculations agree favourably with standard known results, despite the relatively large mesh sizes used. The use of the classical boundary layer profile at the nose as the initial boundary condition is also justified, as far as prediction of the separation point is concerned, as is the assumption that the initial boundary condition at a station x, has little effect in comparison with the two boundary conditions in the $\psi$-direction.

In conclusion it should be stressed that all the numerical work in this thesis was carried out on a desk calculating machine. The time factor prevented great accuracy being obtained, particularly in the neighbourhood of the plate. The use of high speed calculating machines would result in an overall increase in detailed information. In particular, in the compressible case, the temperature near the plate, the heat transfer and the separation point could be obtained accurately for a large range of initial Mach numbers. The calculations performed, however, are sufficient to stress the need for information on the stability of step-by-step solutions of non-linear partial difference equations.

## REFERENCES.


[1] Modern developments in Fluid Dynamics, Volume 1 (1933).

[2] Modern developments in Fluid Dynamics, High Speed Flow, Volume 1 (1953).

[3] Schlichting Boundary layer theory, English Edition (1955).

[4] Navier Mémoire sur les Lois du Mouvement des Fluides. Mem. de l'Acad. d. Sci. 6,389 (1827).

[5] Poisson Mémoire sur les Équations générales de l'Equilibre et du Mouvement corps Solides Élastiques et des Fluides. J. de l'Ecole polytech. 13, 1 (1831).

[6] Prandtl Über Flüssingkeitsbewegung bei sehr kleiner Reibung. Proc (111) Interm. Math. Congr. Heidelberg (1904).

[7] Cope and Hartree The laminar boundary layer in a compressible flow. Phil. Trans. Roy. Soc. A 200, 84 (1949).

[8] Blasius Grenzschichten in Flüssigkeiten mit kleiner Reibung. Z. Math. u. Phys., 56, 1, (1908)

[9] Töpfer Bemarkungen zu dem Aufsatz von H. Blasius [8]. Z. Math. u. Phys. 60, 397, (1912).

[10] Bairstow Skin Friction. J. of the Roy. Aero. Soc. 19, 3 (1925).

[11] S. Goldstein Concerning some solutions of the boundary layer equations in hydrodynamics. Proc. Camb. Phil. Soc. 26, 19, (1930).

[12] Howarth On the solution of the laminar boundary layer equations. Proc. Roy. Soc. London A 164, 547 (1938).

[13] Hartree A solution of the laminar boundary layer equation for retarded flow. A.R.C. Rep. and Memo. No. 2426 (1949).

[14] Von Karman. Über laminare und turbulente Reibung. Z.A.M.M. 1, 233 (1921).

[15] Polhausen. Zur näherungsweisen Integration der Differentialgleichung der laminaren Reibungschict. Z. A.M.M. 1, 252 (1921).

[16] Prandtl Zur Berechnung der Grenzschichten. Z.A.M.M. 18, 77, (1938).

[17] Görtler Weiterentwicklung eines Grenzschichtprofiles bei gegebenem Druckverlauf. Z.A.M.M. 19, 129 (1939).

[18] Görtler Ein Differenzenverfahren zur Berechnung laminarer Grenzschichten. Ing. Arch. 16, 173 (1948).

[19] Schroeder Verwendung der differenzenrechnung zur Berechnung der laminaren Grenzschicht. Math. Nachr. 4.439 (1951).

[20] Witting Verbesserung des Differenzenverfahrens von H. Goertler zur Berechnung laminaren Grenzschichten Z.A.M.P. 4, 376 (1953).

[21] Leigh The laminar boundary layer, a method of solution by means of an automatic computer. Proc. Camb. Phil. Soc. 51, 320 (1955).

[22] Howarth Concerning the effect of compressibility on laminar boundary layers and their separation. Proc. Roy. Soc. London A 194 16 (1948).

[23] Stewartson Correlated compressible and incompressibl boundary layers. Proc. Roy. Soc. A, 200, 84, (1949).

[24] Crocco Sullo strato limite laminare nei gas lungo una lamina plana. Rend. Math. Univ. Roma. V, 2, 138(1941).

[25] Busemann Gasströmung mit laminarer Grenzschicht entlang einer Platte. Z.A.M.M. 15, 23 (1935).

[26] Hantzschd and Wendt. Zum Kompressibilitätseinflus bei der laminaren Grenzschicht an der ebenen Platte. Jb. dt. Luftfahrtforschung I, 517 (1940).

[27] Illingworth The effect of heat transfer on the separation of a compressible laminar boundary layer. Quarterly Journal of Mechanics and Applied Mathematics VII 8, (1954).

[28] Brainerd and Emmons Temperature effect in a laminar compressible fluid boundary layer alon a flat plate. J. Appl. Mech. 8, A. 105 (1941) and 9, 1 (1942).

[29] Gadd On the numerical integration of the laminar boundary layer equations. A.R.C. Repand Memo 15-101.

[30] Flugge-Lotz The computation of the laminar compressible boundary layer. Report of Dept. Mech. Eng'g. Stanford University (1954).

[31] Siekmann Ein Differenzenverfahren zur Berechnung stationärer laminarer kompressible Grenzschichten. Thesis Faculty of Mechanical Engineering (1955).

[32] Von Mises Bemerkungen zur hydrodynamik Z.A.M.M. 7, 425 (1927).

[33] Luckert. Über die Integration der Differentialgleichung einer Gleitschicht in zäher Flussigkeit. Schriften d. Math. Seminars u. Inst. F. angew. Math. d. Universität Berlin 1,245 (1933).

[34] Von Karman and Millikan On the theory of lamina boundary layers involving separation. N.A.C.A. Rep. 504 (1934).

[35] Von Karman and Tsein Boundary layer in compressible fluid. J. Aero. Sci. 5, 227 (1938).

[36] Illingworth Steady flow in the laminar boundary layer of a gas. Proc. Roy. Soc. A 199, 533 (1949).

[37] O'Brien, Hyman and Kaplan A Study of the numerical solution of partial differential equations. J. of Math. and Phys. 29, 223, (1951).